

**McGill**  
UNIVERSITY

**Additive Manufacturing Leveraged  
Microfluidic Setup for Sample to Answer  
Nucleic Acid-based Detection of Pathogens**

Sripadh Guptha Yedire

Master of Engineering

Department of Bioengineering

McGill University

Montréal, Quebec, Canada

July 2022

A thesis submitted to McGill University in partial fulfillment of the requirements of the  
degree of Master of Engineering

© Sripadh Guptha Yedire, 2022

## Table of contents

Abstract-English.....	1
Abstract- Français.....	3
Preface and Author contributions.....	5
Acknowledgments.....	6
List of Figures and Tabela.....	7
List of Abbreviations.....	9
<b>1. Introduction.....</b>	<b>10</b>
<b>2. Literature review.....</b>	<b>12</b>
2.1. Colorimetric assays for molecular detection of pathogen.....	13
2.1.1. Dye based techniques.....	14
2.1.2. Turbidimetry.....	14
2.1.3. Fluorescent techniques.....	14
2.2. Point of care/need technologies for colorimetric molecular detection.....	15
2.2.1. Sample collection and processing.....	16
2.2.2. Fluid manipulation.....	17
2.2.2.1. Active flow manipulation.....	19
2.2.2.2. Passive flow manipulation.....	21
2.2.3. Signal transduction.....	26
2.2.3.1. Influence of incident illumination on plasmonic nanostructures.....	26
2.2.3.2. Imaging setups for POC applications.....	27
<b>3. Additive Manufacturing Leveraged Microfluidic Setup for Sample to Answer</b>	
<b>Nucleic Acid-based Detection of Pathogens.....</b>	<b>31</b>
3.1. Abstract.....	31
3.2. Introduction.....	33

3.3. Experimental.....	39
3.3.1. Outline of operation.....	39
3.3.2. Optical train setup.....	39
3.3.3. Fabrication of microfluidic cartridge.....	40
3.3.4. Fabrication protocol for suction cups.....	43
3.3.5. Fabrication of 3D printed components.....	43
3.3.6. Electronic components of automation.....	44
3.3.7. RT-LAMP assay.....	45
3.4. Results and discussion.....	45
3.4.1. Optical setup development and characterization.....	45
3.4.1.1. Field of view and resolution characterization.....	46
3.4.1.2. Light source selection.....	47
3.4.1.3. Illumination column characterization.....	47
3.4.2. Characterization of microfluidic cartridge.....	50
3.4.2.1. COMSOL simulation and discussion.....	51
3.4.2.2. Suction cups characterization.....	53
3.4.2.3. Characterization of volume suctioned.....	53
3.4.2.4. Fluid flow control.....	55
3.4.2.5. 3D printed fluid handling attachment characterization.....	56
3.4.2.5.1. 3D printed membrane characterization.....	57
3.4.2.6. Extent of mixing.....	57
3.5. Design of automated setup.....	60
3.6. Assay imaging.....	61
3.6.1. Comparative study of Imaging of assay droplet on platform.....	66
3.7. Conclusion.....	68

3.8. Supplementary Information.....	70
3.9. References.....	79
<b>4. Discussion and future perspectives.....</b>	<b>86</b>
<b>5. Summary.....</b>	<b>91</b>
<b>6. Master Bibliography.....</b>	<b>92</b>

## **Abstract- English**

The colorimetric signal transduction technique has been extensively applied for the detection of biological analytes. Specifically, a colorimetric readout for the detection of infectious diseases is gaining traction for application at the point of care/need settings. This can mainly be attributed to the standout features of colorimetric readout which include high sensitivity, ease of analysis and interpretation, minimal training requirements, and affordability. In addition to this, colorimetric readout provides ease of integration and conductivity with Loop-mediated isothermal amplification (LAMP) assay, which is a popular alternative to the gold-standard polymerase chain reaction (PCR) test for infectious pathogen detection. Recently, our lab reported a specialized nanostructured platform, QolorEX, that enhances the colorimetric readout of a LAMP assay via plasmonic excitation. The two main challenges impeding its potential application at the point of care/need are, (i) the requirement of a brightfield microscope for capturing the colorimetric change and (ii) user involvement to execute multiple sequential steps of the LAMP assay. The nanostructured platform is sensitive to the nature of the incident light irradiated for the interpretation of the colorimetric readout. This necessitates an imaging setup customized to the signal capture over the color-sensitive platform.

In this thesis, I proposed an automated setup that encompasses an imaging setup for recording the colorimetric change; and a microfluidic setup to automate the sequential steps in the LAMP assay. First, for imaging, we designed a portable reflected-light imaging setup with controlled epi-illumination (PRICE). It features an infinity-focused objective (magnification 20x) with an optical train that forms an image on a CMOS sensor. More importantly, the setup uses an illumination column that provides uniform illumination with spatial and intensity control. The second key challenge is user involvement in one or more assay steps. This was addressed with a microfluidic cartridge. To integrate all the assay steps, from sample collection to endpoint

detection onto this microfluidic cartridge, we leveraged four key technologies, (1) negative pressure-based suction cups, (2) microfabrication, (3) additive manufacturing, and (4) open-source hardware and software. Suction cups were designed and employed to execute sequential fluid manipulation steps upon compress and release cycles. A silicon-based microfluidic chip houses the detection platform as well as microchannels for transporting and mixing fluid. Stereolithography (SLA) 3D printing (additive manufacturing) was employed to design a module that houses sample collection, sample lysis, and amplification reagents storage chambers. In addition to this, this 3D printed module also houses a simple screw-nut-based contraption for mechanical actuation of the suction cups. Finally, the different steps in the operation of the cartridge are automated/concerted by a control module (encompassing linear, actuators, heaters, servos, stepper motors, and CMOS sensor) concerted by Arduino UNO and Raspberry Pi microprocessors. The entire control module is centrally controlled by a mobile application installed on the user's mobile phone.

The imaging setup showed promising results in imaging the colorimetric change on par with a commercial brightfield microscope. We were able to detect the presence of viral nucleic acid in 15 minutes at a clinically relevant load of  $8 \times 10^5$  RNA copies/ $\mu\text{L}$ . The screw-nut mechanical actuation system was successfully demonstrated for angle-dependent precise fluid metering. The fluidic cartridge in conjugation with the control module was demonstrated to automate the sequential steps in the nucleic acid amplification assay.

**Keywords:** Colorimetric readout, nucleic acid amplification, portable imaging, suction cups, additive manufacturing, automation, open-source hardware

## **Abstract- French**

La technique de transduction du signal colorimétrique a été largement appliquée pour la détection d'analytes biologiques. Plus précisément, la lecture colorimétrique pour la détection d'agents pathogènes infectieux gagne en popularité dans les points de soins/besoins, en raison de ses caractéristiques remarquables, telles que sa haute sensibilité, sa facilité d'analyse et d'interprétation, ses exigences minimales en matière de formation et son prix abordable. En outre, la lecture colorimétrique facilite l'intégration avec le test d'amplification isothermique médiée par une boucle (LAMP), qui est une alternative populaire au test de référence qu'est la réaction en chaîne par polymérase (PCR) pour la détection des agents pathogènes infectieux. Récemment, notre laboratoire a présenté une plateforme nanostructurée spécialisée, QolorEX, qui améliore la lecture colorimétrique d'un test LAMP par excitation plasmonique. Les deux principaux défis qui entravent son application au point de soins/besoins sont : (i) la nécessité d'un microscope à fond clair pour capturer le changement de couleur et (ii) l'implication de l'utilisateur pour exécuter les étapes séquentielles du test LAMP. La plateforme nanostructurée est sensible à la nature de la lumière incidente pour l'interprétation de la lecture colorimétrique. Cela nécessite une configuration d'imagerie personnalisée pour la capture du signal sur la plateforme sensible à la couleur.

Dans cette thèse, j'ai proposé une installation automatisée qui comprend une installation d'imagerie pour l'enregistrement du changement colorimétrique et une installation microfluidique pour automatiser les étapes séquentielles du test LAMP. Nous avons conçu un dispositif portable d'imagerie par lumière réfléchiée avec épi-illumination contrôlée (PRICE) avec un objectif 20x à focalisation infinie et un train optique qui forme une image sur un capteur CMOS. Le dispositif utilise une colonne d'illumination qui fournit un éclairage uniforme avec des contrôles spatiaux et d'intensité. Le deuxième défi majeur, à savoir l'implication de

l'utilisateur dans une ou plusieurs étapes du test, a été relevé grâce à une cartouche microfluidique qui intègre différentes étapes du test (du prélèvement de l'échantillon à la détection du point final) en exploitant quatre technologies: (1) les ventouses à pression négative, (2) la microfabrication, (3) la fabrication additive et (4) le matériel et les logiciels libres. Des ventouses ont été utilisées pour exécuter des étapes séquentielles de manipulation de fluides lors de cycles de compression et de relâchement. Une puce microfluidique à base de silicium abrite la plateforme de détection ainsi que des microcanaux pour le transport et le mélange des fluides. L'impression 3D par stéréolithographie (SLA) a été utilisée pour concevoir un module qui abrite les chambres de collecte des échantillons, de lyse des échantillons et de stockage des réactifs d'amplification. En outre, ce module imprimé en 3D abrite un dispositif à base de vis et d'écrous pour l'actionnement mécanique des ventouses. Enfin, les différentes étapes du fonctionnement de la cartouche sont automatisées/concertées par un module de contrôle concerté par des microprocesseurs Arduino UNO et Raspberry Pi. L'ensemble du module de contrôle est piloté par une application mobile installée sur le téléphone portable de l'utilisateur.

Le dispositif d'imagerie a montré des résultats prometteurs en imagerie du changement colorimétrique, à égalité avec un microscope à fond clair commercial. Nous avons pu détecter la présence d'acide nucléique viral en 15 minutes à une charge cliniquement pertinente de  $8 \times 10^5$  copies d'ARN/ $\mu$ L. Le système d'actionnement mécanique vis-écrou a été démontré avec succès pour le dosage précis du fluide en fonction de l'angle. La cartouche fluidique conjuguée au module de contrôle a été démontrée pour automatiser les étapes séquentielles du test d'amplification de l'acide nucléique.

**Mots-clés:** Lecture colorimétrique, amplification de l'acide nucléique, imagerie portable, ventouses, fabrication additive, automatisation, matériel open-source

## **Preface and Author contributions**

Chapter 3 of this thesis titled, ‘Additive Manufacturing Leveraged Microfluidic Setup for Sample to Answer Nucleic Acid-based Detection of Pathogens’ is under preparation for submission to the Lab on a Chip journal from the Royal Society of Chemistry family with Sripadh Guptha Yedire as the co-author. The fabrication of the microfluidic device was carried out at the McGill Nanotools-Microfab facility at McGill University. 3D printing of the preliminary prototypes was carried out at the The Gearbox facility at the Department of Physics. Further processing of the microfluidic chip fabrication was performed at NanoQAM. Seyed Imman Isaac Hosseini and Tamer AbdElFatah helped with the design and brainstorming on the microfluidic chip. Professor Sara Mahshid provided insights into the execution, discussion and presentation of pertinent results.

## **Acknowledgments**

I would like to start by thanking my thesis advisor as well as my mentor, Professor Sara Mahshid of Bioengineering Department at McGill University. Throughout my Master's degree, she supported me and guided me in the right direction. She was always there for me whenever I encountered problems or needed advice. A special mention is in place for Imman Isaac Hosseini for his contribution and dedication to brainstorm, plan and help me with crucial troubleshooting. His contributions to the project were crucial for its success. I would also like to acknowledge the contribution of Tamer Abdel Fatah for helping me accelerate the process of learning several important microfabrication techniques. My gratitude goes out to all members at Mahshid lab, for their advice, encouragement, and providing a great working environment.

I would like to thank members at McGill Nanotools-Microfab for their assistance and support in the microfabrication protocols. The Gearbox facility at the Department of Physics and especially Robert Turner deserves a special mention for their immense help with 3D printing during the pandemic. Also, I would like to acknowledge NanoQAM for their support with plasma cleaner and profilometer equipment.

Starting my graduate degree during the pandemic has not been easy and I am extremely grateful for my mother, father, sister and friends in Hyderabad, Arizona, Toronto and Montreal for their immense support and motivation all through this journey. They motivate me to always push myself and go above and beyond. Lastly, I would like to thank Prof. Shirish Sonawane, at National Institute of Technology, Warangal, who introduced me to this fascinating world of research and Prof. Satya Sai, who motivated me to pursue research as a career option right from the nascent days of undergrad.

# List of Figures and Tables

## Chapter 2: Literature review

**Fig. 1.1.** Suction cup parameters

**Table 1.1.** Brief survey on integrated microfluidic approaches for NAAT based detection pathogens with a colorimetric readout

## Chapter 3: Additive Manufacturing Leveraged Microfluidic Setup for Sample to Answer Colorimetric Detection of Pathogens

**Fig.3.1.** Experimental workflow of sample to answer microfluidic based system for pathogen detection

**Fig. 3.2.** Schematic representation of major components in the automated setup for colorimetric point of care/need detection

**Fig 3.3.** Stepwise fabrication process of the fluid handling module

**Fig. 3.4.** Characterization of the PRICE setup

**Fig. 3.5.** Overview of microfluidic cartridge operation

**Fig. 3.6.** Characterization of components involved in fluidic module

**Fig. 3.7.** Sample collection to analysis protocol

**Fig. 3.8.** Camera captured pictures of prototypes of the imaging and fluidic modules

**Fig. 3.9.** Comparison study between Nikon microscope and the imaging setup for RT-LAMP assay

**Fig. S1.** Components of illumination

**Fig. S2.** COMSOL analysis for design of the microfluidic platform

**Fig. S3.** Suction cup fabrication protocol

**Fig S4.** Depiction of experimental setup for suction cup characterization

**Fig S5.** Characterization of 3D printed components

**Fig S6.** Overview of electronic components

**Fig S7.** Infrared images of the heating module

**Fig. S8.** Overview of operation of the mobile enabled automation

## **List of Abbreviations**

**PCR**- Polymerase chain reaction

**LAMP**- Loop-mediated isothermal amplification

**POC**- Point-of-care

**ASSURED**- Affordable, Sensitive, Specific, User-friendly, Rapid/Robust, Equipment-free and Deliverable

**NAAT**- Nucleic acid amplification tests

**RPM**- Rotation for minute

**PDMS**- Polydimethylsiloxane

**LFA**- lateral flow assay

**PRICE**- Portable Reflected-Light Imaging Setup with Controlled Epi-Illumination

**LOC**- Lab on chip

**IPA**- Isopropyl alcohol

**SLA**- Stereolithography

**CMOS**-Complementary Metal Oxide Semiconductor

**FoV**-Field of view

**CRI**- Color rendering index

# 1. Introduction

Infectious diseases are a significant burden on global health. A primary example is the devastating impact of the COVID-19 pandemic, which has killed millions of lives, damaged economies worldwide, and tremendously disrupted social operations. Infectious diseases are driven by pathogens which include bacteria, viruses, fungi, and protozoa. Pathogens create a healthcare challenge as they can rapidly propel the spread of infectious diseases through quick transmission from one host to another<sup>1</sup>. As such, effective pathogen diagnosis is a crucial step in reducing the load of deadly infectious diseases. Combatting the COVID-19 pandemic has been a hotspot of recent research and there have been strong efforts worldwide for rapid disease diagnosis and isolation<sup>2</sup>. While polymerase chain reaction (PCR) and culture techniques remain the gold standard techniques, next generation and advanced pathogen sensing platforms have been recently reported<sup>3-10</sup>. Specifically, Loop-mediated isothermal amplification (LAMP), an isothermal nucleic acid amplification technique, is garnering attention owing to requirement of constant temperature, high specificity and sensitivity<sup>11,12</sup>. LAMP is combined with several signal transduction techniques like fluorescence, colorimetric and turbidimetric readouts<sup>13</sup>. Recently, our lab has reported a specialized nanostructured platform, QolorEX<sup>14</sup>, that enhances the colorimetric readout of a LAMP assay via plasmonic excitation. Although this platform carries with it several advantages, they bring along some challenges for application at the point of care/need. Firstly, colorimetric readout lacks from error in signal interpretation from user to user, hence often requiring brightfield microscope. To add to this, the sequential nature of LAMP assay often requires user involvement in one or more steps. Hence these challenges necessitate a platform that can automate the process of color change mediated pathogen detection assay using LAMP. In this work we leveraged three technologies to make this automation possible, (i) Additive manufacturing leveraged fluid handling systems to encompass the assays steps in hand-free format, (ii). Imaging with off-the-shelf optics for

signal interpretation, (iii). Open-source hardware and software technologies for control, data interpretation and data transmission.

## 2. Literature review

Centralized laboratories remain the dominant hub of pathogen testing worldwide for gold standard techniques like Polymerase chain reaction (PCR)<sup>15</sup>. However, centralized laboratories are limited by the delay in results, the need for bench-top analyzers, and highly trained personnel<sup>16</sup>. Therefore, it is necessary to employ rapid, sensitive, and economic pathogen detection techniques. Point-of-care (POC) diagnostic systems aim to overcome the challenges presented by traditional diagnostic techniques as they offer prompt diagnostic results for on-site diagnosis and treatment. Some features of POC diagnostics are rapid tests to allow patients to receive immediate treatment plans, sensitive and specific results comparable to those of traditional methods, and user-friendly systems<sup>17</sup>. This enables healthcare practitioners to make quick medical decisions leading to improved health outcomes for patients, due to disease diagnosis at the earliest stage<sup>18</sup>. To aid to the development of POC devices, the world health organization (WHO) proposed a framework dubbed, ASSURED to evaluate and better design the POC diagnostic tool. This framework expects a POC diagnostic tool to be, Affordable, Sensitive, Specific, User-friendly, Rapid/Robust, Equipment-free and Deliverable (ASSURED)<sup>19</sup>.

In compliance to ASSURED criteria, there are three defining features of a POC system, (i). biochemical assay of detection, (ii). Sample handling, (iii). Signal transduction<sup>20</sup>. The choice of assay for pathogen detection plays an important role in designing a POC diagnostic test. The desired features include cost-effectiveness; high sensitivity and specificity; ease of integration with POC tools like microfluidics and digital signal transduction techniques<sup>20</sup>. In this context, POC systems were proposed integrating isothermal nucleic acid amplification techniques (NAAT) with microfluidic systems<sup>21</sup>.

On the other hand, microfluidics has been crucial in designing sample handling systems for POC devices for the past decade. Microfluidic platforms are miniature devices which enable the precise manipulation of flow and reaction conditions of fluids on a submilliliter scale. A crucial feature of microfluidic platforms for pathogen detection is that they enable the integration of sample processing, extraction, detection, and analysis onto a single platform<sup>22,23</sup>. Moreover, confined reaction volumes allow for fast and high throughput analysis<sup>24</sup>. Microfluidic platforms also carry with them features like portability, automation and precise handling of small reaction volumes<sup>25</sup>. These factors make them ideal candidates for POC applications. Microfluidic platforms for pathogen detection have picked up pace in the past decade<sup>26-28</sup>. Microfluidics can potentially be integrated with different read-out systems including electrical, optical, and colorimetric<sup>29-34</sup>. Colorimetric readouts when combined with NAATs benefit from high sensitivity, ease of analysis and interpretation, minimal training requirements, and affordability<sup>35-37</sup>. Hence microfluidic platforms integrated with colorimetric NAAT assays, make for inexpensive, portable, fast, and highly suitable platforms for POC and low-resource settings.

## **2.1. Colorimetric assays for molecular detection of pathogen**

The molecular techniques or NAATs for pathogen majorly comprise of assays such as Polymerase chain reaction (PCR), Loop-mediated isothermal amplification (LAMP), Helicase-dependent amplification (HDA), Nicking endonuclease amplification reaction (NEAR), Transcription mediated amplification (TMA), Strand displacement amplification (SDA), and Clustered regularly interspaced short palindromic repeats (CRISPR)<sup>38</sup>. LAMP, amongst all the amplification techniques is the most researched at POC settings, as an alternative to gold standard PCR<sup>13,39</sup>. The end point detection of these colorimetric assays can be broadly categorized into dye-based and turbidimetry and fluorescence readouts.

### **2.1.1. Dye based techniques**

Dye based techniques involves use of an external dye that enables end-point detection with naked eye. Specifically for LAMP assays naked eye-based detection usually employs either metal ion indicators like hydroxynaphthol blue (HNB) dye, Eriochrome Black T (EBT), Malachite green (MG)<sup>13</sup>, and calcein/Mn<sup>+2</sup><sup>40</sup> or pH sensitive dyes like phenol red and cresol red<sup>41</sup>. The colorimetric changes were either attempted to be analyzed with naked eye<sup>42</sup> or via digital quantification methods<sup>43</sup>. The main idea to employ digital methods is to overcome the user-to-user variability and challenges with quantification with naked-eye detection<sup>44</sup>. To apply colorimetric dyes for POC pathogen detection, Papadakis et al.<sup>44</sup> proposed a portable POC device for SARS-CoV-2 detection using quantitative colorimetric LAMP (qcLAMP). They proposed two channels for real-time RGB tracking of either phenol red or HNB colorimetric dyes in Eppendorf tubes.

### **2.1.2. Turbidimetry**

In one of the initial attempts to track the end-point detection of LAMP assay, a turbidity based naked-eye detection was proposed<sup>45</sup>. The underlying principle relies on the strong cation binding property of pyrophosphate (a by product of LAMP reaction), which precipitates combining with protons, resulting in a turbid solution<sup>13</sup>. The change in turbidity can be visualized using naked eye or turbidimeter<sup>46</sup>. Previously, turbidimetric based readout was applied for detection of several pathogen<sup>46,47</sup> including, H1N1<sup>48</sup>, West Nile virus<sup>49</sup> and adenovirus<sup>50</sup>.

### **2.1.3. Fluorescent techniques**

Fluorescence based end-point detection technique is the most widely reported for LAMP and other amplification techniques alike<sup>46</sup>. Specifically for LAMP assay, the amplified products

were visualized using intercalating dyes like SYBR green I, picogreen and evagreen<sup>51</sup>. The visualization of fluorescence readout usually requires specialized equipment like optical filters, UV or LED light, when compared to naked eye detection techniques. Previously, fluorescence detection techniques were applied for detection of several pathogens using LAMP<sup>46</sup> including, SARS-CoV-2<sup>52</sup>, Ebola<sup>53</sup>, Hepatitis B<sup>54</sup>, mycobacteria<sup>55</sup>, and MERS-CoV<sup>56</sup>.

## **2.2. Point of care/need technologies for colorimetric molecular detection**

The recent COVID-19 outbreak has re-emphasized the importance of tools to contain the infectious pathogen and ultimately lower the mortality rate. Moreover, countries with weaker healthcare infrastructure and inadequate resources faced the larger brunt of the pandemic. Point of care/need (POC) diagnostic tools can help address these shortcomings and help curb the spread of the pathogen. To meet the WHO's ASSURED criteria, microfluidic technologies have emerged as an important tool. Microfluidic platforms are miniature devices which enable the precise manipulation of flow and reaction conditions of fluids on a submilliliter scale. Moreover, confined reaction volumes allow for fast and high throughput analysis<sup>57</sup>. Microfluidic platforms also carry with them features like portability, automation and precise handling of small reaction volumes. Choice of detection assay also plays an important role in determining the closeness of the diagnostic tool with the ASSURED criteria. Isothermal nucleic acid amplification tests (NAAT) present as promising alternative to the gold standard polymerase chain reaction (PCR). Isothermal NAATs include variety of assays previously reported like, Loop-mediated isothermal amplification (LAMP), Helicase-dependent amplification (HDA), Nicking endonuclease amplification reaction (NEAR), Transcription mediated amplification (TMA), and Strand displacement amplification (SDA)<sup>58</sup>. Among these assays, LAMP is an attractive alternative owing to requirement of constant temperature<sup>59</sup>, higher specificity and sensitivity compared to conventional techniques<sup>60</sup>, and stability against amplification inhibitors<sup>61</sup>. LAMP assay typically involves disparate steps of sample collection,

sample preprocessing, nucleic acid enrichment, nucleic acid amplification, signal transduction and data transmission<sup>39</sup>. A crucial and positive feature of microfluidic platforms for pathogen detection is its conducive nature for integration these assay steps on to single platform<sup>22,23</sup>. This feature of microfluidic setups for LAMP assay ensures the compliance of the designed system with multiple ASSURED criteria.

Over the past decade several microfluidic technologies were reported to integrate multiple steps of the detection assay onto a single platform. These platforms, simply dubbed as integrated microfluidic systems, require innovations in technologies pertaining to different assay steps, i.e. sample collection and processing, reagent mixing (fluid manipulation), amplification and signal transduction, to ultimately device a miniaturized system with a potential application at point of care/need. The recent advances in innovations in packing these assay steps onto an integrated platform are discussed in the following sections.

### **2.2.1. Sample collection and processing**

The choice of sample is a crucial step that defines the choice of downstream microfluidic processing techniques utilized. Nasal swab, saliva, blood, urine and stool samples are among the commonly employed samples for NAAT testing of infectious pathogen. More specifically, nasal swab and saliva have been choice of sample for colorimetric NAAT assays<sup>62</sup>. There is a growing interest in saliva owing to the ease of sample collection by untrained individuals, reduced risk and reduced discomfort<sup>62</sup>. Recently, Azzi<sup>63</sup> and co-workers showed saliva as a reliable tool to detect SARS-CoV-2 under 33 threshold cycles using rRT-PCR. Irrespective of the sample of choice, pathogen lysis and subsequent nucleic acid extraction are crucial in determining the POC applicability.

Several POC approaches to pathogen lysis were proposed in previous works and can be broadly categorized into four categories, (i) thermal lysis, (ii) chemical lysis, (iii) mechanical lysis and

(iv) electrochemical lysis<sup>64,65</sup>. Thermal lysis relies on the application of high temperature to rupture the lipid membrane, capsid, encompassing the genetic material of the pathogen<sup>66</sup>. Moreover, thermal lysis method takes only few minutes to release the nucleic acid from the lysed sample<sup>67,68</sup>. Previously, Packard et al.<sup>69</sup> designed a serpentine shaped resistive heater for bacterial cell lysis via joule heating. In another work Cho et al.<sup>70</sup> reported photothermal lysis using plasmonic nanoparticles that absorbs incident light at specific wavelength. Chemical lysis has also been reported<sup>71</sup> previously by Ma et al.<sup>72</sup>, by storing lysis buffer on-chip. Another technique, mechanical lysis was also packed in a POC format to tear the pathogenic membrane<sup>13,73</sup>. Yan et al.<sup>74</sup>, reported a bacterial lysis system on a centrifugal microfluidic platform using magnetically rotated pair of magnets to generate mechanical beating phenomena. Recently, Hügler et al.<sup>75</sup> reported a thermoelectrical lysis technique using a microfluidic chip equipped with micro-sized electrodes.

Following the lysis step, the nucleic acid is separated from other intracellular components. Previously, solid-phase extraction methods were incorporated for nucleic concentration in POC settings<sup>65,76</sup>. In previous works, lysate was concentrated using several techniques like using filter papers<sup>77</sup>, silica membranes<sup>78</sup>, nanomaterial-based approaches<sup>79</sup>, magnetic nanoparticle techniques<sup>77,80</sup>, and miniaturized silicon micropillars as filters<sup>81</sup>. In a recent work, Yoon et al.<sup>71</sup> reported a pH dependent nucleic acid isolation technique for pathogen lysates. Their technique employs a pH-dependent reversible binding of dimethyl adipimidate (DMA) to free RNA.

### **On-chip heating strategies for amplification**

The required temperature for amplification reaction depends on the type of amplification reaction employed i.e. PCR, LAMP, RCA, RPA etc. In any case, an accurate temperature profile is desired. Along the similar lines as heating for lysis, several heating strategies were proposed for the amplification step suitable for POC settings. Few techniques include, thin film

heating, Peltier heating, induction heating, photothermal heating, and continuous flow heating and are well reviewed in the past<sup>64,82,83</sup>. Peltier heating has been widely applied for amplification techniques requiring thermal cycling<sup>84</sup>. In a recent work Chen et al.<sup>85</sup> reported a finger-actuated microfluidic chip equipped with a Peltier heater to carry out LAMP assay for detection of bacterial pathogen. Qiu et al.<sup>86</sup> demonstrated a PCR based POC diagnosis device for H1N1 virus using resistive type thermocycler. In a more recent study, Deng et al.<sup>87</sup> proposed an ultra-portable SARS-CoV-2 POC device with incorporates two micro metal-ceramic heaters that carries lysis and provides the necessary temperature profile for the LAMP assay. In another work, Cho et al.<sup>70</sup> utilized a photothermal heating employing a nano-plasmonic optical antenna for ultrafast transduction of light to heat.

### **2.2.2. Fluid flow manipulation**

Another major criterion determining the extent of closeness of the point of care system to the outlined ASSURED criteria is the ability to manipulate and control the fluid flow in the microfluidic setups. Fluid manipulation becomes even more important in the context of NAAT due to the presence of sequential assay steps. Specifically, the sample preparation step (which includes sample lysis, nucleic acid purification and mixing of amplification reagents) largely require user involvement or use of costly setups<sup>88</sup>. In this context, the fluid manipulation method employed becomes a major difference between lab-on-chip and lab-around-a-chip for pathogen detection at POC<sup>89</sup>. There are certain desired features for the fluid handling systems to be applied in the integrated microfluidic setups, these include, (a). minimal user involvement, (b). precise metering of fluids, (c). capability to handling small fluidic volumes (pertaining to volume handled by microfluidic setups). Fluid handling systems, in other words, micro pumping techniques can be categorized as active and passive pumping systems<sup>90</sup>. Active pumping systems typically require external power source to be activated to enable fluid flow control<sup>91</sup>. On the other hand, passive pumping systems largely do not require external power

source and rely on the pressure gradient inherently engendered in the device. Previously micropumps were reported for several microfluidic applications including, cell culturing, biomedical assays and drug delivery analysis<sup>92,93</sup>. However, they employed sophisticated techniques like piezoelectric actuation, osmotic pressure and gravity assisted techniques, which are not ideal for POC testing applications<sup>91</sup>. Passive micropumping techniques emerged as a powerful technique to manipulate fluid at POC, with several techniques used in commercial POC testing devices<sup>94,95</sup>.

### **2.2.2.1.Active flow manipulation**

Fluid flow is actuated in an active micropumping technique by an external signal. Although this type of pumping adds complexity to the operation, they offer better control over the temporal and spatial parameters of the fluid flow<sup>96</sup>. Active micropumps can further be divided into mechanical and non-mechanical pumps. Mechanical micropumps are mainly characterized by the presence of a moving components actuated by an external signal. Some major mechanical micropumping techniques include pneumatic micropumps, piezoelectric micropumps<sup>97</sup>, thermal actuation micropumps and electromagnetic actuation micropumps<sup>98</sup>. On the other hand, non-mechanical micropumps, also called dynamic micropumps<sup>93</sup> do not comprise of any moving part but utilize to non-mechanical forces for fluid actuation<sup>91</sup>. Non-mechanical micropumps include, magnetohydrodynamic (MHD) micropumps, electrohydrodynamic (EHD) micropumps, electroosmotic and electrowetting micropumps<sup>99</sup>. Active micropumps.i.e. both mechanical and non-mechanical variants were previously explored for pathogen detection using NAAT coupled with colorimetric readout<sup>100-108</sup>.

Centrifugal microfluidics, a type of active micropumping system, is an actively researched platform for colorimetric pathogen detection using NAAT. In a recent study, Seo et al.<sup>100</sup> reported a centrifugal microfluidic device for the detection of pathogen using LAMP assay

with a colorimetric change mediated by Eriochrome Black T (EBT). The work employs a polymethyl methacrylate (PMMA) chip patterned with microchannels and chambers for sample loading, sample aliquoting and detection assay reaction. The work employs two capillary valves for sample aliquoting and sample injection into the reaction chambers. At a maximum rotational speed of 5000RPM, the sample is overcoming the capillary pressure of a cross capillary valve to enter the reaction chamber, thus avoiding overflow. In another study, Oh et al.<sup>101</sup> reported a centrifugal microfluidic systems for detection of bacterial pathogen (*Escherichia coli* O157:H7, *Salmonella typhimurium* and *Vibrio parahaemolyticus*) using a LAMP assay mediated by colorimetric change of EBT. This system employs a four layered micropatterned polycarbonate-based chip employing dimensionally controlled microchannels connecting various chambers for LAMP assays. The burst force for the connecting channels was characterized for the chip with the employed rotation for minute (RPM). Stepwise increments in rotational speed results in fluid transfer between different chambers.

Recently, centrifugal microfluidics were combined with active means of pumping and valving<sup>109</sup>. Geissler et al.<sup>102</sup> presented a centrifugal microfluidic platform for the detection of *E. coli* O157:H7 colonies using a PCR protocol followed by cloth-based hybridization array system (CHAS), with a tetramethylbenzidine (TMB) mediated color change. This platform combines centrifugal effects with tilting effects to complement the limitation of unidirectional fluid manipulation in typical centrifugal systems. The work employs two standalone microfluidic cartridges mounted on motorized shafts. These shafts can be tuned to tilt the cartridges at certain angle while they spin at high speeds. The flow between different assay chambers, connected with siphoning channels, is controlled by a combination of the tilt angle and the direction of centrifugation field.

Another major active micropumping technique is pneumatically driven systems for pumping and valving of fluid flow. Lee et al.<sup>103</sup>, designed a pneumatic controlled integrated microfluidic

platform for the detection of bacterial growth in presence of antibiotics via phenol red color change. This work demonstrates a thin Polydimethylsiloxane (PDMS) membrane-based reciprocating circular micropump and series of microvalves. The thin membrane is manipulated by a programmed application of compressed air and vacuum to emulate fluid injection phenomena between reaction chambers.

#### **2.2.2.2. Passive flow manipulation**

Passive micropumping techniques do not require external power source to be operated for subsequent fluid manipulation. They also require minimal user involvement, although with a trade off with better fluid flow control<sup>98</sup>. This feature makes them more suitable for incorporation into pathogen testing systems for application at POC. They have been widely reported for micropumping at POC for pathogen detection<sup>91,96,98</sup>. These passive techniques can be broadly divided into self-powered and human-powered flow manipulation techniques.

##### **a) Self-powered flow manipulation**

###### **i) Micropumping utilizing capillary force**

Capillary-driven fluid flow is based on capillary action that eliminates the need for external pumps for flow manipulation. At microscales, the surface tension at the fluid-channel interface engenders capillary flow, overcoming the viscosity of the liquid and the gravity<sup>110</sup>. This flow is defined by the microchannel's geometry and surface properties<sup>110</sup>. Previously capillary flow assisted technologies were reported for colorimetric detection of pathogen using NAAT utilizing either porous material (ex. Paper, polyester and wool) or solid materials (ex. PDMS, glass and silicon)<sup>111,112</sup>. The microfluidic platforms employing porous material for carrying out detection assay are called lateral flow assay (LFA) setup. LFAs have been the preferred platform for colorimetric NAAT assays<sup>113</sup>. These works leveraged capillary microfluidics to simplify one or several steps of a NAAT assay.

To simplify and reduce use of auxiliary components for nucleic acid extraction, amplification and detection, Fu et al.<sup>114</sup> presented a facile capillary-based setup for polymerase chain reaction (PCR). They presented surface modified silicon dioxide capillary fluidics to extract nucleic acid and perform amplification with eternal micro-pumps. On the other hand, by far, porous material-based microfluidics (especially paper substrates) are the most popular for colorimetric readout based NAAT. They have been extensively reviewed in the past<sup>115</sup>. One key highlight is the ability to integrate passive capillary fluid pumping with conventional microfluidics to form hybrid systems<sup>115</sup>. In a study by Lafleur et al.<sup>116</sup>, they for the first time demonstrated fully integrated paper microfluidic setup for multiplexed colorimetric detection of bacterial pathogen. They present a two-dimensional paper network lateral flow assay (LFA) without any requirement of auxiliary units for fluid manipulation involved in sequential assay steps. Several integrated paper microfluidic devices have been proposed in recent years for nucleic acid-based pathogen detection<sup>43,117-120</sup>, where the underlying principle is the capillary forces controlled with up-and-coming technologies including multidimensional paper networks, and control of capillary wicking rates<sup>93,117</sup>.

#### ii) Air transfer-based flow manipulation

Flow manipulation based on air transfer is based on the incorporation of materials capable of air transfer through either (i). solubility of air from microchannels to porous materials generating a pressure gradient, or (ii) permeability of air from high pressure to low pressure regions within the chip<sup>79,121,122</sup>. These underlying operation principles make them self-powered and suitable for POC applications. However, solubility-based flow manipulation lacks from better control over fluid flow, whereas permeability-based manipulation offer better control over the flow parameters by adjusting the material properties<sup>98</sup>. Previously NAAT platforms driven by air transfer-based pumping were reported for pathogen detection<sup>123-126</sup>. In a recent work, Yeh et al.<sup>127</sup> reported a self-powered microfluidic platform for LAMP assisted detection

of methicillin-resistant *Staphylococcus aureus* DNA. In brief, the fluid pumping is achieved by using a vacuum battery with flow regulated by thin PDMS walls in the vacuum lungs. This results in a more uniform pressure gradients compared to solubility based degas pumping where air flows through bulky PDMS.

### **b) Human-powered flow manipulation**

This category of fluid flow manipulation relies on the generation of pressure gradient in the microchannels via a manual operation by the user. The underlying physical phenomena relies on engendering fluid flow upon simple actuation by the user. In the context of POC diagnostics, two major fluid operations- centrifugation and pumping- were reported as portable and easy to use systems<sup>88,128</sup>. These fluid operations served as tools for one or more steps of the NAAT assay. Hand-powered centrifugation systems were developed for POC detection of infectious pathogen<sup>129-132</sup>. In a recent work, Michael et al.<sup>131</sup> reported hand powered fidget spinner based colorimetric detection of bacterial pathogen. The rotational movement of the fidget spinner engenders centrifugal force that is utilized for sample enrichment via entrapment in a nitrocellulose membrane. The end point is detected by a color change of commercial detection kit from colorless to red.

On the other hand, hand-powered pumping was demonstrated either by a deformable elastomeric chamber<sup>133,134</sup> or solid piston actuation<sup>135</sup>. The former method i.e., use of deformable elastomeric chambers was widely explored for range of POC diagnostic applications<sup>133,136-140</sup>. Specifically, there is growing interest in applying this technology for colorimetric NAAT assay<sup>141</sup>, owing to the assay's sequential nature. In a recent study Choi et al.<sup>142</sup>, proposed a microfluidic device with finger-actuation driven pumping for LAMP based colorimetric detection of *E. coli* in lysate samples. In brief, they reported cylindrical shaped PDMS based actuators for pumping the liquid across different chambers for nucleic acid

extraction, amplification, and detection. They also incorporate a unidirectional valve between chambers to avoid backflow, upon finger release. In a bid to further increase the functionality of this elastomeric chamber-based finger actuation, Deng et al.<sup>87</sup> designed an integrated microfluidic device for LAMP based colorimetric detection of SARS-CoV-2. Their system consists of complex network of actuation chambers and valves, with the former actuated using a finger and the latter actuated by a screw (ultimately manipulated by external user). In these elastomeric chamber systems, the relationship between pressure applied and the deformation of the chambers is directly related to the volume of fluid pumped. Previous studies have established a theoretical relationship between deformation of the chamber and the pressure loading<sup>143</sup>. The volume of the chamber (spherical in most cases) is given by<sup>144</sup>,

$$V = \frac{\pi f}{6} (3r^2 + f^2) \tag{1}$$

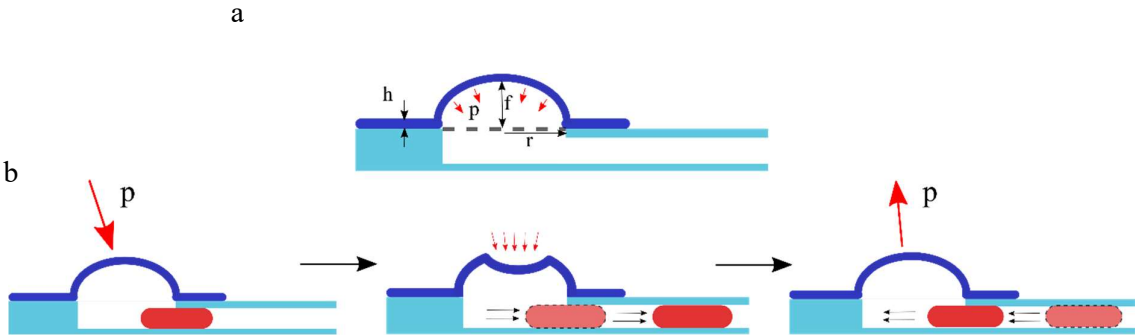


**Fig. 1.1. Suction cup parameters.** (a) Image depicting the important parameters of the elastomeric chambers that define the flow characteristics. (b). Short graphical depiction of the fluid flow. The droplet (shown in red) moves bidirectionally in the microfluidic channels (shown in light blue) upon the actuation of the suction cup (shown in navy blue).

Here,  $V$  is the volume of the chamber (at a chamber radius  $r$ ) at deflection,  $f$ . The deflection,  $f$ , is modeled theoretically via solid mechanics theory considering the system to be circular, reservoir bound elastic<sup>144</sup>. The deflection is therefore modelled as a function of loading pressure, chamber materials properties and the geometry,

$$f = \left( \frac{3r^4}{16Eh^3} \right) (1 - \nu^2)p, \quad \text{for } f \leq h \quad (2)$$

$$f = \left( \frac{3r^4(1-\nu)}{8Eh^4} \right)^{1/3} hp^{1/3}, \quad \text{for } f > h \quad (3)$$

Here  $E$  is the elastic modulus of the chamber material,  $h$  is the chamber membrane thickness,  $\nu$  is the Poisson's ratio and  $p$  is the loading pressure. The elastomer used to fabricate these actuation chambers is silicone based in most of the cases. Hence the Poisson's ratio becomes 0.5 for this case. These equations hold valid for chambers where size ( $r$ ) is greater than the membrane thickness ( $h$ ). As observed from equations (2) and (3), the deflection is linear in the regime where  $f \leq h$  and non-linear in the regime  $f \geq h$ .

In the recent years, with the advent of additive manufacturing techniques, 3D printing is being explored for developing innovative microfluidic flow manipulation systems, ultimately making POC testing systems more affordable and user-friendly<sup>145,146</sup>. In one of the first demonstrations, Begolo et al.<sup>147</sup> reported a 3D printed setup that pumps liquid in microchannels using a locking lid that helps compress or decompress air above the liquid. In a different iteration of similar concept, Chan et al.<sup>148</sup> proposed a 3D printed microfluidic device for colorimetric detection of urinary protein. One of core ideas for the fluid manipulation involves a torque actuated pump that works on the principle of air compression and decompression using a piston like setup.

### **2.2.3. Signal transduction**

Colorimetric readout assisted detection assays carry with them several advantages like high sensitivity, ease of analysis and interpretation, minimal training requirements, and affordability<sup>149–152</sup>. However, they lack from inaccuracies in interpretation from user to user owing to influence of ambient light and variability of vision quality for each individual color interpreter<sup>149</sup>. Employing a standardized imaging setup to record the colorimetric signal will help address these inaccuracies. Another major advantage to using a computerized imaging setup is the ability to analyze the signal quantitatively and temporally for multiple pathogens<sup>153</sup>. Employing a smart unionized imaging setup would also ease the process of data collection and subsequent analysis. Several setups were reported in the past aiming at optical imaging of microfluidic setups. Specifically, the work in this thesis necessitates an imaging setup for opaque substrate, in other words, it necessitates an epi-illumination imaging modality. There are three important components encompassing a setup targeted for imaging microfluidics setup, (i) Illumination system, (ii) Imaging optics, (ii) data acquisition and interpretation.

Illumination is a crucial component that ultimately effects the optical characteristics of the image ultimately recorded. Hence it of utmost importance to identify the properties of incident light that are most crucial to imaging the target substrate. Hence, before discussing the different imaging modalities reported in the past, it is important to discuss the influence of incident light on the plasmonic nanostructures employed in this work.

#### **2.2.3.1. Influence of incident illumination on plasmonic nanostructures**

In the recent years, plasmonic nanostructures are being widely reported as color printing alternatives to dye-based colorants<sup>154</sup>. The underlying phenomena of color generation relies on the interactions of light with metallic surfaces micropatterned at sub-diffraction limit scales<sup>155</sup>. More specifically, the surface plasmon resonance (SPR) can be utilized to trap optical

excitation and eventually manipulate the optical properties of light<sup>154</sup>. These properties of SPR were employed to generate colors using plasmonic nanostructures<sup>156,157</sup>. The SPR and the subsequent optical response is strongly influenced by the size, arrangement, periodicity and the material utilized<sup>158</sup>. In addition to this, the optical response is also affected by the properties of the incident light. Previous studies reported the influence of angle, polarization and uniformity of incident light on the engendered optical response, more specifically the color<sup>156,159</sup>. This dependency on angle and uniformity was prominently shown in patterned surfaces incorporating gold<sup>160</sup>, silver and aluminum<sup>161</sup> as plasmonic substrates. In a recent work by Wang et al.<sup>158</sup>, silver-insulator-aluminum oxide sandwiched nano disks were employed for color generation of entire gamut. The work reported the dependency of reflection and transmission spectra on the angle of incident light between the angles 15<sup>0</sup>-85<sup>0</sup> with the normal. Moreover, a commercial brightfield microscope with halogen lamp was employed to image the platform. These properties point out to the inherent necessity to employ controlled illumination for optimally viewing/imaging of these plasmonic nanostructured platforms.

### **2.2.3.2. Imaging setups for POC applications**

Accurate interpretation of colorimetric readout is crucial for prompt diagnosis of pathogens. This becomes more important in POC and low resource settings where there is dearth of specialized equipment and trained personnel. Moreover, an automated signal transduction and analysis system would be necessary for quantitative detection of the pathogen. In majority of the works in the past, colorimetric readout was packed in the form of an LFA<sup>153,162,163</sup>. Several imaging modalities were reported for capturing the color change in the detection window in microfluidic channels or the reaction bands on the lateral flow assay test strips<sup>164-166</sup>. Furthermore, with the ubiquity of smartphones and open-source hardware, portable and handheld imaging setups were proposed<sup>167</sup>. In a recent work Jung et al.<sup>168</sup> reported a smartphone based imaging of a lateral flow strip for semi-quantitative detection of *E.coli*

O157:H7. The compact imaging setup illuminated the LFA strip by a LED-diffuser system and is imaged using a plano-convex lens that projects the image on the camera lens of the smartphone. Similar technologies were applied for molecular testing of pathogens. Nguyen et al.<sup>162</sup> recently reported a smartphone-based analyzer for LAMP based colorimetric detection of pathogen. The end point color change is captured by a smartphone fitted with a 3D printed attached with an on-chip illumination LED and a macro lens that projects the detection chamber's image on the in-built lens of the smartphone. Furthermore, the inherent capability of smartphone was also leveraged to transmit and/or analyze the data recorded<sup>169,170</sup>.

**Table 1.1.** Brief survey on integrated microfluidic approaches for NAAT based detection pathogens with a colorimetric readout.

Pathogen	Detection assay	Sample processed	On-chip Sample lysis	On-chip reagent storage	Flow control mechanism	Time for detection	Reference
Influenza A (H1N1)	RT-LAMP assisted color change of pH sensitive hydroxynaphthol blue dye	Diluted lab provided samples	Chemical lysis	Liquid reagents stored on-chip	Passive capillary flow controlled by hydrophobic soft valves.	40 min	Ma 2019 <sup>72</sup>
Zika Virus	RT-LAMP assisted color change of phenol red	Tap water, urine, plasma	NA	NA	Capillary flow in porous paper substrate	40 min	Kaarj 2018 <sup>171</sup>
SARS-CoV-2	Fluorescence analysis using EvaGreen intercalating dye	Nasopharyngeal swab	Thermal lysis at 95°C for 1 min	Liquid RT-LAMP reagents stored in syringe	Hand-powered active pumping	30 min	Ganguli 2020 <sup>172</sup>
<i>E. coli</i> O157:H7	LAMP assisted color change of phenol red	<i>E. coli</i> lysate samples	NA	Dehydrated LAMP reagents	Finger-actuated pumping mediated by PDMS valves	80 min	Choi 2021 <sup>142</sup>

SARS-CoV-2	LAMP assisted color change of phenol red	RNA spiked DI water	Thermal lysis at 95°C for 5 min	LAMP master mix stored as liquid	Finger actuated pressure chambers for pumping and torque actuated valves	35 min	Deng 2021 <sup>87</sup>
Methicillin-resistant Staphylococcus aureus (MRSA)	Gold nanoparticle mediated color detection	Nasal swab	Thermal lysis at 95°C for 10 min	Lyophilized reagent storage	Capillary flow in 2D paper network with flow controlled by valve pad	30 min	Lafluer 2016 <sup>116</sup>
C. difficile and Enterovirus	Fluorogenic detection using PCR	Fecal samples	Chemical lysis	Liquid reagents	Active pumping using system of peristaltic pumps	60min	Kang 2017 <sup>77</sup>
SARS-CoV-2	RT-LAMP detection mediated by florescence intensity change	Swab samples spiked with viral particles	Chemical lysis with reagent stored on-chip	Liquid reagents	Centrifugal microfluidics	60min	Tian 2020 <sup>173</sup>
<i>Salmonella typhimurium</i>	Turbidity analysis of LAMP reaction.	Spiked samples and meat samples	Lysis buffer	Liquid reagents stored in a chamber	Active pumping using syringe pumps	90 min	Wang 2020 <sup>174</sup>
<i>Staphylococcus aureus</i> , <i>Salmonella</i> , Shigella, enterotoxigenic Escherichia coli, and Pseudomonas aeruginosa	Color change of LAMP mixture	Spiked samples and contaminated water	Mechanical lysis	Liquid reagent stored	Centrifugal system with flow controlled by rotation speed	70 min	Liu 2020 <sup>175</sup>
<i>Salmonella spp.</i> , <i>Staphylococcus aureus</i> , and <i>Escherichia coli</i> O157:H7	Color change of LAMP assay mediated by fuchsin	Bacteria spiked milk and juice samples	Chemical lysis	Dried reagents on paper disc	Capillary flow between porous paper discs	75 min	Trinh 2019 <sup>176</sup>

<i>Escherichia coli</i> O157:H7, <i>Salmonella typhimurium</i> and <i>Vibrio parahaemolyticus</i>	LAMP assay with color change mediated by Eriochrome Black T (EBT).	Extracted genomic DNA and cultured bacterial cells.	NA	Air dried reagents	Centrifugal microfluidic system with flow controlled by capillary valves	60 min	Seo 2017 <sup>177</sup>
Influenza A (InFA, H1N1) and <i>MRSA</i>	LAMP assisted change of Hydroxynaphthol blue (HNB)	Sample spiked with pathogen	Chemical lysis	Liquid reagents preloaded into the chamber	Passive capillary flow controlled by hydrophobic soft valves	<40min	Ma 2019 <sup>72</sup>

### **3. Additive Manufacturing Leveraged Microfluidic Setup for Sample to Answer Nucleic Acid-based Detection of Pathogens**

Sripadh Guptha Yedire<sup>1</sup>, Imman Isaac Hosseini<sup>1</sup>, Tamer AbdelFatah<sup>1</sup>, Sara Mahshid<sup>1</sup>

<sup>1</sup> Department of Bioengineering, McGill University, Montréal, QC, H3A 0C3, Canada

#### **3.1. Abstract**

Colorimetric readout for detection of infectious diseases is gaining traction at the point of care/need owing to its ease of analysis and interpretation; minimal training requirements; and ease of integration with highly specific Loop mediated amplification (LAMP) assay. However, the colorimetric readout coupled LAMP assay is rife with challenges impeding its potential application at the point of care/need. Major challenges include, (i) the requirement of a brightfield microscope for recording colorimetric change, (iii). Lack of quantitative assessment of the colorimetric readout signal, and (ii) user involvement in sequential steps of the LAMP assay. To address these challenges, in this work we propose an automated setup that encompasses an imaging module for signal capture and analysis; and a microfluidic module to automate the sequential steps in the LAMP assay. First, for imaging, we proposed a portable reflected-light imaging setup with controlled epi-illumination (PRICE). This setup offered better illumination with the maximum relative intensity varying only 17% while achieving a resolution of  $0.155\mu\text{m}/\text{pixel}$ . To automate different steps of the LAMP assay, a microfluidic cartridge that leverages technologies of suction cups and 3D printing was proposed to bring different steps of the LAMP assay onto a single platform. The mechanically actuated suction cups demonstrated pumping of fluid volumes down to  $0.1\ \mu\text{l}/\text{per } 30\text{degrees}$  rotation. The operation of the cartridge is automated/concerted by a control module concerted by Arduino UNO and Raspberry Pi microprocessors. The automated setup was able to demonstrate the

detection of viral nucleic acid in 15 minutes at a clinically relevant load of  $8 \times 10^5$  RNA copies/ $\mu\text{L}$ .

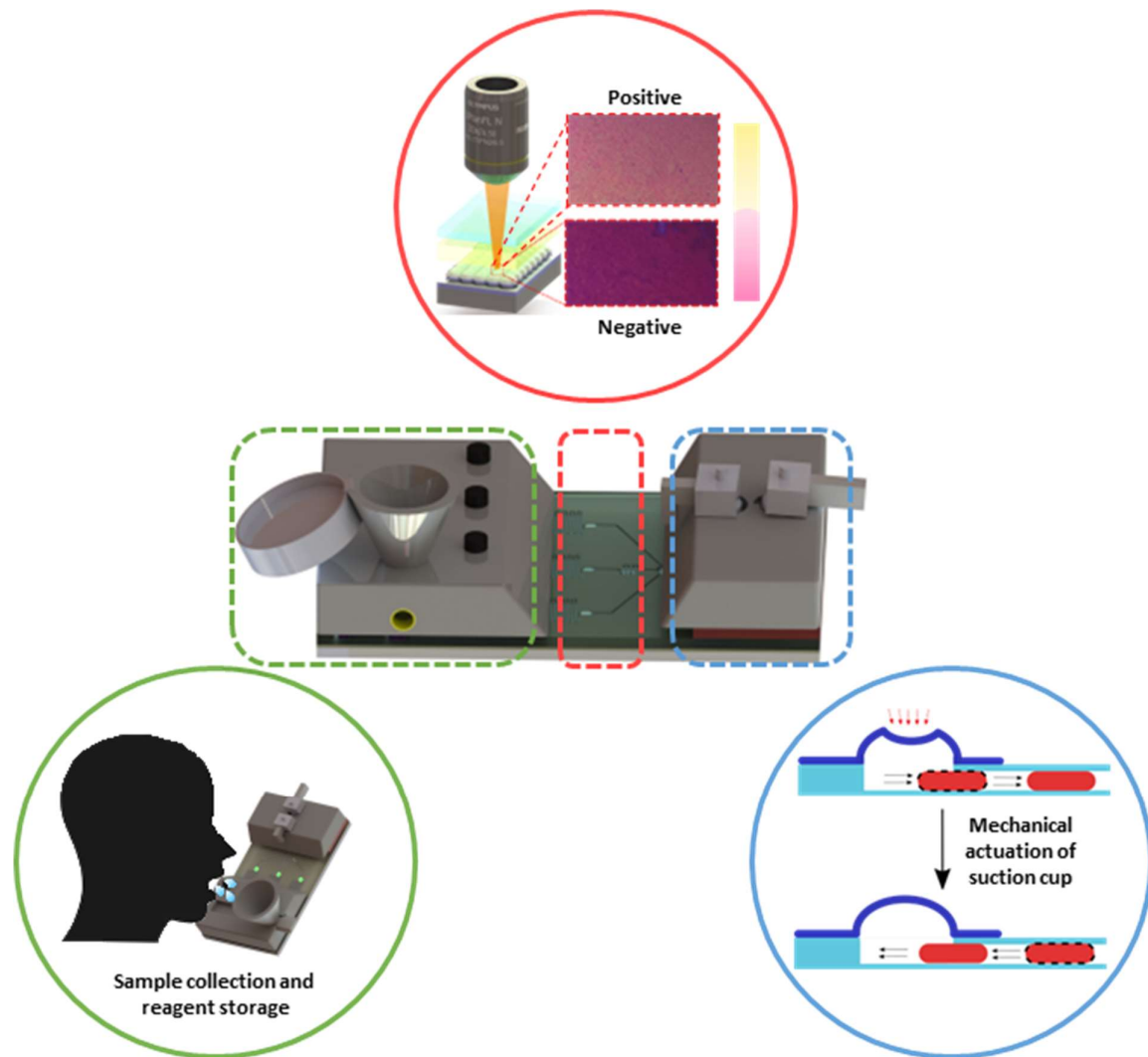


**Fig.3.1.** Experimental workflow of sample to answer microfluidic based system for pathogen detection

## 3.2. Introduction

Colorimetric signal transduction technique has been extensively applied for the detection of biological analytes<sup>1,2</sup>. There has been increasing evidence on the suitability of colorimetric readout techniques for pathogen detection at the point of care<sup>3,4</sup>. This can majorly be attributed to key features of colorimetric readouts, like high sensitivity, ease of analysis and interpretation, minimal training requirements, and affordability<sup>5-9</sup>. However, one of the major drawbacks with colorimetric readout systems is the challenge with the interpretation of results, the major reason being variability of vision from user to user leading to misinterpretation and/or requiring sophisticated instrumentation like a brightfield microscope<sup>10</sup>. To offset these drawbacks, recently, there is an increasing work on portable imaging setups for interpreting the colorimetric readout with smartphones and open-source technologies at the core of automation and data transmission units<sup>8,11-18</sup>. Implementing smartphone and open-source technologies, allowed miniaturization and eased the process of data collection and analysis<sup>19,20</sup>. This is only complemented by an increasing trend in accessibility and affordability of open-source technologies and smartphones<sup>21</sup>. Most of the previously reported imaging setups were designed for assays where the color change is driven by the assay and imaging setups acted as a proxy to the human eye to either reduce user-to-user variability, facilitate quantification and/or enable automation<sup>8,22-24</sup>. In the current work we employ, QolorEX, a platform that offers rapid sensing of colorimetric assay via plasmonic excitation<sup>25</sup>. This opaque metallic nanostructured plasmonic platform is sensitive to characteristics of incident light like intensity, spectral profile, uniformity, and the angle of incidence<sup>26,27</sup>. Hence the work necessitates an epi-illumination imaging setup that offers better control over illumination and imaging modalities. A broad range of colorimetric readout techniques have been combined with nucleic acid amplification assay for pathogen detection<sup>28,29</sup>. While polymerase chain reaction (PCR)

technique remains the gold standard technique, isothermal nucleic acid amplification techniques (NAAT), especially Loop-mediated isothermal amplification (LAMP) has gained traction. Several advantages of LAMP include a requirement for constant temperature for amplification<sup>30</sup>, higher specificity and sensitivity compared to conventional methods<sup>31</sup>, and stability against some amplification inhibitors<sup>32</sup>. Among different colorimetric techniques, naked-eye/dye-based readouts are suitable for integration with LAMP<sup>33,34</sup>. This technique also allows for easy integration with Lab on chip (LOC) platforms for point of care/need applications, as they require simple imaging setups allowing easy interpretation<sup>33,35,36</sup>.

A major feature of a point of care/need diagnostic system is the ability to integrate of all the discreet assay steps in a fashion more suitable for point of care/need settings<sup>37</sup>. In the case of nucleic acid amplification assays, these steps are sample collection, sample processing, reagent mixing, amplification reaction, and detection sub-steps<sup>38</sup>. In addition to this, the sequential nature of a typical RT-LAMP assay, i.e pathogen lysis, metering of sample and reagents followed by controlled heating for amplification<sup>39</sup>, necessitate not only precise but also a facile setup for the end user in a point of care/need setting. To address these broad needs, microfluidic setups could help implement techniques that allow metering and precise control of fluids and heat transfer, onto a single platform<sup>40-42</sup>. Microfluidic systems have been crucial in designing point of care/need pathogen detection platforms in the past<sup>43</sup>. Moreover, confined reaction volumes allow for fast and high throughput analysis, and enhanced heat transfer<sup>41,44,45</sup>. Although, previous research on colorimetric readout-based pathogen detection platforms utilized microfluidic setups to integrate major assay sub-steps i.e., sample collection, sample processing, reagent mixing, amplification reaction, and detection, they often involve user involvement in one or more of these sub-steps, especially in sample collection, sample preprocessing, and/or fluid manipulation steps.

Another significant feature of microfluidic setups is their conductivity to incorporate auxiliary components that could help reduce user involvement while achieving features suitable for point of care settings<sup>46,47</sup>. Specifically, there has been growing interest in leveraging additive manufacturing techniques to fabricate auxiliary components that could offset the need for expensive equipment and/or trained personnel<sup>48,49</sup>. Previous works used 3D printing (a type of additive manufacturing technique) and open-source hardware to bring multiple steps of colorimetric detection assay onto a single platform<sup>46,50-52</sup>. For colorimetric detection assays, in both 3D printing leveraged and conventional integrated microfluidic systems alike, most of them lack from requiring user involvement and/or off-chip processing in one or more of the sequential assay steps, especially in sample collection, sample preprocessing, and/or fluid manipulation steps<sup>53,54</sup>. For example, Tian et al.<sup>55</sup> reported an integrated and automated centrifugal microfluidic device for fluorescence-based RT-LAMP assay for viral pathogens. The system integrates multiple assay steps including lysis, amplification, and fluorescence detection steps into an automated setup. However, there are some drawbacks with sample collection requiring a swab, employing relatively complex fabrication and automation procedures, and using a commercial computer. Consumer 3D printing techniques also bring with them advantages like rapid and repeated prototyping, and cost-effectiveness<sup>52,56</sup>.

In this work, we implement a phenol red assisted colorimetric readout technique for the end-point detection of a RT-LAMP assay for SARS-CoV-2. We employ QolorEX<sup>25</sup>, the pathogen detection platform we previously reported<sup>25</sup>. To automate the process the LAMP assay and colorimetric signal detection, an automated setup (Fig.3.2) was proposed with three modules, (i). Imaging module (Fig.3.2(d)), (ii). An additively manufactured microfluidic cartridge (Fig.3.2(c)), (iii). An automation control unit (Fig.3.2(b&e)). The imaging module is majorly comprised of a portable reflected-light imaging setup with controlled epi-illumination (PRICE), to image the assay liquid over the nanostructure assisted (QolorEX) detection

window. Assay droplet imaged on QolorEX enabled the detection of SARS-CoV-2 wild-type RNA at a concentration of  $8 \times 10^5$  RNA copies/ $\mu\text{L}$  within 15 minutes. We validated the assay with a Nikon Ni-U upright brightfield microscope and observed the detection within 15 minutes. With PRICE, we achieved a Field of view of  $298 \mu\text{m}$  at a resolution of  $0.155 \mu\text{m}/\text{pixel}$ . To achieve controlled illumination, we demonstrated a low-cost Koehler illumination modality. Furthermore, we demonstrated a 3D printing leveraged multiplexed microfluidic cartridge that in tandem with opensource electronics and software offers automation of sequential steps in a LAMP assay and subsequent data analysis with minimal user involvement.

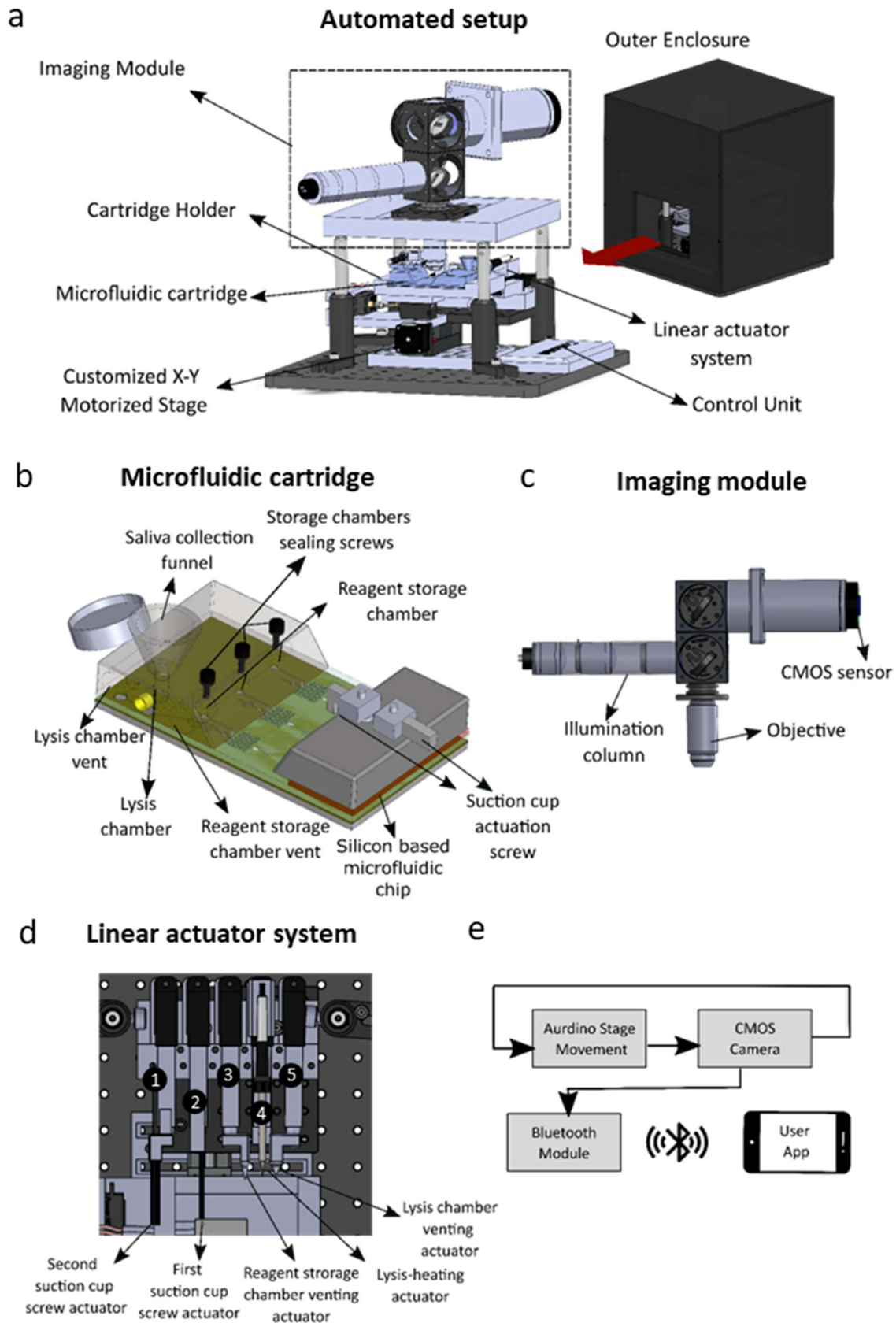


**Fig. 3.2. Schematic representation of major components in the automated setup for colorimetric point of care/need detection.** The automated setup comprises of two modules, (i) microfluidic cartridge; and (ii) imaging module. (a) Schematic of uncovered unit with labeled main components. This portable setup houses the imaging module; the cartridge holder mounted on an x-y translation stage for scanning the detection chambers; components of automation (linear actuators and heaters); and a central control unit housing the microcontrollers. The imaging setup is an epi-illumination setup deigned on reflected light microscopy principles. (b) The schematic representation of the microfluidic cartridge designed to aid in the automation the process of sequential steps in a LAMP assay, with the main components highlighted. (c) Different parts imaging module, including CMOS sensor, illumination column, and an objective. The image module is named- portable reflected-light imaging setup with controlled epi-illumination (PRICE). (d) Actuator system employed for the automation of the cartridge. Each actuator carries out a specific function, actuators 1 and 3 hosts a sharp tip for rupturing the membranes; actuators 2 holds a solder tip for supplying heat for lysis; Actuators 4 and 5 are required for actuation of the suction cups. (e) Block diagram of overall steps of colorimetric imaging using the automated setup. After amplification, the first image will be captured by CMOS camera. Then by moving the customized x-y motorized stage, the detection platform is scanned, and images are captured. Simultaneously, each captured image will be sent to the android app via Bluetooth module. The automated setup contains imaging system, actuators for cartridge operation for amplification assay, centrally controlled by a microcontroller setup, which allows cross-communication between linear actuator system, heaters, and imaging module.

### **3.3. Experimental**

#### **3.3.1. Outline of operation**

The current pathogen detection system has three major steps (Fig.3.7), (i) sample collection from the user, (ii) amplification assay, and (iii) image capture and data analysis. In the first step, the user spits into the saliva collection funnel (Fig.3.2(b)) on the microfluidic cartridge until the saliva fills up to the specified level. The user then covers the saliva inlet by closing a sliding door above the inlet. Following this, the user opens the sliding door and places the microfluidic cartridge on a stage inside the imaging box (Fig.3.2(a)). The user then connects to the system via a mobile application and starts the system. A concerted effort between different components inside the box will facilitate all the key assay steps namely, (a) sample lysis, (b) mixing with amplification reagents, (c) heating for amplification reaction. Once the assay is completed, the colorimetric endpoint is imaged, and data is analyzed. The results are then transmitted to the user's mobile application (Fig.3.2(e)).

#### **3.3.2. Optical train setup**

The portable reflected-light imaging setup with controlled epi-illumination (PRICE) has two main important modules, (i). illumination module and (ii). image capture module (Fig.3.2©). To implement the illumination module, we mimicked a Koehler illumination<sup>57</sup> optical train with off-the-shelf optics. A 5000K 90CRI LUXEON LED (Lumileds Inc.) was used as the primary illumination source. To collimate the LED, a diffusive aspheric condenser lens (d= 25.4mm, f= 20.1mm, Thorlabs) was used. A ring-actuated iris diaphragm (Thorlabs) was used as a field diaphragm with aperture diameters ranging from 8mm (minimum aperture opening) to 12mm (maximum aperture opening). The collimated light is then illuminated on the back of an achromatic doublet lens (d= 25.4mm, f= 30mm, Thorlabs), creating an imaging at the focal length of the lens. A ring-actuated iris diaphragm (Thorlabs) was used as an aperture diaphragm

with aperture diameters ranging from 8mm (minimum aperture opening) to 12mm (maximum aperture opening). Finally, the image of the light at the aperture diaphragm is collimated by an achromatic doublet lens ( $d= 25.4\text{mm}$ ,  $f= 30\text{mm}$ , Thorlabs). The collimated light is then projected onto the back aperture of the objective (TU Plan Fluor EPI 20x, N.A. 0.45, W.D. 4.5mm, Nikon Inc.) via a beamsplitter (Reflectance: Transmittance- 30:70,  $d= 25.4\text{mm}$ , Thorlabs) placed at an angle of 45degrees with the vertical. The reflected light from the sample placed the working distance is collected by the objective. Since the objective is infinity focused, a condenser lens (tube lens,  $f=200\text{mm}$ ) was used to project the image onto the CMOS sensor (Sony IMX477R, 12.3MP, Raspberry Pi Inc.).

### **3.3.3. Fabrication of the microfluidic cartridge**

The microfluidic cartridge presented here has two major modules, (i). Cleanroom fabricated microfluidic chip and (ii). 3D printed fluid handling attachment (Fig. 3.3). Together these two modules enable the integration of sample collection, sample lysis, reagent mixing and amplification steps as a single platform. All the microfluidic chip and the cartridge components were designed using AutoCAD™ and SolidWorks software. The first step of the fabrication process is the patterning of the fluidic channels ( $400\mu\text{m}$  width and  $50\mu\text{m}$  thick) using UV photolithography process. A lithography mask was designed to pattern a  $50\mu\text{m}$  thick SU-8 layer (SU-8 2050, MicroChem Corp., MA, USA) (Fig.3.3a (2)) on a silicon substrate (Fig.3.3a (1)) via a straightforward lithography process. In the second step (Fig.3.3b), the color sensitive platform (Fig.3.3b (3)) was fabricated using a fabless nano-patterning technique. Briefly, a generic approach is used to develop a colloidal self-assembly monolayer (SAM) of nanoparticles at a water/air interface. Next, the resulting honey-comb structures are transferred to the Si Substrate. Subsequently, a ZnO thin film ( $120\text{nm}$ ) was deposited as a low dielectric constant back reflector. Last, a thin aluminum layer ( $10\text{nm}$ ) was deposited to provide a tunable localized surface plasmon resonance with a white background. Fig.3.3(b) (Inset) shows the

various materials involved in the fabrication of the color sensitive platform (Fig.3.3(b) (3)). In the next step, a thin polydimethylsiloxane-PDMS layer (10:1, PDMS SYLGARD 184 silicone elastomer, Dow Consumer Solutions, QC, Canada) was punched with holes at channel inlets. The punched PDMS layer was plasma treated for 40sec at maximum power (Harrick Plasma cleaner, PDC-32G (115V), 18W). This surface activated PDMS layer was bonded to the SU-8 fluidic layer to create closed microfluidic channels (Fig.3.3(c) (4)). Next, PDMS based suction cups layer was fabricated using SLA printed molds (Fig.S2). This suction cup layer was bonded to the fluidic-PDMS layer by plasma treatment for 40sec at maximum power (Fig.3.3(d) (5)). Finally, the Stereolithography (SLA) 3D printed cartridge (printed at 50 $\mu$ m resolution with the Form 3, Formlabs, USA) is bonded to the PDMS covered microfluidic chip using a double-sided tape conducive to plasma activated bonding<sup>58</sup> (treated at maximum power for 40sec and placed in 95<sup>0</sup>C for 90min) (Fig.3.3(e) (6&7) & Fig.3.3(f)). The figure (Fig.3.3(f)) shows the exploded view of the cartridge showing multiple components. The saliva slider (Fig.3.3(f) (8)) is used to seal off the inlet once the saliva is collected. The brass metal inserts (Fig.3.3(f) (9&10)) are employed for lysis of the sample. Small screws (Fig.3.3(f) (13)) are used to seal-off the inlets (in the printed cartridge) used for reagent loading. The components (Fig.3.3(f) (11&12)) are 3D printed screws to actuating the suction cups by applying a small lateral force during automation, resulting in negative pressure gradient and subsequent flow of liquid from the inlets.

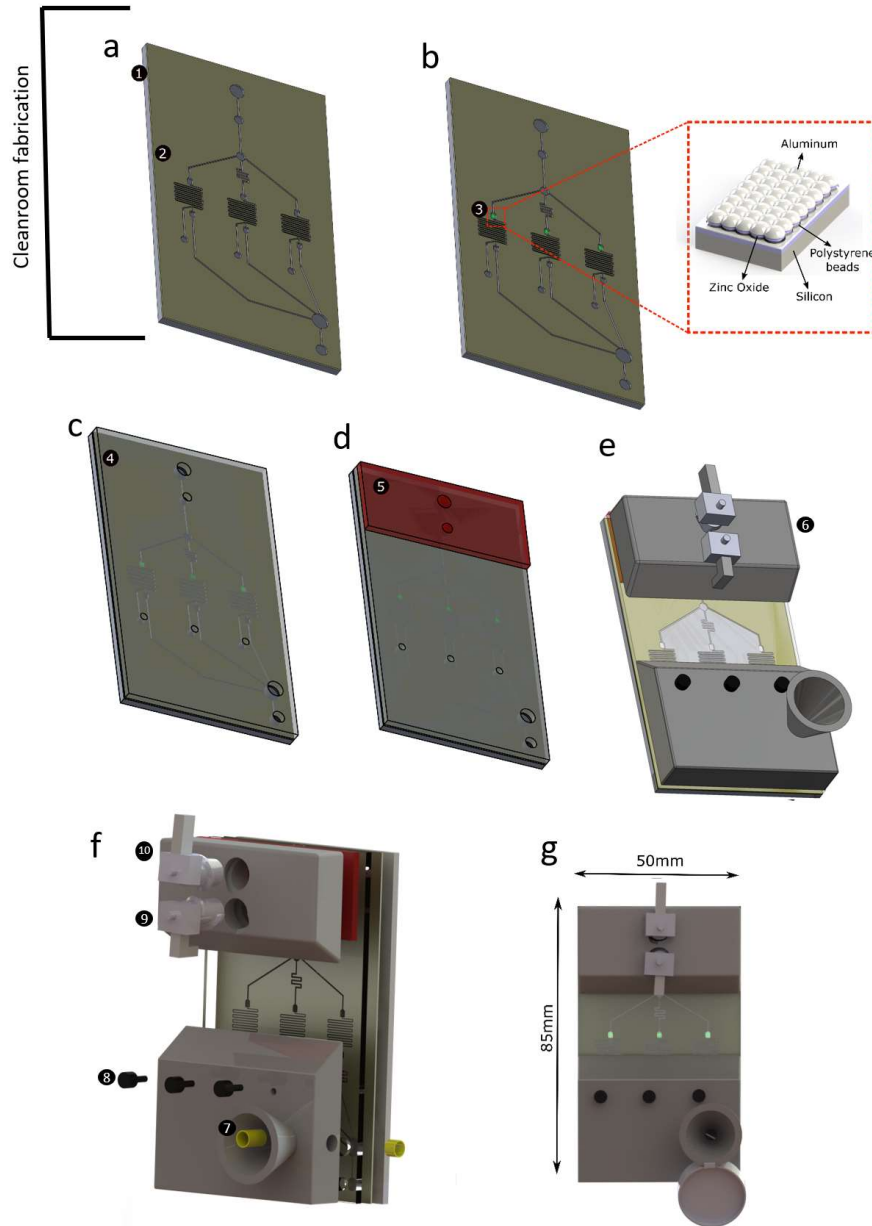


**Fig 3.3. Stepwise fabrication process of the fluid handling module** (a-b) The silicon based microfluidic chip was fabricated in a specialized cleanroom facility to pattern the SU-8 fluidic layer. (c-d) The fluidic channels are closed off with a 10:1 PDMS layer with holes punched at the inlets. This is followed by plasma activated bonding of PDMS-based suction cups layer to the fluidic-PDMS layer. In the final step, the SLA 3D printed cartridge is bonded via plasma

activated double sided tape. (f) 3D exploded view of the multiple layers involved in fabrication of the fluid handling module. (g) Front view of the fluid handling module with dimensions shown.

### **3.3.4. Fabrication protocol for suction cups**

In this work we employed 3D printed molds for the fabrication of suction cups with PDMS. SolidWorks software was used to design the master mold. We employed high resolution SLA 3D printing (Form 3, Formlabs, USA) at a layer thickness of 25 $\mu$ m in the z-axis as per the company's specifications. The post-printing treatment included a wash in isopropyl alcohol (IPA) for 20min followed by drying and UV curing at 60<sup>0</sup>C for 20min. Once the curing is done, the supports are removed. The master mold had two components, male and female molds (Fig.S3). Before proceeding to pour PDMS for molding, the 3D printed parts were surface treated by established protocol<sup>59</sup> to avoid curing inhibition at the PDMS-mold interface<sup>60,61</sup>. In brief, the 3D printed master mold post curing is first heated at 130<sup>0</sup>C in oven for 4h, following by an air plasma treatment (Harrick Plasma cleaner, PDC-32G (115V), 18W) for 3 min. The molds are then treated with 10 $\mu$ l trichlorosilane (Sigma Aldrich) in a vacuum desiccator overnight. Finally, the PDMS-curing agent mixture in the ratio of 10:1 (PDMS to curing agent ratio), is poured into the female mold. The male mold fits tightly onto the female mold via the guides at the corners. The male mold has vertical openings to accommodate the overflow of excess PDMS upon insertion into the female mold (Fig.S3). The mold combination is then placed in the oven at 65<sup>0</sup>C overnight for curing.

### **3.3.5. Fabrication of 3D printed components**

All the 3D printed components are designed with SolidWorks software and fabricated using an SLA 3D printer (Form 3, Formlabs, USA) at a layer thickness of 50 $\mu$ m in the z-axis as per the company's specifications. The post-printing treatment included a wash in isopropyl alcohol

(IPA) for 20min followed by drying and UV curing at 60<sup>0</sup>C for 20min. Once the curing is done, the supports are removed. Following this, the collection funnel, lysis funnel, and reagent storage chambers housed in the 3D printed fluid handling attachment, are coated with Epoxy resin (Artresin, Canada) to make the surface biocompatible<sup>62</sup>. Finally, a hollow biocompatible aluminum insert (McMaster-Carr Inc, Canada) is incorporated into the 3D printed fluid handling attachment as the lysis chamber.

### **3.3.6. Electronic components of automation**

The automation module had three main components, (i) Linear actuator system, (ii) Heating module, (iii) x-y translation stage and (iv) Imaging and data processing module (Fig.3.2). Two main microcontrollers were used here, Arduino UNO (Arduino Inc.) and Raspberry Pi 4 (Raspberry Inc.). The Arduino was employed to control components (i), (ii), (iii), (iv) and the Raspberry Pi controlled the imaging and data processing module. Five linear actuators (Actuonix Inc.) were employed to facilitate sequential fluid handling steps (Fig.3.2(d)). This detection platform requires heating for the lysis and amplification steps of the assay, to facilitate this employed two heating components, a portable solder iron (TS-100) for saliva lysis and ceramic thermal heater (Bolsen Tech Inc.) for LAMP reaction at 65<sup>0</sup>C. The two heating elements are controlled with a two-channel relay module (Yizhet Inc.). As previously mentioned, here a multiplexed approach with three detection chambers was used. Hence it is essential to have a x-y translation stage to scan and image across multiple intra-chambers as well as inter-chamber regions. To realize this a linearly guided CNC stage that is driven by a stepper motor (FUYU Inc.) was employed for stage movement in x-direction, with a guide length of 50mm and a resolution of 0.25mm. To move the chip in y-direction we used a single axis manual translation stage (Edmund Optics Inc.) attached to a 3D printed holder that firms the microfluidic cartridge in place. The screw head of this y-axis translation component is controlled by a knob attached to a continuous servo (SPT digital, SPT5325LV). The image

once captured by the CMOS sensor is captured and analyzed on-board the Raspberry Pi 4. Finally, the results are transmitted and communicated via a mobile application created with MIT App inventor.

### **3.3.7. RT-LAMP assay**

The RT-LAMP assay employed in this work uses the primer set against the ORF1ab gene obtained from Sigma-Aldrich, USA. The individual oligonucleotide concentrations of the 10x primer mix were, 0.2  $\mu\text{mol/L}$  of forward outer primer, 1.6  $\mu\text{mol/L}$  of Forward inner primer and backward inner primer, 0.4  $\mu\text{mol/L}$  of forward loop primer and backward loop primer. The primer mix was mixed with WarmStart® Colorimetric LAMP 2X Master Mix (NewEngland Biolabs, MA, USA), and RNase free water (Thermo Fischer Scientific, MA, USA). The standard reaction volume is 20  $\mu\text{l}$  that consisted of 2  $\mu\text{l}$  10X primer mix, 10  $\mu\text{l}$  2X master mix, 7  $\mu\text{l}$  RNase free water, and 1  $\mu\text{l}$  synthetic SARS-CoV2 RNA (VR-3276SD ATCC, VA, USA) sample. The samples were incubated at 65°C for different periods to visualize color change versus time for different samples.

## **3.4. Results and discussion**

### **3.4.1. Optical setup development and characterization**

A portable reflected-light imaging setup with controlled epi-illumination (PRICE) was designed to capture the colorimetric change of the assay solution (Fig.3.4a). In the current scheme of SARS-CoV-2 detection, we employed QolorEX platform that enhanced the colorimetric change via plasmonic excitation. QolorEX is a nanostructured platform fabricated in cleanroom with deposition of multiple layers of metals<sup>25</sup>. This novel platform elicits structure and material dependent-color upon irradiance of white light, extensively studied in

the past and termed as plasmonic based coloring<sup>26,63</sup>. The mechanism of interference of these surfaces with the colorimetric assay is described in our previous<sup>25</sup>. These metallic surfaces are sensitive to illumination properties which could ultimately affect the colorimetric readout. Hence it was important to ensure to have a uniform, consistent, and controlled illumination and subsequently use PRICE as a replacement to a commercial brightfield microscope. The PRICE has two main modules (i). illumination module and (ii). imaging module.

### **3.4.1.1. Field of view and resolution characterization**

The optical train of the system as shown in Fig.3.4(a)(ii) is a combination of many different off-the-shelf optical components. The imaging module uses a 20x objective as the condensing lens with the detection platform placed at the focal plane of the objective Fig.3.4(a). The image of the detection platform is then focused onto the CMOS sensor using a tube lens of 200mm focal length. Since we intended to capture the color change on the detection platform, it is desirable to have a large field of view (FoV) while maintaining a high numerical aperture (determined by the objective). Using a tube lens of standard focal length (200mm) eliminated spherical and chromatic aberration while providing high FoV. A CMOS sensor with a diagonal length of 7.9mm was selected to maximize the FoV. Moreover, this combination of tube lens with the CMOS camera provided a digital magnification of 275x (calculated at a Field number (FN) of 22mm) since the CMOS only captures a part of the image created by the tube lens. The FoV and the resolution of the imaging module was characterized using a 1951 US Air Force (USAF) resolution target (Fig.3.4(b)). The system could resolve the lateral lines in Group 7 Element 6, which yields a resolution of 228lp/mm or 4.4 $\mu$ m. Subsequently the field of view is also determined across the entire area of CMOS as 298  $\mu$ m. The detection chamber size employed here approximately is, 1500  $\mu$ m in the lateral direction, hence this FoV 298  $\mu$ m would allow the complete imaging of the detection chamber in 3 scans of different inter-chamber regions while not losing crucial information.

### **3.4.1.2.Light source selection**

Source of illumination is an important property that can have predominant effect on the final color captured and observed<sup>63</sup>. The platform we employ in this work, QolorEX, was characterized using UV-Vis spectroscopy to obtain the resonance wavelength (Fig.S1). The 5000K LED employed for illumination has the spectral profile shown in Fig.S1. The two intensity peaks in the wavelength interval of ~430nm-500nm (narrower peak) and in the interval ~550nm-660nm (broader peak). Majority of the intensity falls in the ~430nm-500nm, which matched with the resonance wavelength of the platform. Color rendering index (CRI) is another important parameter and signifies the extent of closeness of colors revealed by the light source when compared with ideal lighting conditions<sup>64</sup>. The LED has a specified CRI of 90, making it an ideal candidate for illumination.

### **3.4.1.3.Illumination characterization**

Ensuring uniform illumination is crucial for capturing accurate colorimetric reading. Having a controlled illumination column would also facilitate more control over the illumination parameters, specifically area of illumination and the intensity of illumination. One key issue with achieving uniform illumination is the diverging angle of irradiance of an LED. The 5000K LED employed in this work has a total viewing angle (defined as the angle from the LED centerline after which the luminous intensity drops to half of the maximum) of 60°. Among different illumination methods employed in standard microscopes, Koehler illumination is widely adopted owing to its illumination uniformity<sup>65</sup>. Moreover, Koehler illumination setup is more resilient to external disturbances like dust and optical imperfections, making them suitable for imaging outside of controlled environments<sup>66</sup>. These features also facilitate minimal variations in the images obtained by the camera over long and repeated cycles<sup>66</sup>. Hence, a portable illumination column mimicking the Koehler setup would address the

challenges with controlled illumination. Although previous work reported a 4f setup for achieving Koehler illumination setup<sup>66</sup>, it was designed for benchtop educational purpose and lacked portability. Moreover, it was designed a setup aimed at trans-illumination that works only for imaging translucent samples. In the current work however, we require an epi-illumination since the detection chamber is opaque in nature (Fig 4c(i)). In brief we employ a 5000K 90CRI LED placed at the focal plane of an aspheric condenser with a diffuser. A diaphragm is placed after the aspheric lens that allows the control over the ‘area of illumination’ by controlling the radius of diaphragm aperture opening. The collimated light is then focused an achromatic lens that forms real image of the light source of a diaphragm placed at the focal length of the lens. The aperture opening of this diaphragm allows control over the ‘intensity of illumination’. In the final step, the real image comes out as a collimated beam of light after passing through another achromatic lens placed at the focal length. Different LED and optics setup for illumination were first compared visually (Fig. S1). It is evident from Fig. S1, visually, illumination column employed in PRICE (Fig.S1(b)(iv)) offers a more uniform spectral profile. This is further validated by examining the uniformity of illumination by placing an aluminum sample at the focal plane of the objective and analyzing the intensity values of the image (Fig.3c). The differences in intensity for the PRICE setup varied only 17% whereas the regular LED-diffuser lens setup with an aspheric diffuser varied 65% (Fig.3.4c(ii)).

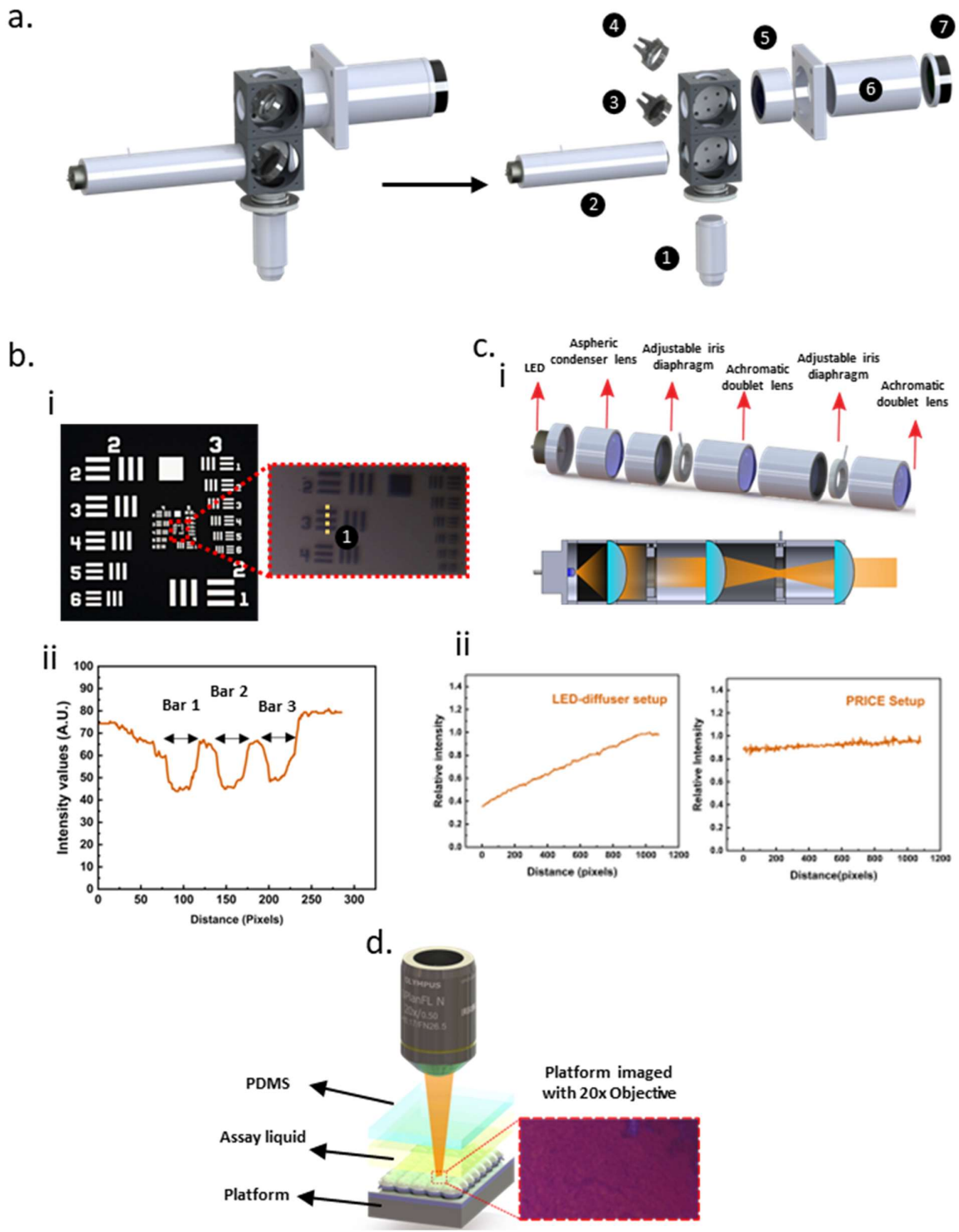


**Fig. 3.4. Characterization of the PRICE setup,** (a) Shows the exploded view of all the off-the-shelf optics involved in the setup. The components are number coded as follows, (1) 20x objective, (2) illumination column, (3) beam splitter, (4) Fully reflecting mirror, (5) Tube lens,

(6) (6) CMOS sensor. (b) The image shows the characterization of the imaging setup for obtaining the Field of View (FoV) using a UASF 1951 target. The bars horizontal bars in Group 6 Element 3 are clearly depicted in the intensity plot. Based the standardized calculation, we obtained the resolution for the system as  $4.4\mu\text{m}$  and a FoV of  $298\mu\text{m}$  in horizontal direction (c). The illumination column is characterized for uniformity of irradiation. (i) depicts various lenses and optics incorporated in the illumination column labelled. (ii). The relative intensity distribution is depicted for both the illumination setups, illumination column designed in this setup and for LED with no illumination modification. (d) The CAD depiction of imaging the detection platform placed at the focal plane of the objective and illuminated with the proposed illumination column.

### **3.4.2. Characterization of the microfluidic cartridge**

In this work we employ pressure driven flow induced by suction cups as the core technology to enable fluid flow with minimal user involvement. The key features of an amplification assay are, (a). discrete sequential steps involved in the assay, (b). Metering of fluids involved (sample and reagents). To expand, the sequential steps in a typical amplification assay are, (i) sample collection, (ii) sample lysis, (iii) mixing with amplification reagents (in a fixed volumetric ratio), (iv) amplification reaction, and (v) end point detection. In this work we leverage three key technologies to enable integration of all these sequential steps (Fig.3.5(a)) on to a single microfluidic cartridge, they are, (1) mechanically actuated suction cups, (2). microfabrication, (3). additive manufacturing. The suction cups facilitate power free, user less fluid flow manipulation via mechanically actuating with a 3D printed screw-nut like setup. Microfabricated silicon-based chip housed the channels and chambers required for mixing, amplification, and detection steps. Additive manufacturing (3D printing in our work) enabled fabrication of a 3D printed fluid handling module that is coupled with the silicon microchip. This fluid handling module houses sample collection, sample lysis, reagent storage and suction

cup actuation components. The components driven by these three technologies at the core are characterized in this section.

### **3.4.2.1.COMSOL simulation and discussion**

One of key technologies in the integration of all the assay steps onto a microfluidic cartridge is microfabrication. We employed SU-8 microchannels for enabling fluid handling. COMSOL simulation methods were employed for designing the microfluidic chip. One key requirement is the mixing of lysed saliva sample with the reagents in the volumetric ratio of 1:10. To execute this, a Y-junction mixing followed by a serpentine channel was used to ensure complete mixing. Sin area of cross section of all the channels is the same, the channel widths were manipulated to ensure a flow rate ratio of 1:10 Fig. (3.5a(iv)). The right combination of channel widths was arrived at by using 2D COMOL simulation, modeled at creeping flow conditions. The central idea is that the area of cross section of the channels is the same and the widths can be manipulated to change the overall volumetric flow rate (Fig.3.5(c)). The change of widths ultimately effects the distribution of the negative pressure produced by the suction release. Given the multiplexed nature of the proposed system the lysed sample should be distributed into the channels leading up to mixing module. Considering the design requirements for the automation, a pressure distribution simulation was performed to ensure uniform pressure distribution (Fig.S2(a)). In addition to this, the mixing module was simulated to ensure perfect mixing over the length of the serpentine (Fig.S2(b)). The microfluidic design showed rapid mixing when analysed for the lysed sample diffusion into the reagent inlet stream along the channel centerline shown in grey (Fig.S2(d)). This analysis resulted in a mixing length of at least 20mm to ensure full mixing (Fig.S2(c)). This short mixing length can be attributed to the mixing promoted by the serpentine channel with groovy walls (Fig.S2(d)).

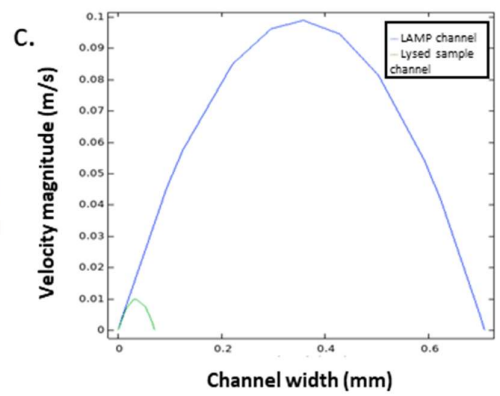
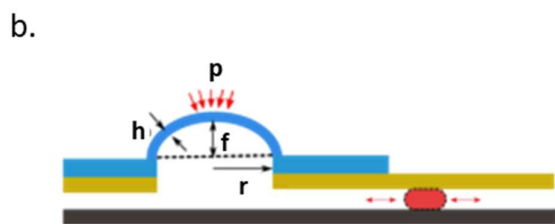
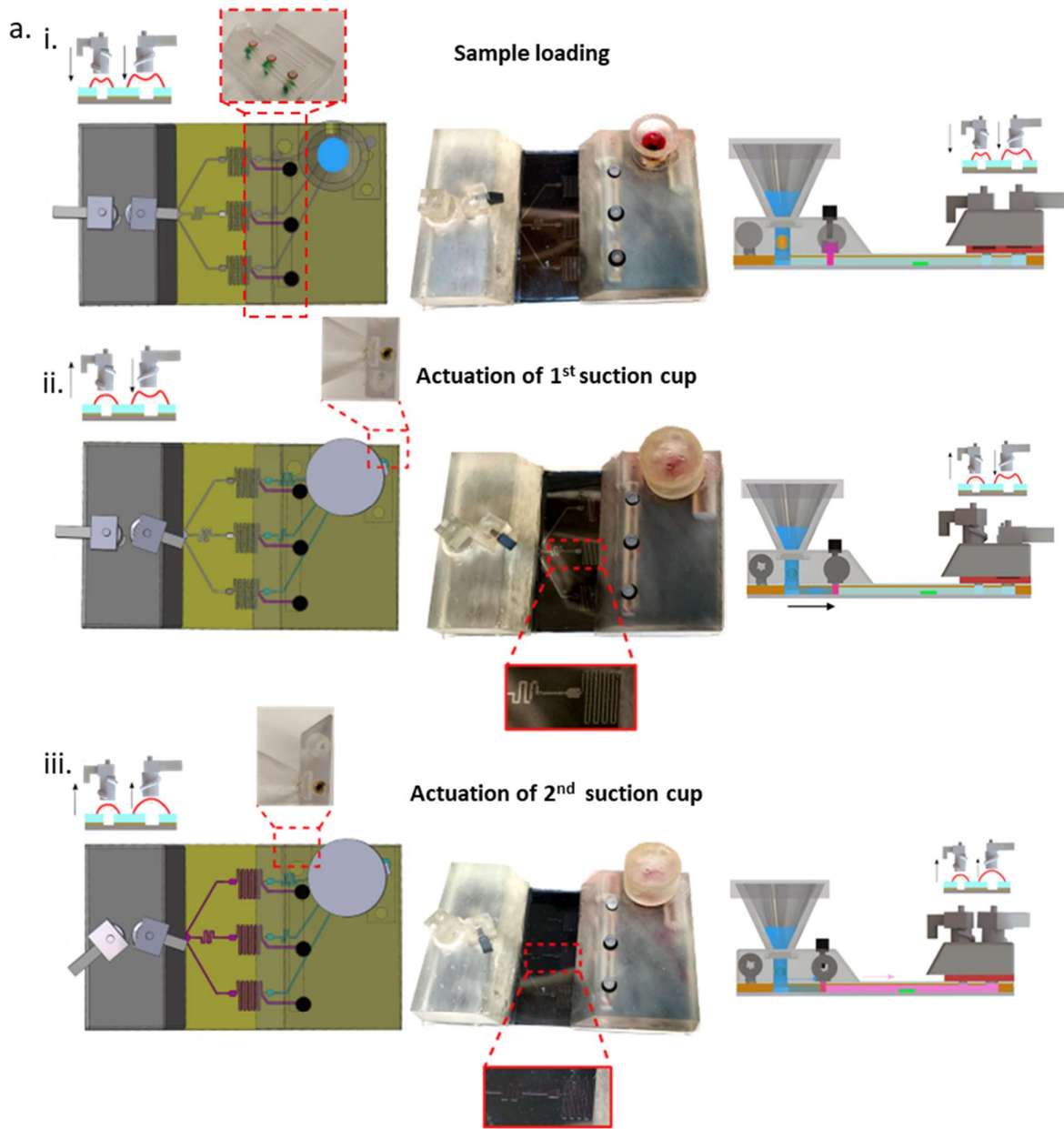


**Fig. 3.5. Overview of microfluidic cartridge operation.** (a). The overview of the steps involved in the operation of the cartridge are depicted a top view schematic (left hand side), top view real images (middle panel) and cross sectional view(on the right most side). (i) In the first step, the amplification reagents were loaded into the reagent storage chambers with the suction cups in pressed state and the saliva is collected in the funnel for lysis and the saliva inlet is sealed off with a tightly sealed lid, (ii) Once the lysis step is completed, the saliva channel is vented by breaking the membrane and the first suction cup is released from the compressed state, (iii) Once the saliva reaches the Y-junction of the mixing channel, second membrane is broken, exposing the reagent inlets to the atmosphere. The second suction cup is now released causing the lysed saliva and reagents to enter the mixing channel. (b) A schematic showing the various important parameters of the fabricated suction cup. (c). COMSOL study showing the surface velocity distribution at the reagent channel inlet cross section (shown in blue) and the lysed sample channel cross section (shown in green).

### **3.4.2.2.Suction cups characterization**

In this work, PDMS based suction cups were employed to drive the fluid flow with no user involvement or expensive external equipment (like syringe pump, peristaltic pump). The suction cups work on the principle of air displacement giving rise to a negative pressure in the microfluidic channels thereby inducing fluid flow along the pressure gradient<sup>67,68</sup>.

### **3.4.2.3.Characterization of volume suctioned**

The volume of liquid that can be moved/pumped by the suction cup is dependent on the volume of air displaced upon compression of the cup. Previous works that reported power-free micropumps, used finger for actuation of the pumps<sup>69-71</sup>. In this work we employed a mechanical actuation system with a nut and screw mechanism. In the context of fluid flow in

microchannels, it is important to employ suction cups that can precisely pump desired volumes. However, the mechanical actuation system is prone to having residual volume when the cup is pressed down<sup>72</sup>. Hence, correlating the experimental suction cup volume to the theoretical volume is important to account for the residual volume. Specifically, the affect of mechanical actuation in current system on the residual volume. Initially the cup is assumed to be a hemisphere, hence the initial volume ( $V_{in}$ ) is given by<sup>84</sup>,

$$V_{in} = \frac{\pi}{6} * d^2 * f_{max} \quad (1)$$

Here,  $d$  is the diameter of the suction cup and  $h$  is the central height of the hemisphere (Fig.3.5(b)). The suction cups were fabricated using SLA printed mold (Fig S3). In this work, the lysed saliva sample is suctioned to the mixing junction. A key design criterion is that the suction cup volume correlates to the volume of the fluid suctioned. The volume of microchannels up to this point was calculated to be 3.4  $\mu$ l. Following this, the lysed sample with amplification reagents at a ratio of 1:10. The volume of serpentine mixing channel and detection chambers cumulatively resulted in a volume of 8.3 $\mu$ l. Hence correlating the theoretical volume (actual volume) of the suction cup given by equation 1 should be correlated to volume of fluid suctioned with the mechanical actuation setup. The mechanical actuation of the suction cups is carried out using a 3D printed screw-nut system, which exerts a normal force of around 11N (Fig. S4(c)). Fig.3.6a(v) shows the correlation between the theoretical volume of the suction cup to the volume of the fluid suctioned when actuated with the 3D printed screw-nut system employed (Fig. S4(a&b)). It can be interpreted that the mechanical actuation effects the residual volume which in turn effects the empirical volume of fluid pumped. From (Fig.3.6a(v)) it is evident that the volume of fluid suctioned deviates from the theoretical volume, this can be attributed to the fact that there is residual volume when a mechanical actuation system with screw-nut type setup is used. It is also interesting to note

that the volume of the fluid suctioned follows a linear trend (Fig.3.6a(v)). The linear trend profile equation was used to accurately design the suction cups for the desired volumes.

### 3.4.2.4. Fluid flow control

We further built upon the effect of mechanical actuation on the volume of fluid suctioned. We hypothesized that the volume of fluid suctioned/pumped ( $V_p$ ) can be varied by manipulating the deflection of the PDMS membrane ( $f$ ) (Fig.3.5(b)). This volume,  $V_p$ , is controlled by the mechanical actuation of a screw and nut system (Fig. S4(c&d)). The central idea revolves around the concept that the volume,  $V_p$ , can be controlled via fine threaded screws mechanically pressing on the buttons. For each rotation, the screw moves a distance equivalent to the pitch which in turn manipulates the deflection of the suction membrane ( $f$ ). This is demonstrated in Fig.3.6(a)(i), where the screw head is rotated clockwise (CW) and counterclockwise (CCW) to pump fluid in and out of the channels in multiple cycles. The volume of the spherical suction cup is given by the equation<sup>73</sup>,

$$V = \frac{\pi f}{6} (3r^2 + f^2) \quad (2)$$

Where  $V$  is the volume stored by the suction cup,  $f$  is the deflection,  $r$  is the radius of the suction cup. The deflection  $f$  is in turn a function of applied pressure and for silicone polymer (Poisson's ratio of 0.5) is given by,

$$f = \left( \frac{9r^4}{64Eh^3} \right) p, \quad \text{for } f \leq h \quad (3)$$

$$f = \left( \frac{3r^4}{16Eh^4} \right)^{1/3} hp^{1/3}, \quad \text{for } f > h \quad (4)$$

Here  $E$  is the elastic modulus of the chamber material,  $h$  is the chamber PDMS membrane thickness, and  $p$  is the loading pressure. These equations hold true only when  $2r > h$ , which is

the case in our current work. From equations, (2), (3) and (4), it can be inferred that volume of the suction cup ( $v$ ) varies cubically with loading pressure ( $p$ ) in the  $f \leq h$  and varies non-linearly in the regime  $f > h$ . The experimental results stand correlate with the theoretical profile as in Fig.3.6(a)(ii). Specifically, we demonstrated the control of fluid flow with actuation varying in steps of  $30^\circ$  angle either CW or CCW. Different sizes of suction cups (Diameters ( $d$ )- 2mm, 7mm, 8mm and height( $h$ )- 1mm) were employed to demonstrate this controlled flow actuation, Fig.3.6(a)(ii). Given the pitch of the screw used is 1.4mm (distance moved by the screw in 1 full rotation), the volume suctioned plateaus after  $300^\circ$  of rotation.

The delta volume suctioned is given by first order differential of the equation (4), given by,

$$\frac{dV}{df} = \frac{\pi}{2}(r^2 + f^2) \quad (5)$$

This equation shows that change in suction cup volume (i.e volume of fluid suctioned), is in quadratic relationship with the deflection. The experimental results are in correlation with this as demonstrated in Fig.3.6(a)(iii), showing a parabolic profile. In other words, the angular control allows for precise manipulation of the fluid volume in the channel. By incorporating this screw-nut actuation system with a screw of pitch 1.4mm, we demonstrated pump of fluid volumes as low as  $0.1 \mu\text{l}$  (Fig.3.6(a)(iii)). This process of fluid pumping into the channel is found out to be in correlation with the fluid pumping out of the channel in one full cycle (Fig.3.6(a)(iv)). This precise and reliable manipulation of fluid could have potential implications for facile metering of fluid at very low volumes with minimal user training.

### **3.4.2.5.3D fluid handling attachment characterization**

The silicon based microfluidic chip is bonded to the 3D printed attachment (Fig.3.2) to facilitates automation of all the assay steps. More specifically, the 3D printed attachment houses sample collection, sample lysis, reagent storage and suction cup actuation components

(Fig.3.2). The sequential steps involved in the operation of the cartridge to carryout lysis and metered reagent mixing are described in Fig.3.5(a). One key technology driving this process is 3D printing, more specifically, high resolution, micron thick 3D printed membrane.

#### **3.4.2.5.1. 3D printed membrane characterization**

The sequential nature of the amplification assays requires the amplification reagents mixing with the sample only after the lysis. To facilitate this, the amplification reagents are stored on the cartridge in the storage chambers (Fig.3.5a(i)). The chambers are sealed off from atmospheric pressure, to impede the amplification reagents from entering the serpentine mixing channel before the flow of the lysed saliva to the y-shaped mixing junction. To realize this, we leveraged high resolution of SLA 3D printer to print membrane in the order of microns in thickness. This membrane upon breakage, causes the atmospheric venting leading to the flow of the reagents to the Y-junction and subsequent mixing with lysed sample (Fig.3.5). As we will discuss, in the final step of automation, this membrane breakage step is executed with a linear actuator with sharp tip. Hence the thickness of the membrane plays an important role, as the force required for breaking the membrane should be a value that can be executed by the tip of the linear actuator. Membranes were fabricated at different thicknesses starting from 100  $\mu\text{m}$  up to 600  $\mu\text{m}$  (Fig.S5). The membranes were then manually broken to evaluate the required force to inflict damage. We obtained that an average force of 6.26N (Fig.S5(b)) was required to break a 100  $\mu\text{m}$  thick membrane, which within the limit range of force inflicted by an average human's finger. Hence, we hypothesized that this thickness would be ideal for application in an automated setup, owing to the requirement of minimal force.

#### **3.4.2.6.Extent of mixing**

The extent of mixing module is evaluated by employing image analysis of images captured by a microscope (Fig.3.6(b)). The whole cartridge operation as shown in Fig.3.5(a), but with green

dyed water was used to simulate lysed saliva and non-dyed clear water was loaded into the reagent storage chambers as simulation fluid. Ultimately, it desired to have the lysed saliva and reagent mix the ratio of 1:10. In addition to this, mixing should be ensured to be perfect in the detection chamber, where the amplification is carried out and the colorimetric change is recorded. To ensure that the mixing occurs in the desired ratio, a PDMS replicate of the current microfluidic chip was used to capture the color of the final mixed liquid. Images of the detection chamber with the mixed liquid were captured. These images were then compared with images of the detection chamber taken when loaded with pre-mixed liquid (green dye to water in the ratio of 1:10) (Fig.3.6(b)). The green value of the RGB is same for mixed liquid in the detection chamber (G= 248) and the premixed liquid (G= 243). Whereas, the water filled channel have a green value of 183.

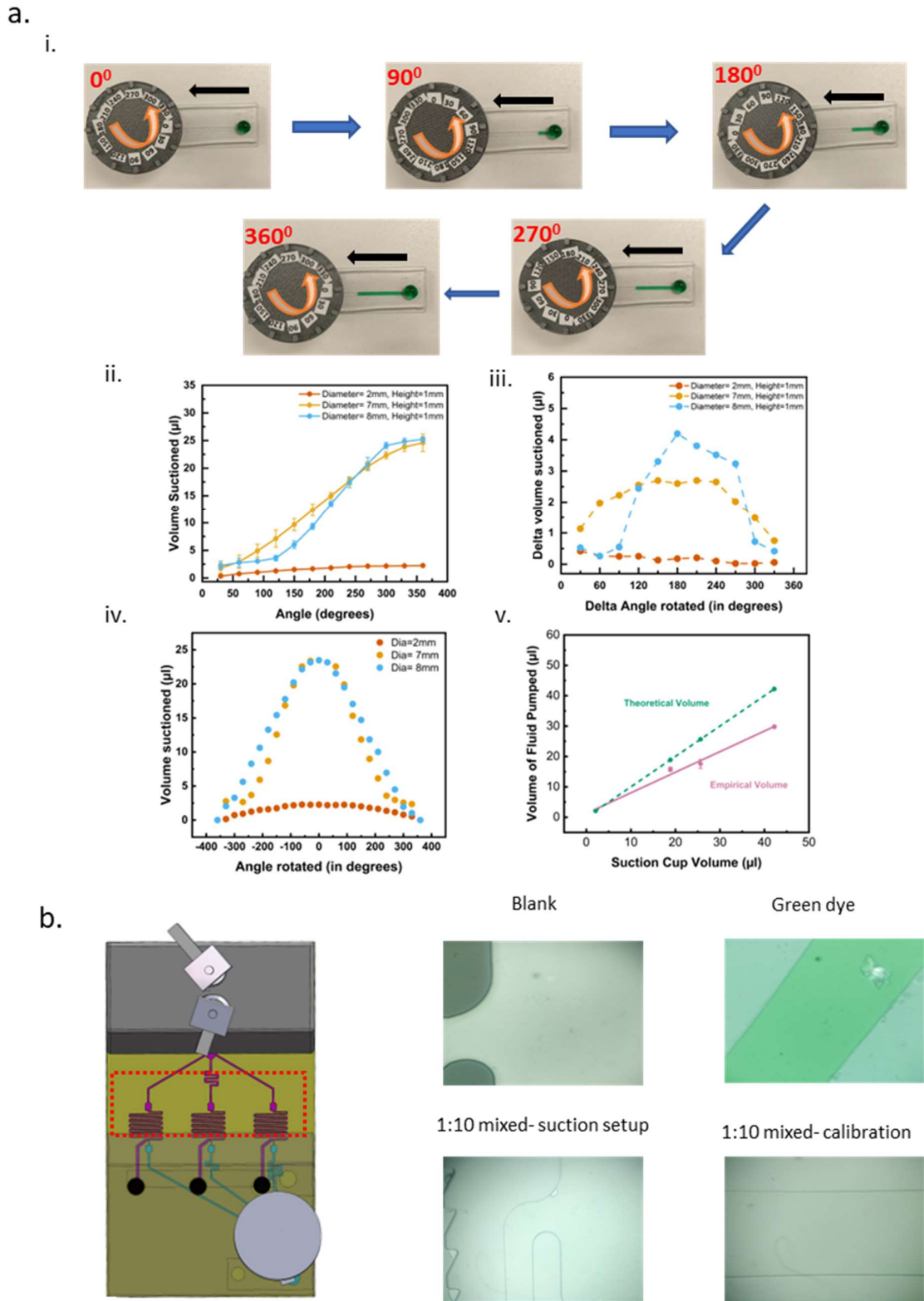


**Fig. 3.6. Characterization of components involved in fluidic module.** (a) Demonstration of various of aspects of fluid flow manipulation. (i) The fluid pumping is depicted by the

controlled mechanical actuation of the PDMS suction cup. The tip of the screw exerts a perpendicular force on the suction cup displacing/releasing the air underneath causing a pressure gradient conducive to fluid flow. The demonstration shows volumetric fluid metering based on the angle of the screw rotated in either CW or CCW directions. (ii) Graph characterizing the volume of fluid pumped in relation with the angle of the screw turned, for different sizes of suction cups. (iii) Characterization of minimum volume of fluid that can be manipulated for a set degree of screw rotation (here,  $30^{\circ}$ ). (iv) The precision of fluid volume pumped in one full cycle of pumping is demonstrated to be correlated. (v) The theoretical volume of suction cup is correlated to the empirically observed volume pumped with the 3D printed screw-nut system. (b) The channels were imaged to evaluate the extent of mixing with the microfluidic cartridge setup. The channel is imaged when there is no fluid (blank), filled with complete green dye. Then the detection chamber is imaged when cartridge is operated with saliva simulated with green dye and LAMP reagents simulated with water mixed in the ratio of 1:10. Finally images are captured with chamber filled with calibration liquid mixed in 1:10 ratio.

### **3.5. Design of automated setup**

For the successful application of the current setup at the point of need, it is necessary to integrate PRICE (imaging setup) and operation of the cartridge in an automated fashion. In first, as depicted in Fig.3.5(a), the operation of cartridge has sequential steps, with key steps that could require user involvement in absence of an automated setup. These key steps, include (i) breakage of the membrane, (ii) release of the suction cups (by twisting the screws holding them in place), (iii) heating for saliva and amplification steps. To automate these steps, a system of five linear actuators was employed (coded- A1, A2, A3, A4, A5) (Fig.3.2) controlled by an Arduino UNO microcontroller (Fig.S6). The actuators, A1 and A3 were attached with sharp

ended tips that assists with breakage of the membrane with a force of 6.2N. Actuators, A4 and A5 were fitted with cylindrical shaped tips to push the extension of the screw and actuate the suction cups (Fig.3.7(steps 4&6)). The linear actuator A2 was fitted with a portable pocket solder to carry out the sample lysis step (Fig.3.7(step 2)). It is desired to reach 95<sup>0</sup>C for 3min to complete the lysis process. The temperature is controlled from overshooting by employing cycles of linear movement of the actuators. The desired temperature was reached in under 1min as represented by infrared images in Fig.S7(a). For the carrying out the amplification reaction, it is desired to reach a temperature of 65<sup>0</sup>C for 15min, to execute this, a ceramic heater directly in contact with cartridge was employed. The temperature profile is achieved by employing a proportional–integral–derivative (PID) controller in conjunction with the ceramic heater (Fig.S7(b)). Additionally, to ensure loss of liquid due to evaporation engendered by the breaking of the membranes, the tips of actuators A1 and A3 were fitted with silicone O-rings to tightly seal the broken membrane area (Fig.3.7 (step 7)).

Once the amplification reaction was carried out for 15min, the colorimetric was desired to be captured by PRICE. The imaging setup is completely controlled by Raspberry Pi 4 microcontroller. The PRICE works in tandem with Arduino microcontroller to scan different chambers and different regions in the chambers. This movement is enabled by an X-Y translation stage directly controlled by the Arduino. For the X-translation, a CNC linear stage was employed. For the Y-translation a unique contraption involving a linear manual actuation stage and continuous servo motor. The linear stage moves in a single direction with rotation of a screwhead. This screwhead is attached to the rotating shaft of the servo motor via a 3D printed knob. The cartridge holder is firmly fitted to this linear translation stage (Fig.3.2). The duration of rotation and the direction of rotation of the servo motor shaft therefore determines the movement of the cartridge. The entire setup is covered with a 3D printed enclosure (Fig.3.8) with a sliding door for insertion of the cartridge.

This concerted interplay between (i) imaging (executed by Raspberry Pi 4), (ii) execution of fluidic steps (operation of cartridge) and movement of X-Y translation stage (executed by Arduino UNO) is centrally controlled by a mobile application. Both the Raspberry Pi and Arduino execute commands via Bluetooth commands (Fig.S8).

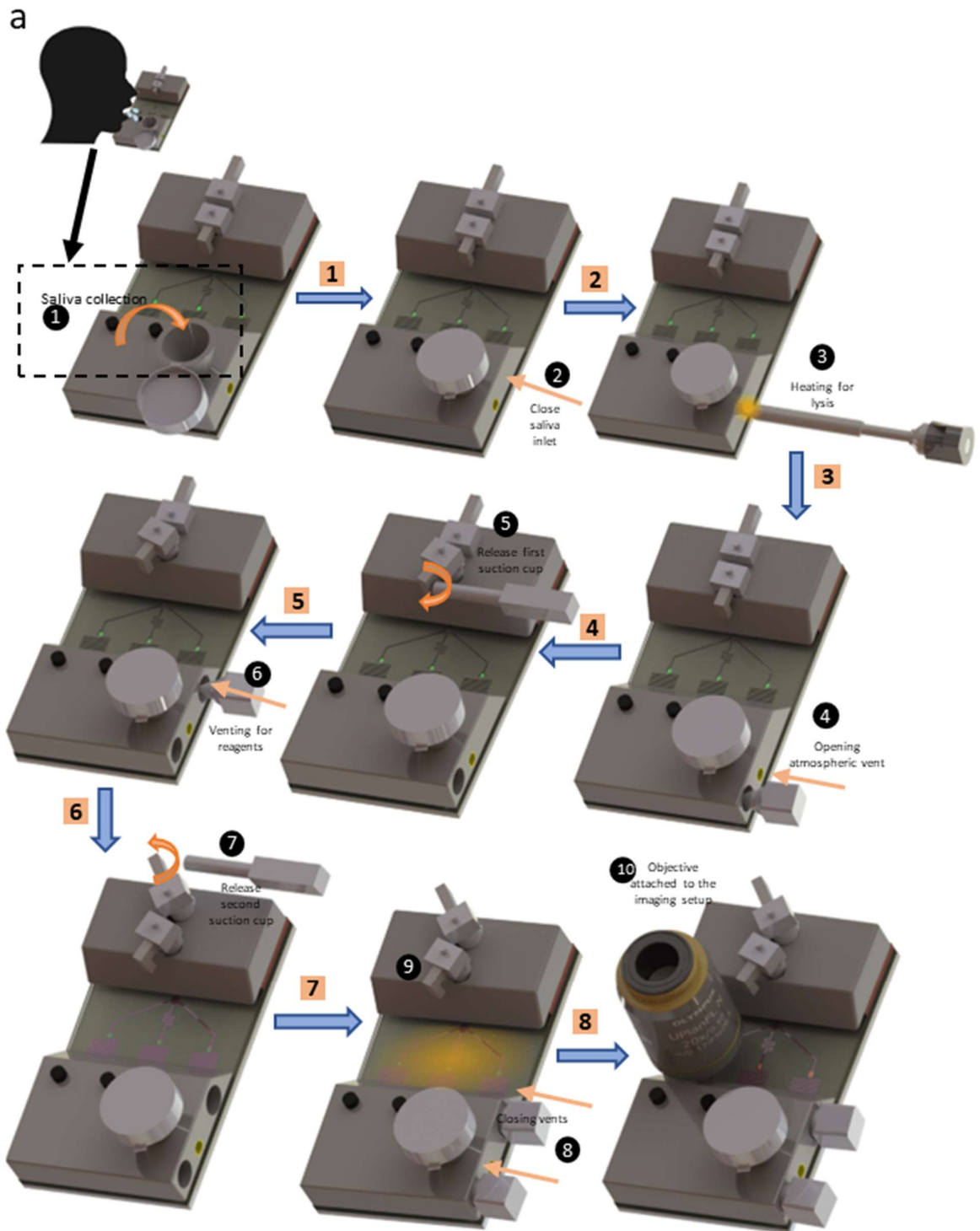
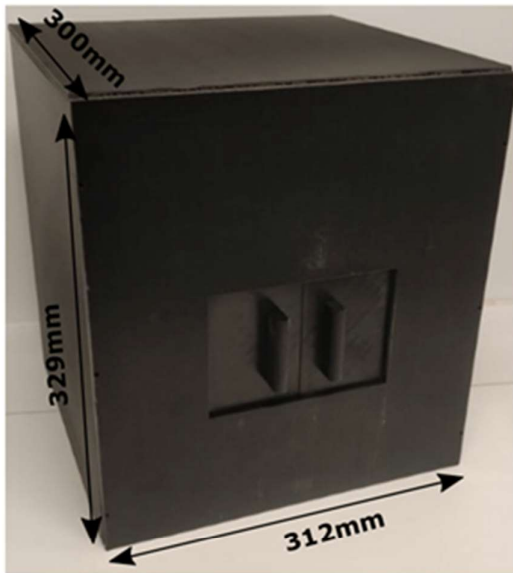


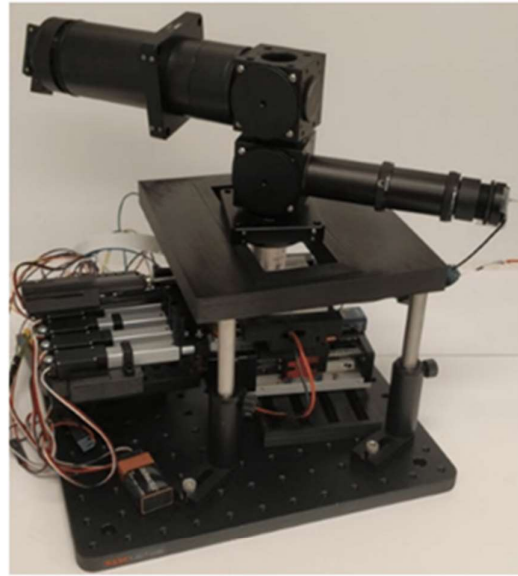
**Fig. 3.7. Sample collection to analysis protocol.** (a) In step (1), the user spits saliva in the funnel on the 3D printed cartridge. The inlet is then closed by covering the inlet with a slider to mitigate evaporation (2) secured by the friction between the parts. In the next step the sample

is heated to 95<sup>0</sup> Celsius by a heating element in contact with metal inserts (3) which in turn are in direct contact with the saliva sample. The closing lid helps mitigate the sample evaporation during heating step. Once the lysis step is done, saliva inlet is exposed to atmospheric pressure (venting) via breaking (4) of a 100micron thick membrane which results in the exposure of the saliva inlet to atmospheric pressure. Following this, the first suction (in compressed state) is released (5) resulting in a negative pressure in the channels, allowing the saliva to flow to the mixing Y-junction. The volume of the suction cups is calculated based of the volume of liquid desired in the channels. Next, the amplification reagents stored are vented to atmospheric pressure by breaking a 100 $\mu$ m thick 3D printed membrane (6). Once this venting is completed, the second suction screw (7) is released resulting in a negative suction pressure enabling the mixing of lysed sample and amplification reagents via a Y-junction followed by a serpentine channel and reaches the detection chamber. Both the vent openings in the 3D printed cartridge are closed to mitigate evaporation (8). The detection chamber is then heated to 65<sup>0</sup> Celsius for 15min to enable the amplification reaction (9). Following the amplification reaction, the detection chamber is imaged and subsequently the images are analyzed, and results are communicated to the mobile phone.

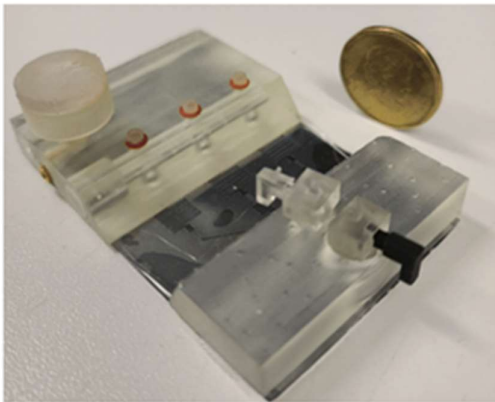
a.



b.



c.



d.



**Fig. 3.8. Camera captured pictures of prototypes of the imaging and fluidic modules (a).** Picture showing the isometric view of the outer enclosure of the setup with dimensions specified. (b) Isometric view, (c-d). Isometric view and side view of the cartridge,

### **3.6. Assay imaging**

The image of the assay on the platform is captured with our custom-built PRICE setup. In brief, the CMOS sensor captures the image of the detection platform. The raw image is stored in the raspberry Pi for further processing. In addition to controlled illumination, the parameters of image capture, namely, white balance, gain (analog and digital) exposure time, framerate and ISO become important. Among these, white balance and gain values were changed in this study. The rationale behind this draws inspiration from traditional brightfield microscope wherein, the gain and white balance values are manipulated to capture the images. All the other parameters were fixed and left changed through the experimental process.

#### **3.6.1. Comparative study of Imaging of assay droplet on platform**

LAMP assay was carried out in Eppendorf tubes for wild type SARS-CoV-2 synthetic RNA for different points. Then 1 $\mu$ l of the droplet was transferred to the detection platform and imaged with the PRICE setup and brightfield Nikon microscope Fig.9d. The Fig.9a shows the  $G^2/R*B$  analysis for images with the PRICE. There is a steep increase of the  $G^2/R*B$  at 10min confirming the presence of viral nucleic acid. The same assay when imaged with Nikon microscope (Fig.9b) shown the change in  $G^2/R*B$  at 10min. This shows good correlation between both the imaging setups.

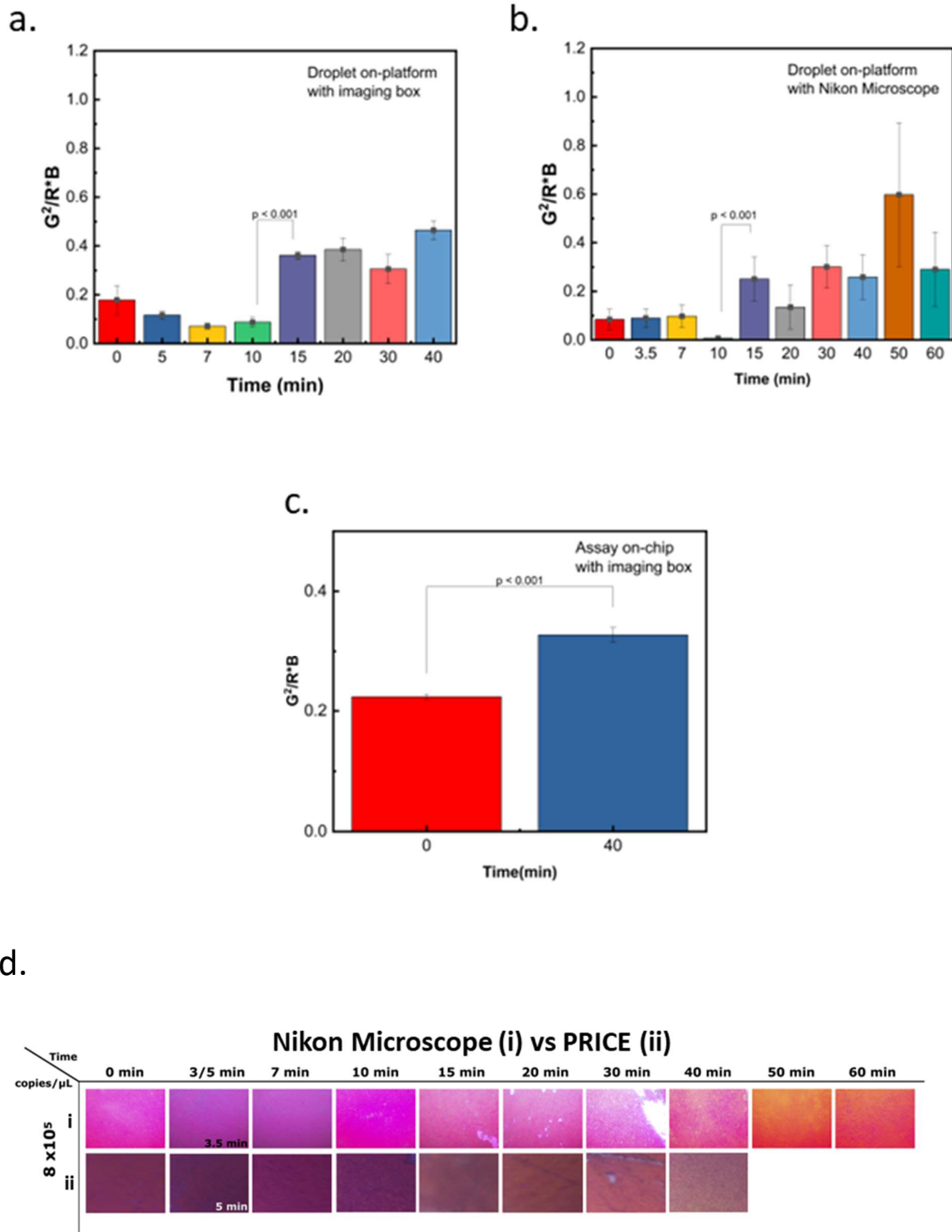


**Fig. 3.9. Comparison study between Nikon microscope and the imaging setup for RT-LAMP assay.** The figure set is a proof-of-concept study of the portable imaging setup to capture phenol red mediated colorimetric change for SARS-CoV-2 detection at point-of-need.

All the analyses are carried out for wild type SARS-CoV-2 synthetic RNA at  $8 \times 10^5$  copies/ $\mu$ L. For these analyses, the RT-LAMP assay is carried out off-chip in an Eppendorf tube and later pipetted out on to color sensitive platform for imaging. (a) The graph depicts temporal change of  $G^2/R*B$  parameter for assay droplet on the color sensitive plasmonic platform. The significant change is observed from time point 10min to 15min ( $p < 0.001$ ). Hence time point 15min is considered as point of differentiation or color change. The images here are capture with a Raspberry Pi HQ CMOS sensor at Red:Blue gain values of 3:3. (b) This graph is a comparative study with a Nikon Eclipse Ni-U microscope. Here, the time point of differentiation is observed to be 15min. The images are captured at Red:Blue gain values of 1.54:2.11. (c) The graph shows the variation of the parameter ( $G^2/R*B$ ) when the assay liquid is imaged in the fabricated chip (with PDMS bonded fluidic layer) at two different time points 0min and 40min. The graph shows significant change ( $p < 0.001$ ) in the parameter for the two time points. This study is a proof-of-concept analysis of the imaging setup to capture colorimetric change in a fully fabricated microfluidic chip.

### **3.7. Conclusion**

In this work we reported an automated setup for sample to answer pathogen detection. The sequential steps of the assay and signal transduction and analysis are automated using three different modules, (i) a portable reflected-light imaging setup with controlled epi-illumination (PRICE), (ii) a microfluidic cartridge and (iii) automation control unit. The QolorEX platform, a specialized nanostructured platform recently developed in our lab that leverages plasmonic excitation for highly sensitive detection of respiratory infectious pathogen is employed as the key detection technology. First, to capture the colorimetric change, PRICE is designed for imaging the assay chamber. The imaging setup offered superior spatial and spectral control with only a 17% variation in the relative intensity and a resolution and FoV of  $4.4 \mu\text{m}$  and

298 $\mu$ m, respectively. Next, to eliminate the involvement of the user, a microfluidic cartridge with mechanically actuated PDMS suction cups coupled is implemented by leveraging additive manufacturing techniques. The flow was shown to be mechanically actuated by a screw-nut mechanism with excellent control over the fluid pumping. This actuation mechanism demonstrated lowest volume of fluid suctioned at 0.1 $\mu$ l for a 30<sup>0</sup>degree rotation of the actuating screw. Subsequently, the microfluidic chip also showed perfect extent in mixing lysed sample with the reagents. With the final automation and control module., the cartridge operation was concerted using system of linear actuators and electrothermal heaters connected via Arduino UNO and Raspberry Pi controlled via mobile application. The imaging was implemented in a direct comparison format with a Nikon brightfield microscope, and a quantifiable colorimetric change was recorded in 15min. In future iterations we plan to package the whole microfluidic cartridge as a fully additive manufactured platform including the microfluidic channels. We believe that this automated system can truly enable the application of highly sensitive QoloEX platform at the POC for pathogen testing.

### 3.8. Supplementary Information

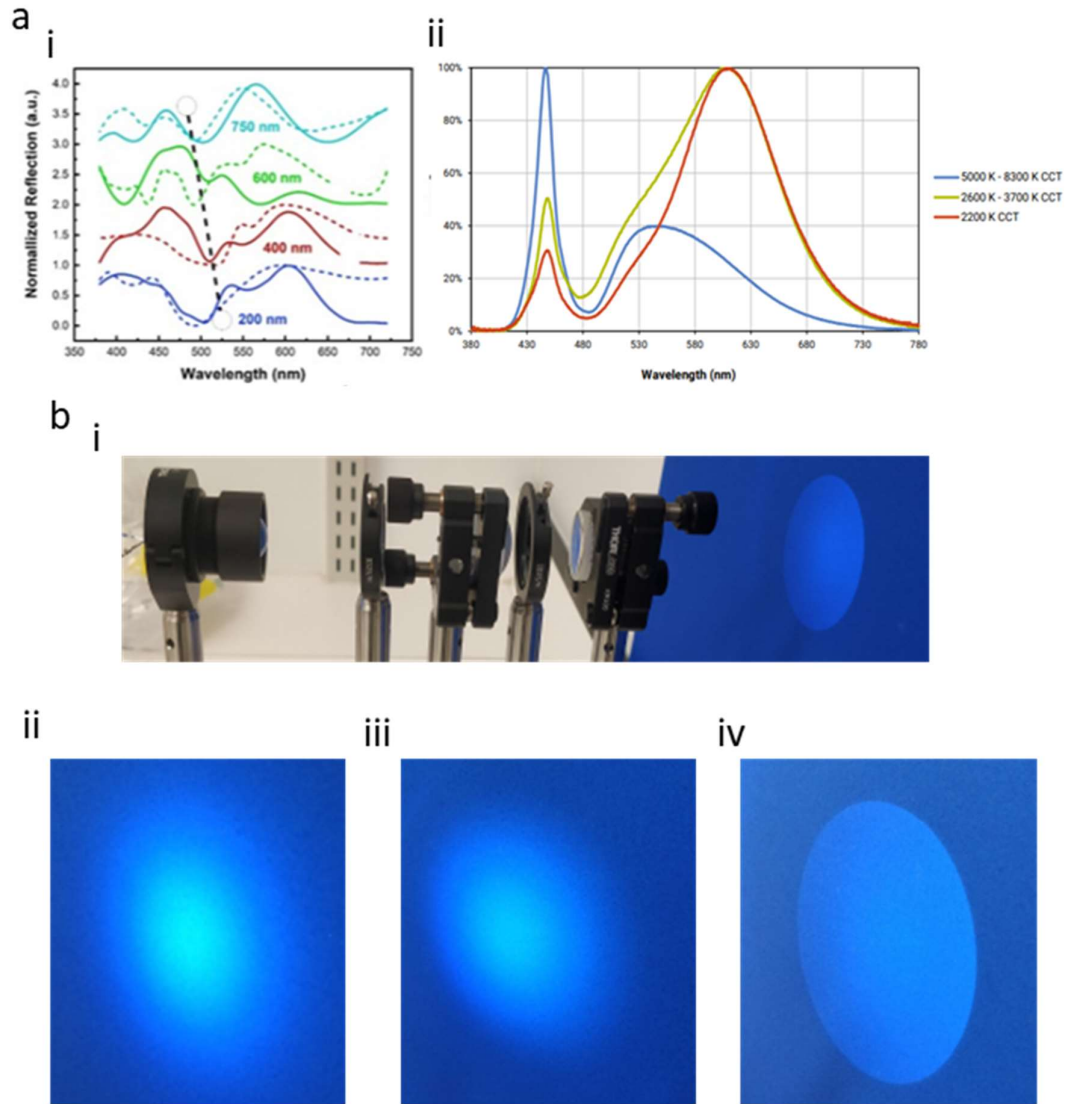


**Fig. S1. Components of illumination** (a) (i) UV-Vis spectroscopy analysis of the detection platform. (ii) The spectral power distribution of Lumileds LEDs at lighting ratings (Lumileds Inc.). (b) Visual characterization of proposed illumination column in PRICE. (i) The benchtop setup employed for visual characterization. The collimated light beam is irradiated onto a blue background and subsequently images were captured with phone

camera. The visual intensity profile of the collimated beam is shown for, (ii) simple LED with no lens setup, (iii) LED-diffusing lens setup, (iv) PRICE illumination column.

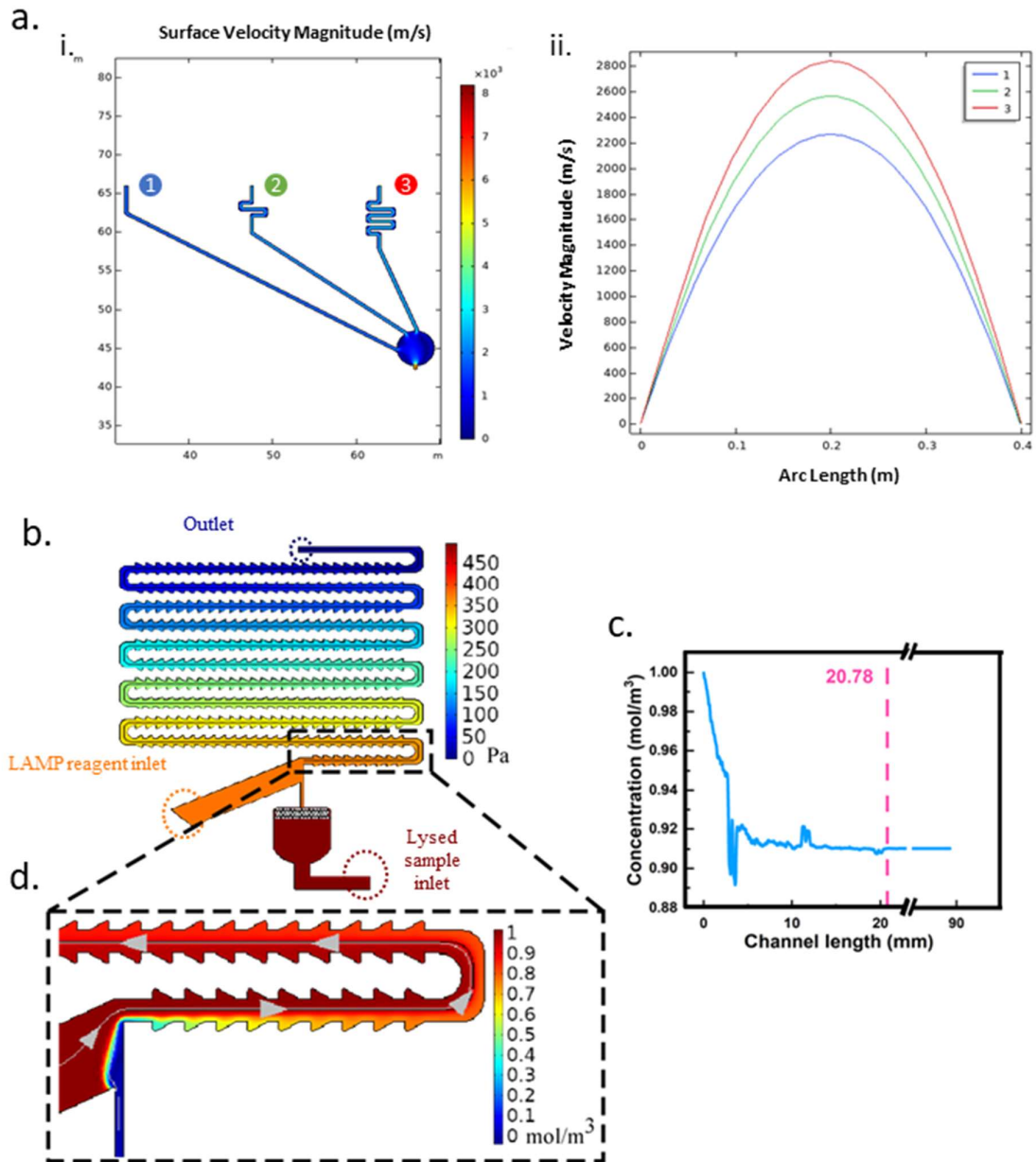


**Fig. S2. COMSOL analysis for design of the microfluidic platform.** (a) The channels were designed to ensure uniform pressure distribution of the lysed sample under the same suction

pressure loading. (i) Surface pressure distribution across the channels for the distribution of lysed sample. (ii). Velocity distribution across the cross-section of the three channels color-coded in blue, green and red. (b). The serpentine channel that aids in the mixing of the lysed sample with the LAMP reagents and is simulated to ensure perfect mixing with the proposed length. (c&d) The simulation showed rapid mixing as depicted with a mixing length of 20mm.

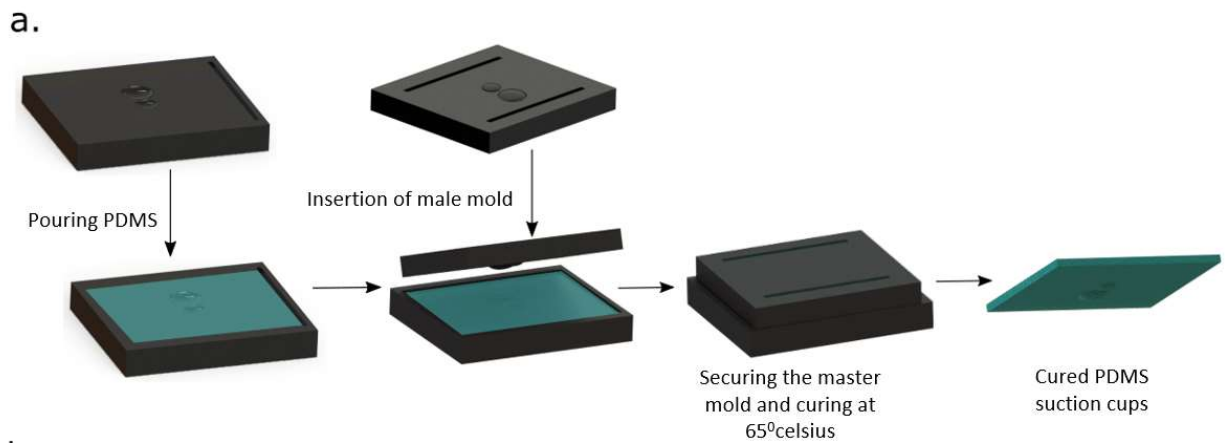


**Fig. S3. Suction cup fabrication protocol.** (a) The suction cups are fabricated using SLA printed molds. The 3D printed molds are first surface treated to avoid curing inhibition at the PDMS mold interface. The high resolution of the printing ensured low roughness of the PDMS thereby ensuring strong bonding.

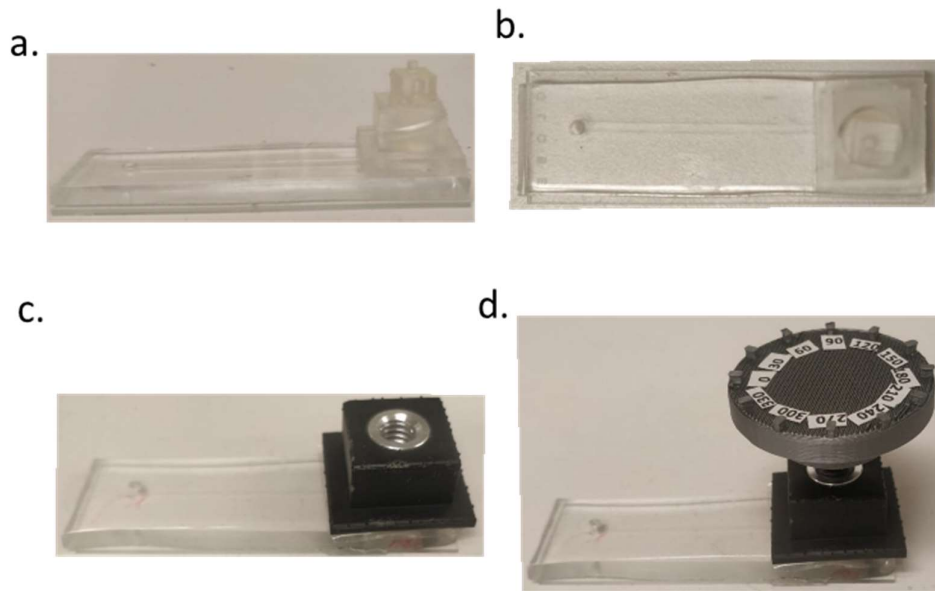


**Fig S4. Depiction of experimental setup for suction cup characterization.** (a&b) 3D printed module employed for characterization of empirical volume of the suction cups. (c&d) The fluidics setup employed for demonstration of fluid manipulation

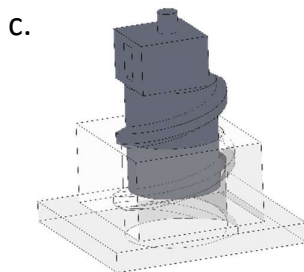
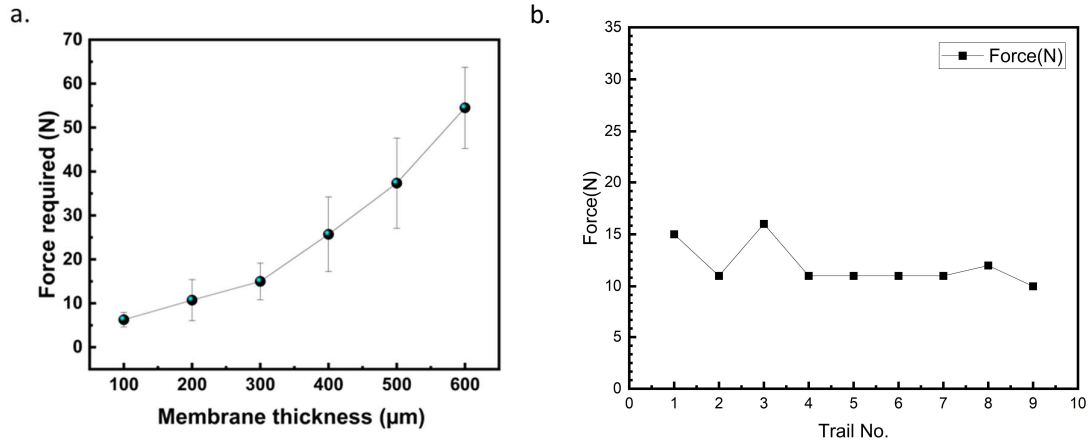


**Fig S5. Characterization of 3D printed components** (a) The figure depicts the manual force required to break the membrane at different thicknesses. The membrane was fabricated using SLA 3D printer. (b) The normal force exerted by the screw-nut system characterized in multiple trails. (c) CAD model depicting the 3D printed nut-screw setup employed for mechanical actuation of the suction cup.

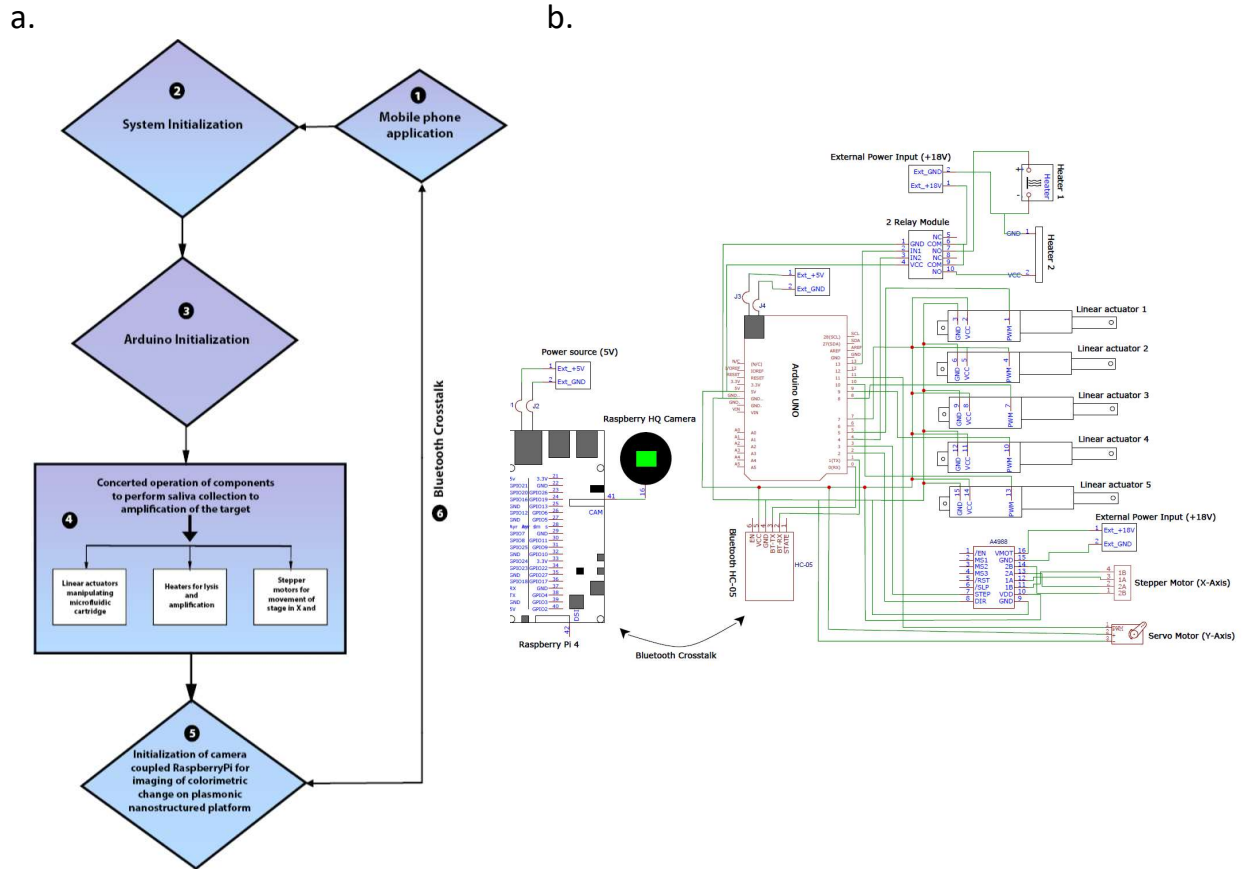


**Fig S6. Overview of electronic components** (a). Flow diagram depicting the high-level operation of microfluidic sample-to-answer pathogen detection platform, with major emphasis on electronic components involved. The number coded blocks indicate the sequence of the individual process involved in the operation. In brief, Step-1 to 3 involves the user to connect to the system via a mobile application enabled by an on-board Bluetooth module connected to the Arduino UNO. In the next subsequent step, the components in the Arduino are activated in

concerted sub steps to complete the processes from sample collection to LAMP reaction incubation. Following the completion of the reaction, the Bluetooth communicates with Raspberry Pi via Bluetooth to initiate imaging and subsequent movement of the stage for multiplexed pathogen detection. (b). The figure shows the electronic CAD layout of all the electronic components enabling the automation of the sample to answer processing of the system. The major constituents involved in the prototype controlled by Arduino UNO and Raspberry Pi are, (i). actuator system (five in number to automate the process of saliva collection and sequential delivery of reagents typically involved in a LAMP assay), (ii). Two DC heating components to controlled heating for pathogen lysis and subsequent nucleic acid amplification reaction, (iii). Raspberry Pi 4 (4GB RAM) coupled with CMOS sensor for imaging of the colorimetric change, (iv). A HC-05 Bluetooth module that enables cross talk between the mobile application and the Arduino UNO, and subsequently between Arduino UNO and Raspberry Pi 4.

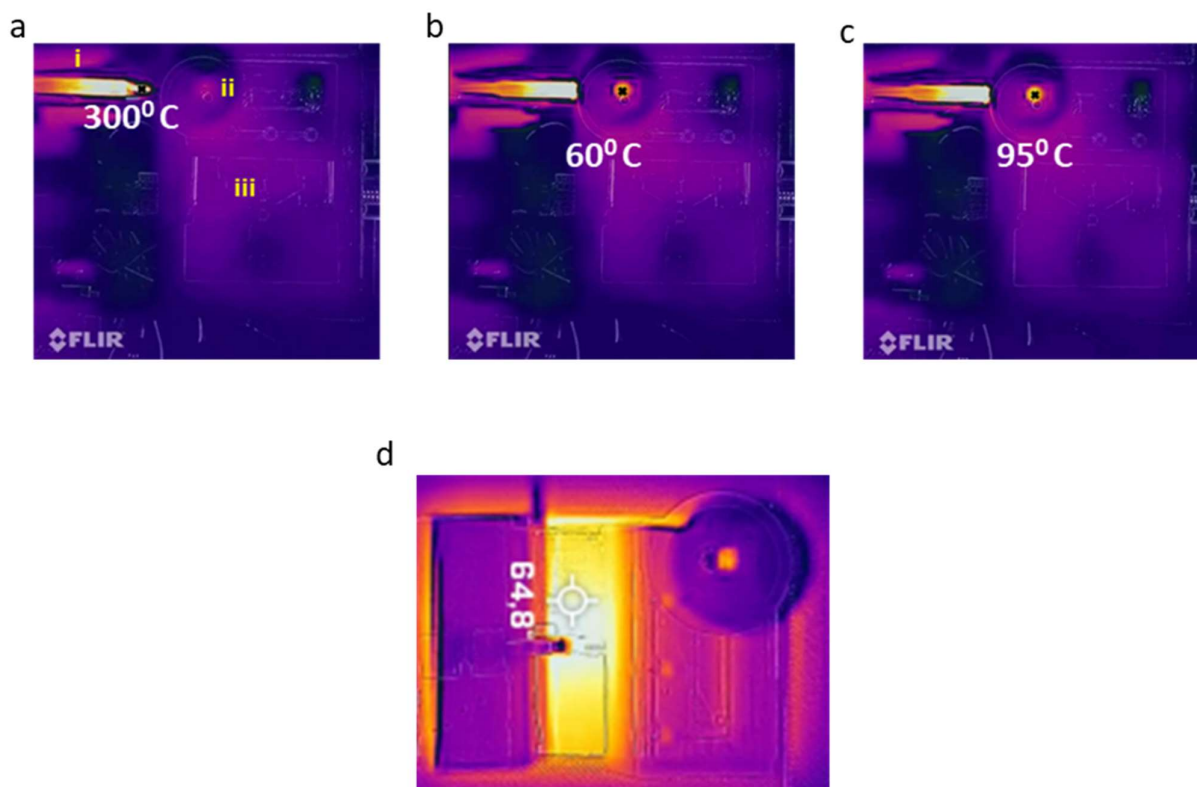


**Fig S7. Infrared images of the heating modules.** (a). Infrared image depicting the surface temperature of the solder tip (i) at 300°C, (b&c). The solder tip is brought in contact with the metal insert (ii), where the sample is heated to 95°C for 3min. (d) The infrared image showing the surface temperature of the cartridge heated up to 65°C for amplification reaction.

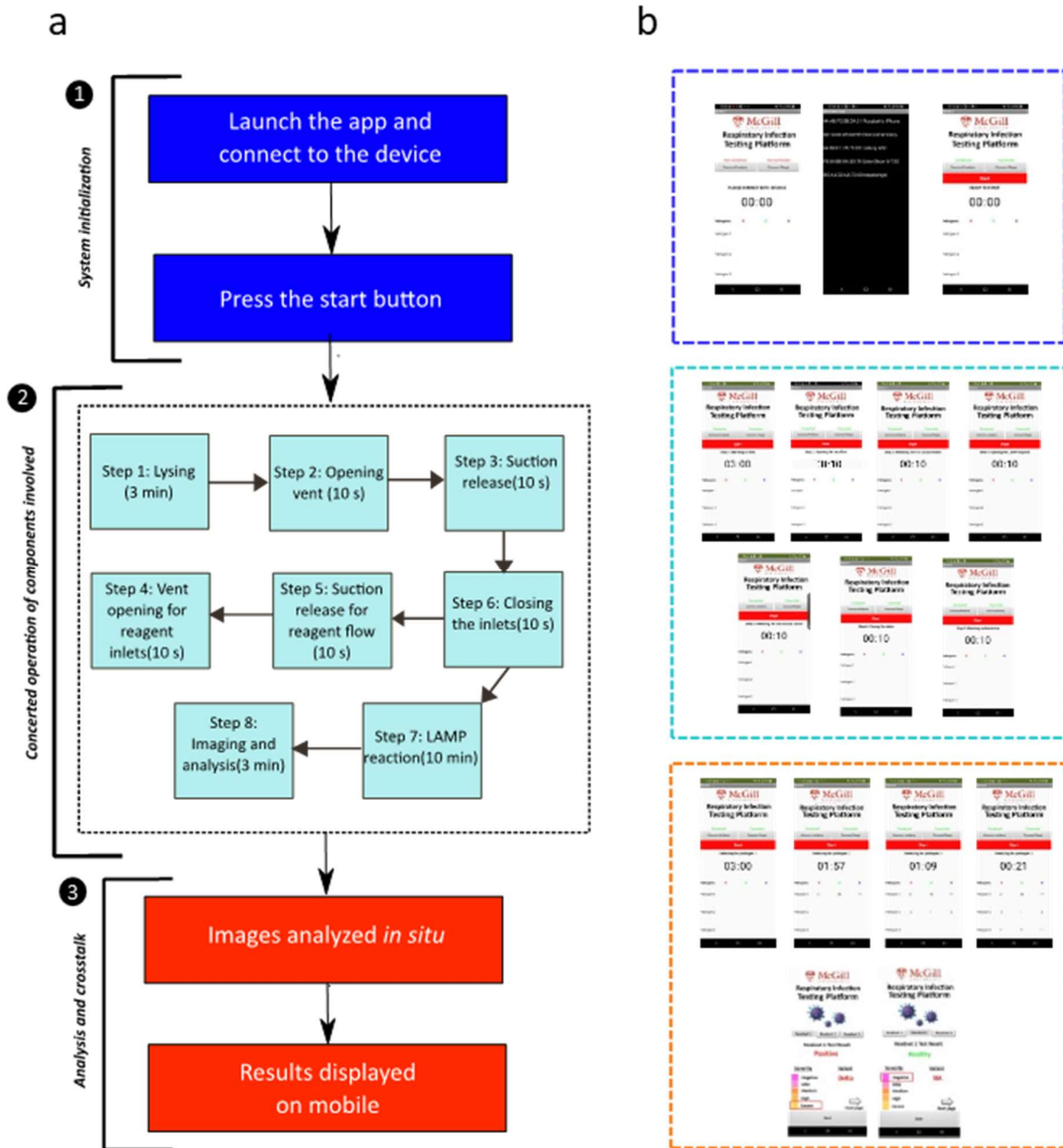


**Fig. S8. Overview of operation of the mobile enabled automation (a&b)** This figure gives an overview of process flow involved in the operation of the mobile application working in tandem with two major microcontroller modules, namely, Arduino UNO and Raspberry Pi 4. The operation of the application can be broadly categorized into three main subsets, (1) System initialization- The crosstalk between the mobile phone and the microcontroller modules is enabled by a stable Bluetooth connection. Hence the first step is establishing a connection

between mobile and the modules and subsequently press the button labelled 'Start' to send a message to the Arduino and Raspberry Pi 4 to start initializing the process (color coded in navy blue). Following this, in subset (2), the components start operating in a concerted fashion. Each component substep is clocked to enable operation in the defined sequence. The user can monitor the progression of the process on the mobile application (color coded in light blue). Once the assay incubation time is completed, the images are captured and analyzed in substep (3). In brief, RGB values are extracted from the images and analyzed further to display the final result on the screen easily interpretable by the user (color coded in red).

### 3.9. References

1. Liu B, Zhuang J, Wei G. Recent advances in the design of colorimetric sensors for environmental monitoring. *Environmental Science: Nano*. 2020;7(8):2195-2213. doi:10.1039/D0EN00449A
2. Piriya V.S A, Joseph P, Daniel S.C.G. K, Lakshmanan S, Kinoshita T, Muthusamy S. Colorimetric sensors for rapid detection of various analytes. *Materials Science and Engineering: C*. 2017;78:1231-1245. doi:10.1016/J.MSEC.2017.05.018
3. Sharafeldin M, Davis JJ. Point of Care Sensors for Infectious Pathogens. *Analytical Chemistry*. 2021;93(1):184-197. doi:10.1021/ACS.ANALCHEM.0C04677/ASSET/IMAGES/ACS.ANALCHEM.0C04677.SOCIAL.JPEG\_V03
4. Zhao VXT, Wong TI, Zheng XT, Tan YN, Zhou X. Colorimetric biosensors for point-of-care virus detections. *Materials Science for Energy Technologies*. 2020;3:237-249. doi:10.1016/J.MSET.2019.10.002
5. Safavieh M, Kanakasabapathy MK, Tarlan F, et al. Emerging Loop-Mediated Isothermal Amplification-Based Microchip and Microdevice Technologies for Nucleic Acid Detection. *ACS Biomaterials Science and Engineering*. 2016;2(3):278-294. doi:10.1021/ACSBBIOMATERIALS.5B00449/ASSET/IMAGES/ACSBBIOMATERIALS.5B00449.SOCIAL.JPEG\_V03
6. Zhao F, Liu Z, Gu Y, et al. Detection of Mycoplasma pneumoniae by colorimetric loop-mediated isothermal amplification. *Acta Microbiologica et Immunologica Hungarica*. 2013;60(1):1-9. doi:10.1556/AMicr.60.2013.1.1
7. Goto M, Honda E, Ogura A, Nomoto A, Hanaki KI. Colorimetric detection of loop-mediated isothermal amplification reaction by using hydroxy naphthol blue. *Biotechniques*. 2009;46(3):167-172. doi:10.2144/000113072
8. Nguyen HQ, Nguyen VD, van Nguyen H, Seo TS. Quantification of colorimetric isothermal amplification on the smartphone and its open-source app for point-of-care pathogen detection. *Scientific Reports 2020 10:1*. 2020;10(1):1-10. doi:10.1038/s41598-020-72095-3
9. Lou-Franco J, Das B, Elliott C, Cao C. Gold Nanozymes: From Concept to Biomedical Applications. *Nano-Micro Letters*. 2021;13(1):1-36. doi:10.1007/s40820-020-00532-z
10. Myers FB, Lee LP. Innovations in optical microfluidic technologies for point-of-care diagnostics. *Lab on a Chip*. 2008;8(12):2015-2031. doi:10.1039/B812343H
11. Ding X, Mauk MG, Yin K, Kadimisetty K, Liu C. Interfacing Pathogen Detection with Smartphones for Point-of-Care Applications. *Analytical Chemistry*. 2019;91(1):655-672. doi:10.1021/ACS.ANALCHEM.8B04973/ASSET/IMAGES/LARGE/AC-2018-04973W\_0009.JPEG

12. Zhu H, Isikman SO, Mudanyali O, Greenbaum A, Ozcan A. Optical imaging techniques for point-of-care diagnostics. *Lab on a Chip*. 2012;13(1):51-67. doi:10.1039/C2LC40864C
13. Papadakis G, Pantazis AK, Fikas N, et al. Portable real-time colorimetric LAMP-device for rapid quantitative detection of nucleic acids in crude samples. *Scientific Reports* 2022 12:1. 2022;12(1):1-15. doi:10.1038/s41598-022-06632-7
14. Ma YD, Chen YS, Lee G bin. An integrated self-driven microfluidic device for rapid detection of the influenza A (H1N1) virus by reverse transcription loop-mediated isothermal amplification. *Sensors and Actuators, B: Chemical*. 2019;296:126647. doi:10.1016/j.snb.2019.126647
15. Mauk M, Song J, Bau HH, et al. Miniaturized devices for point of care molecular detection of HIV. *Lab on a Chip*. 2017;17(3):382-394. doi:10.1039/C6LC01239F
16. Zhang D, Liu Q. Biosensors and bioelectronics on smartphone for portable biochemical detection. *Biosensors and Bioelectronics*. 2016;75:273-284. doi:10.1016/J.BIOS.2015.08.037
17. Priye A, Bird SW, Light YK, Ball CS, Negrete OA, Meagher RJ. A smartphone-based diagnostic platform for rapid detection of Zika, chikungunya, and dengue viruses. *Scientific Reports* 2017 7:1. 2017;7(1):1-11. doi:10.1038/srep44778
18. Song J, Pandian V, Mauk MG, et al. Smartphone-Based Mobile Detection Platform for Molecular Diagnostics and Spatiotemporal Disease Mapping. *Analytical Chemistry*. 2018;90(7):4823-4831. doi:10.1021/ACS.ANALCHEM.8B00283/ASSET/IMAGES/LARGE/AC-2018-00283V\_0006.JPEG
19. Yang K, Peretz-Soroka H, Liu Y, Lin F. Novel developments in mobile sensing based on the integration of microfluidic devices and smartphones. *Lab on a Chip*. 2016;16(6):943-958. doi:10.1039/C5LC01524C
20. Liu J, Geng Z, Fan Z, Liu J, Chen H. Point-of-care testing based on smartphone: The current state-of-the-art (2017–2018). *Biosensors and Bioelectronics*. 2019;132:17-37. doi:10.1016/J.BIOS.2019.01.068
21. Kanchi S, Sabela MI, Mdluli S, Bisetty K. Smartphone based bioanalytical and diagnosis applications: A review. Published online 2017. doi:10.1016/j.bios.2017.11.021
22. Zhou P, He H, Ma H, Wang S, Hu S. A Review of Optical Imaging Technologies for Microfluidics. *Micromachines* 2022, Vol 13, Page 274. 2022;13(2):274. doi:10.3390/MII13020274
23. Yang J, Wang K, Xu H, Yan W, Jin Q, Cui D. Detection platforms for point-of-care testing based on colorimetric, luminescent and magnetic assays: A review. *Talanta*. 2019;202:96-110. doi:10.1016/J.TALANTA.2019.04.054

24. Oh SJ, Park BH, Choi G, et al. Fully automated and colorimetric foodborne pathogen detection on an integrated centrifugal microfluidic device. *Lab on a Chip*. 2016;16(10):1917-1926. doi:10.1039/C6LC00326E
25. Tamer AbdElFatah MJSGYIIHSM. *Plasmonic-Assisted Point-of-Care Rapid and Quantified Identification (or Diagnosis) of Respiratory Infections via a Nano Surface Microfluidic Colorimetry Apparatus.*; 2022.
26. Cheng F, Gao J, Luk ST, Yang X. Structural color printing based on plasmonic metasurfaces of perfect light absorption. *Scientific Reports* 2015 5:1. 2015;5(1):1-10. doi:10.1038/srep11045
27. Docter MW, Young IT, Piciu OM, et al. Measuring the wavelength-dependent divergence of transmission through sub-wavelength hole-arrays by spectral imaging. *Optics Express, Vol 14, Issue 20, pp 9477-9482*. 2006;14(20):9477-9482. doi:10.1364/OE.14.009477
28. Mocan T, Matea CT, Pop T, et al. Development of nanoparticle-based optical sensors for pathogenic bacterial detection. *Journal of Nanobiotechnology*. 2017;15(1):1-14. doi:10.1186/S12951-017-0260-Y/FIGURES/7
29. Yoo SM, Lee SY. Optical Biosensors for the Detection of Pathogenic Microorganisms. *Trends in Biotechnology*. 2016;34(1):7-25. doi:10.1016/J.TIBTECH.2015.09.012
30. Lakshmi BA, Kim S. Recent trends in the utilization of LAMP for the diagnosis of viruses, bacteria, and allergens in food. In: *Recent Developments in Applied Microbiology and Biochemistry*. Elsevier; 2021:291-297. doi:10.1016/b978-0-12-821406-0.00027-8
31. Notomi T, Okayama H, Masubuchi H, et al. Loop-mediated isothermal amplification of DNA. *Nucleic Acids Res*. 2000;28(12):63. doi:10.1093/nar/28.12.e63
32. Shang Y, Sun J, Ye Y, Zhang J, Zhang Y, Sun X. Loop-mediated isothermal amplification-based microfluidic chip for pathogen detection. *Critical Reviews in Food Science and Nutrition*. 2020;60(2):201-224. doi:10.1080/10408398.2018.1518897
33. Garrido-Maestu A, Prado M. Naked-eye detection strategies coupled with isothermal nucleic acid amplification techniques for the detection of human pathogens. *Comprehensive Reviews in Food Science and Food Safety*. 2022;21(2):1913-1939. doi:10.1111/1541-4337.12902
34. Zhang X, Lowe SB, Gooding JJ. Brief review of monitoring methods for loop-mediated isothermal amplification (LAMP). *Biosensors and Bioelectronics*. 2014;61:491-499. doi:10.1016/J.BIOS.2014.05.039
35. Sharma S, Alamgir Kabir M, Asghar W. Lab-on-a-Chip Zika Detection With Reverse Transcription Loop-Mediated Isothermal Amplification–Based Assay for Point-of-Care Settings. *Archives of Pathology & Laboratory Medicine*. 2020;144(11):1335-1343. doi:10.5858/ARPA.2019-0667-OA
36. Kaygusuz D, Vural S, Aytekin AÖ, Lucas SJ, Elitas M. DaimonDNA: A portable, low-cost loop-mediated isothermal amplification platform for naked-eye detection of

- genetically modified organisms in resource-limited settings. *Biosensors and Bioelectronics*. 2019;141:111409. doi:10.1016/J.BIOS.2019.111409
37. Nayak S, Blumenfeld NR, Laksanasopin T, Sia SK. Point-of-Care Diagnostics: Recent Developments in a Connected Age. *Analytical Chemistry*. 2017;89(1):102-123. doi:10.1021/ACS.ANALCHEM.6B04630/ASSET/IMAGES/ACS.ANALCHEM.6B04630.SOCIAL.JPEG\_V03
  38. Chin CD, Linder V, Sia SK. Lab-on-a-chip devices for global health: Past studies and future opportunities. *Lab on a Chip*. 2006;7(1):41-57. doi:10.1039/B611455E
  39. Zhu H, Fohlerová Z, Pekárek J, Basova E, Neužil P. Recent advances in lab-on-a-chip technologies for viral diagnosis. *Biosensors and Bioelectronics*. 2020;153:112041. doi:10.1016/J.BIOS.2020.112041
  40. Mark D, Haeberle S, Roth G, von Stetten F, Zengerle R. Microfluidic lab-on-a-chip platforms: Requirements, characteristics and applications. *NATO Science for Peace and Security Series A: Chemistry and Biology*. Published online 2010:305-376. doi:10.1007/978-90-481-9029-4\_17/TABLES/5
  41. Foudeh AM, Fatanat Didar T, Veres T, Tabrizian M. Microfluidic designs and techniques using lab-on-a-chip devices for pathogen detection for point-of-care diagnostics. *Lab on a Chip*. 2012;12(18):3249-3266. doi:10.1039/C2LC40630F
  42. Battat S, Weitz DA, Whitesides GM. An outlook on microfluidics: the promise and the challenge. *Lab on a Chip*. 2022;22(3):530-536. doi:10.1039/D1LC00731A
  43. Nasseri B, Soleimani N, Rabiee N, Kalbasi A, Karimi M, Hamblin MR. Point-of-care microfluidic devices for pathogen detection. *Biosens Bioelectron*. 2018;117:112. doi:10.1016/J.BIOS.2018.05.050
  44. Pattanayak P, Singh SK, Gulati M, et al. Microfluidic chips: recent advances, critical strategies in design, applications and future perspectives. *Microfluidics and Nanofluidics*. 2021;25(12):1-28. doi:10.1007/S10404-021-02502-2/FIGURES/17
  45. Chen J, Chen D, Xie Y, Yuan T, Chen X. Progress of Microfluidics for Biology and Medicine. *Nano-Micro Letters*. 2013;5(1):66-80. doi:10.1007/bf03354852
  46. Liu W, Yue F, Lee LP. Integrated Point-of-Care Molecular Diagnostic Devices for Infectious Diseases. *Accounts of Chemical Research*. 2021;54(22):4107-4119. doi:10.1021/ACS.ACCOUNTS.1C00385/SUPPL\_FILE/AR1C00385\_SI\_001.PDF
  47. Jue E, Schoepp NG, Witters D, Ismagilov RF. Evaluating 3D printing to solve the sample-to-device interface for LRS and POC diagnostics: example of an interlock meter-mix device for metering and lysing clinical urine samples. *Lab on a Chip*. 2016;16(10):1852-1860. doi:10.1039/C6LC00292G
  48. Ambrosi A, Bonanni A. How 3D printing can boost advances in analytical and bioanalytical chemistry. *Microchimica Acta*. 2021;188(8):1-17. doi:10.1007/S00604-021-04901-2/FIGURES/6

49. Behrens MR, Fuller HC, Swist ER, et al. Open-source, 3D-printed Peristaltic Pumps for Small Volume Point-of-Care Liquid Handling. *Scientific Reports* 2020 10:1. 2020;10(1):1-10. doi:10.1038/s41598-020-58246-6
50. Kadimisetty K, Song J, Doto AM, et al. Fully 3D printed integrated reactor array for point-of-care molecular diagnostics. *Biosensors and Bioelectronics*. 2018;109:156-163. doi:10.1016/J.BIOS.2018.03.009
51. Song J, Mauk MG, Hackett BA, Cherry S, Bau HH, Liu C. Instrument-Free Point-of-Care Molecular Detection of Zika Virus. *Analytical Chemistry*. 2016;88(14):7289-7294. doi:10.1021/ACS.ANALCHEM.6B01632/SUPPL\_FILE/AC6B01632\_SI\_001.PDF
52. Chan HN, Tan MJA, Wu H. Point-of-care testing: applications of 3D printing. *Lab on a Chip*. 2017;17(16):2713-2739. doi:10.1039/C7LC00397H
53. Ganguli A, Mostafa A, Berger J, et al. Rapid isothermal amplification and portable detection system for SARS-CoV-2. *Proc Natl Acad Sci U S A*. 2020;117(37):22727-22735. doi:10.1073/PNAS.2014739117/SUPPL\_FILE/PNAS.2014739117.SM01.AVI
54. Berger J, Aydin MY, Stavins R, et al. Portable Pathogen Diagnostics Using Microfluidic Cartridges Made from Continuous Liquid Interface Production Additive Manufacturing. *Analytical Chemistry*. 2021;93(29):10048-10055. doi:10.1021/ACS.ANALCHEM.1C00654/SUPPL\_FILE/AC1C00654\_SI\_001.PDF
55. Tian F, Liu C, Deng J, et al. A fully automated centrifugal microfluidic system for sample-to-answer viral nucleic acid testing. *Science China Chemistry* 2020 63:10. 2020;63(10):1498-1506. doi:10.1007/S11426-020-9800-6
56. Dixit CK, Kadimisetty K, Rusling J. 3D-printed miniaturized fluidic tools in chemistry and biology. *TrAC Trends in Analytical Chemistry*. 2018;106:37-52. doi:10.1016/J.TRAC.2018.06.013
57. Evennett P. Köhler Illumination: A simple interpretation The problem. 1983;28:189-192.
58. Thompson D, Lei Y. Mini review: Recent progress in RT-LAMP enabled COVID-19 detection. *Sensors and Actuators Reports*. 2020;2(1):100017. doi:10.1016/j.snr.2020.100017
59. Chan HN, Chen Y, Shu Y, Chen Y, Tian Q, Wu H. Direct, one-step molding of 3D-printed structures for convenient fabrication of truly 3D PDMS microfluidic chips. *Microfluidics and Nanofluidics*. 2015;19(1):9-18. doi:10.1007/S10404-014-1542-4/FIGURES/6
60. Venzac B, Deng S, Mahmoud Z, et al. PDMS Curing Inhibition on 3D-Printed Molds: Why? Also, How to Avoid It? *Analytical Chemistry*. 2021;93(19):7180-7187. doi:10.1021/ACS.ANALCHEM.0C04944/ASSET/IMAGES/LARGE/AC0C04944\_0006.JPEG

61. Razavi Bazaz S, Kashaninejad N, Azadi S, et al. Rapid Softlithography Using 3D-Printed Molds. *Advanced Materials Technologies*. 2019;4(10):1900425. doi:10.1002/ADMT.201900425
62. Mansour H, Soliman EA, El-Bab AMF, Abdel-Mawgood AL. Development of epoxy resin-based microfluidic devices using CO2 laser ablation for DNA amplification point-of-care (POC) applications. *International Journal of Advanced Manufacturing Technology*. 2022;120(7-8):4355-4372. doi:10.1007/S00170-022-08992-W/FIGURES/14
63. Lee T, Jang J, Jeong H, Rho J. Plasmonic- and dielectric-based structural coloring: from fundamentals to practical applications. *Nano Convergence* 2018 5:1. 2018;5(1):1-21. doi:10.1186/S40580-017-0133-Y
64. Perikala M, Bhardwaj A. Excellent color rendering index single system white light emitting carbon dots for next generation lighting devices. *Scientific Reports* 2021 11:1. 2021;11(1):1-11. doi:10.1038/s41598-021-91074-w
65. Borovytskyi V. Comparison analysis of illumination systems for digital light microscope according to uniformity of irradiance distribution. <https://doi.org/10.1117/12616531>. 2005;5942:312-320. doi:10.1117/12.616531
66. Madrid-Wolff J, Forero-Shelton M. 4f Koehler Transmitted Illumination Condenser for Teaching and Low-Cost Microscopic Imaging. *The Biophysicist*. 2020;1(2). doi:10.35459/TBP.2019.000113
67. Lee S, Kim H, Lee W, Kim J. Finger-triggered portable PDMS suction cup for equipment-free microfluidic pumping. *Micro and Nano Systems Letters*. 2018;6(1):1-5. doi:10.1186/S40486-018-0063-4/FIGURES/6
68. Park J, Park JK. Finger-Actuated Microfluidic Display for Smart Blood Typing. *Analytical Chemistry*. 2019;91(18):11636-11642. doi:10.1021/ACS.ANALCHEM.9B02129/SUPPL\_FILE/AC9B02129\_SI\_002.MP4
69. Park J, Roh H, Park JK. Finger-Actuated Microfluidic Concentration Gradient Generator Compatible with a Microplate. *Micromachines* 2019, Vol 10, Page 174. 2019;10(3):174. doi:10.3390/MI10030174
70. Iwai K, Shih KC, Lin X, Brubaker TA, Sochol RD, Lin L. Finger-powered microfluidic systems using multilayer soft lithography and injection molding processes. *Lab on a Chip*. 2014;14(19):3790-3799. doi:10.1039/C4LC00500G
71. Park J, Park JK. Finger-actuated microfluidic device for the blood cross-matching test. *Lab on a Chip*. 2018;18(8):1215-1222. doi:10.1039/C7LC01128H
72. Qi W, Zheng L, Hou Y, et al. A finger-actuated microfluidic biosensor for colorimetric detection of foodborne pathogens. *Food Chemistry*. 2022;381:131801. doi:10.1016/J.FOODCHEM.2021.131801
73. Gong MM, MacDonald BD, Vu Nguyen T, Sinton D. Hand-powered microfluidics: A membrane pump with a patient-to-chip syringe interface. *Biomicrofluidics*. 2012;6(4):044102. doi:10.1063/1.4762851



## 4. Discussion and future perspectives

To help support the development of POC pathogen detection tools, world health organization (WHO) proposed an ASSURED framework for systematic evaluation of proposed tools<sup>178</sup>. Currently, the highly specific and a sensitive technique, PCR, is the gold standard and is extensively employed for large scale testing of infectious pathogen. Especially, the current COVID-19 contagion revealed the importance of the rapid testing of widespread population, contracting and quick isolation in curbing the pandemic<sup>179</sup>. However, PCR requires lengthy assay and response times; requires trained personnel; and centralized facilities and relatively expensive equipment<sup>180</sup>. These drawbacks further amplify in the case of testing applied in isolated and resource limited settings. Increasing popularity of the isothermal nucleic acid amplification techniques (NAATs), especially LAMP present attractive alternative to PCR. Moreover, the coupling of isothermal NAATs with colorimetric readouts offer characteristics suitable for POC application. With our lab's recently reported nanostructured microfluidic platform, QolorEX, for highly sensitive colorimetric LAMP assays can potentially address the drawbacks with PCR assays.

In addition to the detection assay, the sample handling system becomes crucial for the real-world translation of the proposed technology. With respect to pathogen diagnosis, major attempts have been made around integrating extremely sensitive nucleic acid methods- PCR and LAMP- into microfluidic platforms, which is evident from the high volume of works pertaining to this in recent years. With the advent of centrifugation-based platforms, high sensitivity and throughput have been achieved. In an analogous way, paper-based microfluidic platforms have enabled acceptable sensitivity, portability, and cost-effectiveness. Despite considerable advances in POC detection by these techniques, an inclusive and comprehensive detection method with the ability to perform all detection steps on-chip is still lacking. In most

of the previously conducted studies, sample pre-processing steps are conducted off-chip, that is, cellular lysis, antigen isolation, antigen extraction, nuclear material extraction, and/or need specialized equipment such as a thermocycler, microscope, bench-top centrifugation setup, and heating oven, among others. Thus, they are not encouraging for application at POC. Nevertheless, earlier works can be improved for integrating extraction, cellular lysis, and detection steps onto a single platform, while being modular for the inclusion/exclusion of other detection assay features, if required. Similarly, pursuing the integration of digital droplet microfluidics with colorimetric detection assays would be interesting since it has been recently shown that they can detect pathogens *in vitro* using LAMP in limited microdroplets and provide great throughput and sensitivity.

A typical LAMP assay consists of series of steps i.e, sample collection, pathogen lysis, mixing of reagents, nucleic amplification and detection. This sequential nature of LAMP assays calls for a fluid handling module that can provide facile way to execute these assay steps without user involvement. Although previous research reported several integrated systems, majority of them require user involvement in one or more assay steps. For example, Tian et al.<sup>173</sup> reported an integrated and automated centrifugal microfluidic device for fluorescence-based RT-LAMP assay for viral pathogens. The system integrates multiple assay steps including lysis, amplification, and fluorescence detection steps into an automated setup. However, there are some drawbacks with requiring a bulky centrifugation system for fluid manipulation; requiring a swab; employment of relatively complex fabrication techniques and automation procedures; and using a commercial computer. Additive manufacturing techniques and innovative fluid manipulation techniques could potentially be leveraged to address these issues. In this thesis, I employed SLA 3D printing to fabricate a microfluidic cartridge, which aids in integrating various assay steps onto a single platform. The fluid manipulation is carried with a novel contraption of a screw-nut like system for mechanical actuation of elastomeric suction cups. In

brief, the operation of the cartridge starts with sample collection via a 3D printed funnel coated with epoxy. The subsequent sample lysis is carried out in a metal insert heated to 95<sup>0</sup>C for 3min, where the steady state temperature is reached within 1min. Following the lysis, the lysed sample is transferred from the lysis chamber (.i.e. the metal insert) to the Y-junction of the mixing module via the mechanical actuation of the suction cup which engenders a pressure gradient. The suction cup, modeled as a hemispherical volume, is fabricated using 3D printed molds, with the volume of the cup correlated to the volume of the channels. Following this, the 3D printed membrane is ruptured, which results in venting the amplification reagent chambers to the atmosphere and the second suction cup is decompressed using mechanical actuation. This results in the mixing of the lysed sample with the amplification reagents and the mixture reaches the detection chambers. The chip is then heated to 65<sup>0</sup>C for 15min using a cartridge heater modulated with an external PID controller. The silicon fabricated microfluidic chip is conducive to quick heating. The fluid manipulation system presented here is based on the controlled actuation of the suction cup using a nut-screw mechanism. The capability of this fluid manipulation system is presented by demonstrating controlled actuation of the suction cup which translated into pumping of fluid in controlled volumes defined by the angle of the screw head. In this work, we demonstrated the fluid pumping by directional rotation of the screw in steps of 30degrees. We believe that this fluid manipulation system could potentially be applied in systems that could require fluid pumping in precise volumes. More specifically, this suction cup mediated flow coupled with 3D printed cartridge could be helpful for assays with sequential nature. For example, application of this fluid manipulation system for Enzyme-linked immunosorbent assay (ELISA) for pathogen detection can be a potential application. ELISA comprises of multiple steps of antibody binding; washing; incubation; and enzyme catalysis<sup>181</sup>. Similarly, the current system with slight modifications can be applied to other nucleic acid assays like RCA, RPA and HDA which require sequential operation. The

microfluidic platform employed in the current work is a silicon substrate patterned with SU-8, fabricated in a cleanroom. This can have potential implications in the context of scale-up. With the current fabrication process, the bulk of the microfluidic cartridge's cost comes from the cleanroom techniques. The advent of rapid and accessible prototyping techniques like 3D printing, present a great avenue for replacing the cleanroom fabrication processes. Previously, microfluidic chips were fabricated using 3D printed approaches for several biomedical approaches<sup>182</sup>. Previously, Kadimisetty et al.<sup>183</sup>, reported a 3D printed microfluidic chip for LAMP based detection of *Plasmodium falciparum*. They employed an SLA 3D printer and fabricated the device for under 1.15\$. This work is one of many works, that bolsters the rationale to shift towards 3D printing and away from cleanroom techniques.

Another challenge with colorimetric detection is quantitative analysis and is an ongoing goal for colorimetric diagnostics. For improving the quantitative assessment capacity, we should adopt a robust automated imaging and subsequent data analysis approaches. The rise of open-source hardware and software technologies could help realize this automation. In addition to this, electronics are becoming more affordable and accessible. In the current work we employed a portable reflected-light imaging setup with controlled epi-illumination (PRICE), that aids in quantitative analysis of the colorimetric change. For subsequently analyzing the images recorded by PRICE, we employed Python environment hosted on Raspberry Pi. In conjunction to the imaging, the operation of the cartridge operation is intended to be automated. An Arduino UNO microcontroller was employed for concerting the operation of a system linear actuators, heaters and the linear X-Y stage. The future iterations would involve experimentation on making the imaging setup more compact by experimenting with employing digital image processing techniques to offset the use of expensive optics while maintaining the quantification capabilities. These improvements would further enable lab-to-bedside translation of the technology.

Considering the future of such assays related to POC/clinical diagnostics, there is still a need to focus on the fundamental research and its clinical translation, with the integration of advanced nanotechnology, biotechnology, and other emerging technologies such as colorimetric-based microfluidic chips and personalized equipment. For accelerating clinical translation, there is a need for collaboration between front-line medical systems and the academic arena. As colorimetric-based microfluidics has a multidisciplinary nature, there is a need for ongoing coordination between all related parties, such as scientists, engineers, end-users (e.g., physicians and medical examiners), and commercial partners (e.g., marketing experts and investors) in a unified and collaborative manner for successful realization of microfluidic tools/technology to the market. Clinical trials should pursue proof-of-concept experiments along with volume-manufacturing considerations so that both commercial and performance success can be obtained.

Integration and standardization are two other challenges with device commercialization. Unreproducible results can appear due to the variability in outcomes of fabricated devices. In addition, many works have shown a failure to integrate all sample analysis steps in an all-inclusive device. It is important to allocate efforts for device integration and standardization improvement for augmenting the scale of pathogen diagnosis and susceptibility testing. Currently, there are many opportunities for the development and application of colorimetric-based microfluidic technologies for addressing different pathogen-related challenges that are globally emerging. With the entry of microfluidics to its third decade, it is expected that growth and expansion will be extended beyond simple proof-of-concept systems into broad, commercial real-world applications, particularly for colorimetric-based microfluidic systems.

## 5. Summary

In this work we reported an automated setup for sample to answer pathogen detection. The setup encompasses three different modules, (i) portable reflected-light imaging setup with controlled epi-illumination (PRICE), (ii) a microfluidic cartridge and (iii) automation control unit. We employed QolorEx, a specialized nanostructured platform recently developed in our lab that leverages plasmonic excitation for highly sensitive detection of respiratory infectious pathogen. First, to capture the colorimetric change, we designed and characterized the PRICE for imaging the assay chamber. The imaging setup was designed to offer control over the spatial and spectral profile of the illumination source while maintaining uniformity. Next, to eliminate the involvement of the user, a microfluidic cartridge with PDMS suction cups coupled with SLA 3D printing and automation was implemented. The flow was shown to be mechanically actuated by a screw-nut mechanism. The microfluidic chip was characterized for mixing efficiency. The cartridge operation was concerted using system of linear actuators and electrothermal heaters connected via Arduino UNO and Raspberry Pi controlled via mobile application. The imaging was implemented in a direct comparison format with a Nikon brightfield microscope, and a quantifiable colorimetric change was recorded in 10min. In future iterations we plan to package the whole microfluidic cartridge as a fully additive manufactured platform including the microfluidic channels. We believe that this automated system can truly enable the application of highly sensitive QolorEX platform at the POC for pathogen testing.

## 6. Master Bibliography

1. Alberts B, Johnson A, Lewis J, Raff M, Roberts K, Walter P. Introduction to Pathogens. Published online 2002. Accessed February 12, 2021. <https://www.ncbi.nlm.nih.gov/books/NBK26917/>
2. Peck KR. Early diagnosis and rapid isolation: response to COVID-19 outbreak in Korea. *Clinical Microbiology and Infection*. 2020;26(7):805-807. doi:10.1016/j.cmi.2020.04.025
3. Yousefi H, Mahmud A, Chang D, et al. Detection of SARS-CoV-2 Viral Particles Using Direct, Reagent-Free Electrochemical Sensing. *J Am Chem Soc*. 2021;143:1722-1727. doi:10.1021/jacs.0c10810
4. Gu W, Deng X, Lee M, et al. Rapid pathogen detection by metagenomic next-generation sequencing of infected body fluids. *Nature Medicine*. 2021;27(1):115-124. doi:10.1038/s41591-020-1105-z
5. Singh NK, Ray P, Carlin AF, et al. Hitting the diagnostic sweet spot: Point-of-care SARS-CoV-2 salivary antigen testing with an off-the-shelf glucometer. *Biosensors and Bioelectronics*. 2021;180:113111. doi:10.1016/j.bios.2021.113111
6. Ning B, Yu T, Zhang S, et al. A smartphone-read ultrasensitive and quantitative saliva test for COVID-19. *Science Advances*. 2021;7(2):eabe3703. doi:10.1126/sciadv.abe3703
7. Dinnes J, Deeks JJ, Adriano A, et al. Rapid, point-of-care antigen and molecular-based tests for diagnosis of SARS-CoV-2 infection. *Cochrane Database of Systematic Reviews*. 2020;2020(8). doi:10.1002/14651858.CD013705
8. Busche J, Möller S, Klein AK, et al. Nanofluidic Immobilization and Growth Detection of Escherichia coli in a Chip for Antibiotic Susceptibility Testing. *Biosensors (Basel)*. 2020;10(10):135. doi:10.3390/bios10100135
9. Wang X, Shang X, Huang X. Next-generation pathogen diagnosis with CRISPR/Cas-based detection methods. *Emerging Microbes & Infections*. 2020;9(1):1682-1691. doi:10.1080/22221751.2020.1793689
10. Lee RA, de Puig H, Nguyen PQ, et al. Ultrasensitive CRISPR-based diagnostic for field-applicable detection of Plasmodium species in symptomatic and asymptomatic malaria. *Proc Natl Acad Sci U S A*. 2020;117(41):25722-25731. doi:10.1073/pnas.2010196117
11. Gomez-Gutierrez S v., Goodwin SB. Loop-Mediated Isothermal Amplification for Detection of Plant Pathogens in Wheat (*Triticum aestivum*). *Frontiers in Plant Science*. 2022;13:604. doi:10.3389/FPLS.2022.857673/BIBTEX
12. Iwamoto T, Sonobe T, Hayashi K. Loop-mediated isothermal amplification for direct detection of Mycobacterium tuberculosis complex, M. avium, and M. intracellulare in sputum samples. *Journal of Clinical Microbiology*. 2003;41(6):2616-2622.

doi:10.1128/JCM.41.6.2616-2622.2003/ASSET/ABCFD794-AC75-44EA-8773-C070FFF793B3/ASSETS/GRAPHIC/JM0631851002.JPEG

13. Moehling TJ, Choi G, Dugan LC, Salit M, Meagher RJ. LAMP Diagnostics at the Point-of-Care: Emerging Trends and Perspectives for the Developer Community. *https://doi.org/10.1080/1473715920211873769*. 2021;21(1):43-61. doi:10.1080/14737159.2021.1873769
14. Tamer AbdElFatah MJSYGIIHSM. *Plasmonic-Assisted Point-of-Care Rapid and Quantified Identification (or Diagnosis) of Respiratory Infections via a Nano Surface Microfluidic Colorimetry Apparatus.*; 2022.
15. St John A, Price CP. Existing and Emerging Technologies for Point-of-Care Testing. *Clin Biochem Rev*. 2014;35(3):155-167. Accessed February 17, 2021. <http://www.ncbi.nlm.nih.gov/pubmed/25336761>
16. Jung W, Han J, Choi JW, Ahn CH. Point-of-care testing (POCT) diagnostic systems using microfluidic lab-on-a-chip technologies. *Microelectronic Engineering*. 2015;132:46-57. doi:10.1016/j.mee.2014.09.024
17. Vashist SK. Point-of-care diagnostics: Recent advances and trends. *Biosensors (Basel)*. 2017;7(4). doi:10.3390/bios7040062
18. Trevino EA, Weissfeld AS. The Case for point-of-care testing in infectious-disease diagnosis. *Clinical Microbiology Newsletter*. 2007;29(23):177-179. doi:10.1016/j.clinmicnews.2007.11.001
19. Naseri M, Ziora ZM, Simon GP, Batchelor W. ASSURED-compliant point-of-care diagnostics for the detection of human viral infections. *Reviews in Medical Virology*. 2022;32(2):e2263. doi:10.1002/RMV.2263
20. Nguyen T, Chidambara VA, Andreasen SZ, et al. Point-of-care devices for pathogen detections: The three most important factors to realise towards commercialization. *TrAC Trends in Analytical Chemistry*. 2020;131:116004. doi:10.1016/J.TRAC.2020.116004
21. Gorgannezhad L, Stratton H, Nguyen NT. Microfluidic-Based Nucleic Acid Amplification Systems in Microbiology. *Micromachines (Basel)*. 2019;10(6). doi:10.3390/M110060408
22. Tsougeni K, Kaprou G, Loukas CM, et al. Lab-on-Chip platform and protocol for rapid foodborne pathogen detection comprising on-chip cell capture, lysis, DNA amplification and surface-acoustic-wave detection. *Sensors and Actuators, B: Chemical*. 2020;320:128345. doi:10.1016/j.snb.2020.128345
23. Dhar BC, Lee NY. Lab-on-a-Chip Technology for Environmental Monitoring of Microorganisms. *Biochip Journal*. 2018;12(3):173-183. doi:10.1007/s13206-018-2301-5
24. Foudeh AM, Fatanat Didar T, Veres T, Tabrizian M. Microfluidic designs and techniques using lab-on-a-chip devices for pathogen detection for point-of-care diagnostics. *Lab on a Chip*. 2012;12(18):3249-3266. doi:10.1039/c2lc40630f

25. Yoon JY, Kim B. Lab-on-a-chip pathogen sensors for food safety. *Sensors (Switzerland)*. 2012;12(8):10713-10741. doi:10.3390/s120810713
26. Shrivastava S, Trung TQ, Lee NE. Recent progress, challenges, and prospects of fully integrated mobile and wearable point-of-care testing systems for self-testing. *Chemical Society Reviews*. 2020;49(6):1812-1866. doi:10.1039/c9cs00319c
27. Zhang D, Bi H, Liu B, Qiao L. Detection of Pathogenic Microorganisms by Microfluidics Based Analytical Methods. *Analytical Chemistry*. 2018;90(9):5512-5520. doi:10.1021/acs.analchem.8b00399
28. Mairhofer J, Roppert K, Ertl P. Microfluidic Systems for Pathogen Sensing: A Review. *Sensors*. 2009;9(6):4804-4823. doi:10.3390/s90604804
29. Jalali M, Filine E, Dalfen S, Mahshid S. Microscale reactor embedded with Graphene/hierarchical gold nanostructures for electrochemical sensing: application to the determination of dopamine. *Microchimica Acta*. 2020;187(1):1-10. doi:10.1007/s00604-019-4059-4
30. Jalali M, AbdelFatah T, Mahshid SS, Labib M, Sudalaiyadum Perumal A, Mahshid S. A Hierarchical 3D Nanostructured Microfluidic Device for Sensitive Detection of Pathogenic Bacteria. *Small*. 2018;14(35):1801893. doi:10.1002/smll.201801893
31. Wang L, Musile G, McCord BR. An aptamer-based paper microfluidic device for the colorimetric determination of cocaine. *ELECTROPHORESIS*. 2018;39(3):470-475. doi:10.1002/elps.201700254
32. Jalali M, Moakhar RS, Abdelfattah T, Filine E, Mahshid SS, Mahshid S. Nanopattern-Assisted Direct Growth of Peony-like 3D MoS<sub>2</sub>/Au Composite for Nonenzymatic Photoelectrochemical Sensing. *ACS Applied Materials and Interfaces*. 2020;12(6):7411-7422. doi:10.1021/acsami.9b17449
33. Sanati A, Jalali M, Raeissi K, et al. A review on recent advancements in electrochemical biosensing using carbonaceous nanomaterials. *Microchimica Acta*. 2019;186(12):1-22. doi:10.1007/s00604-019-3854-2
34. Abdelfatah T, Jalali M, Mahshid S. A nanofilter for fluidic devices by pillar-assisted self-assembly microparticles. *Biomicrofluidics*. 2018;12(6). doi:10.1063/1.5048623
35. Nguyen HQ, Nguyen VD, van Nguyen H, Seo TS. Quantification of colorimetric isothermal amplification on the smartphone and its open-source app for point-of-care pathogen detection. *Scientific Reports*. 2020;10(1):1-10. doi:10.1038/s41598-020-72095-3
36. Zhao F, Liu Z, Gu Y, et al. Detection of *Mycoplasma pneumoniae* by colorimetric loop-mediated isothermal amplification. *Acta Microbiologica et Immunologica Hungarica*. 2013;60(1):1-9. doi:10.1556/AMicr.60.2013.1.1
37. Goto M, Honda E, Ogura A, Nomoto A, Hanaki KI. Colorimetric detection of loop-mediated isothermal amplification reaction by using hydroxy naphthol blue. *Biotechniques*. 2009;46(3):167-172. doi:10.2144/000113072

38. Baldi P, la Porta N. Molecular Approaches for Low-Cost Point-of-Care Pathogen Detection in Agriculture and Forestry. *Frontiers in Plant Science*. 2020;11:1603. doi:10.3389/FPLS.2020.570862/BIBTEX
39. Wong YP, Othman S, Lau YL, Radu S, Chee HY. Loop-mediated isothermal amplification (LAMP): a versatile technique for detection of micro-organisms. *Journal of Applied Microbiology*. 2018;124(3):626-643. doi:10.1111/JAM.13647
40. Gadkar VJ, Goldfarb DM, Gantt S, Tilley PAG. Real-time Detection and Monitoring of Loop Mediated Amplification (LAMP) Reaction Using Self-quenching and De-quenching Fluorogenic Probes. *Scientific Reports 2018 8:1*. 2018;8(1):1-10. doi:10.1038/s41598-018-23930-1
41. Tanner NA, Zhang Y, Evans TC. Visual detection of isothermal nucleic acid amplification using pH-sensitive dyes. *Biotechniques*. 2015;58(2):59-68. doi:10.2144/000114253/
42. Zhang X, Lowe SB, Gooding JJ. Brief review of monitoring methods for loop-mediated isothermal amplification (LAMP). *Biosensors and Bioelectronics*. 2014;61:491-499. doi:10.1016/J.BIOS.2014.05.039
43. Rodriguez-Manzano J, Karymov MA, Begolo S, et al. Reading Out Single-Molecule Digital RNA and DNA Isothermal Amplification in Nanoliter Volumes with Unmodified Camera Phones. *ACS Nano*. 2016;10(3):3102-3113. doi:10.1021/ACSNANO.5B07338/ASSET/IMAGES/LARGE/NN-2015-07338B\_0006.JPEG
44. Papadakis G, Pantazis AK, Fikas N, et al. Portable real-time colorimetric LAMP-device for rapid quantitative detection of nucleic acids in crude samples. *Scientific Reports 2022 12:1*. 2022;12(1):1-15. doi:10.1038/s41598-022-06632-7
45. Mori Y, Nagamine K, Tomita N, Notomi T. Detection of loop-mediated isothermal amplification reaction by turbidity derived from magnesium pyrophosphate formation. *Biochem Biophys Res Commun*. 2001;289(1):150-154. doi:10.1006/BBRC.2001.5921
46. Garg N, Ahmad FJ, Kar S. Recent advances in loop-mediated isothermal amplification (LAMP) for rapid and efficient detection of pathogens. *Current Research in Microbial Sciences*. 2022;3:100120. doi:10.1016/J.CRMICR.2022.100120
47. Dhama K, Karthik K, Chakraborty S, et al. Loop-mediated isothermal amplification of DNA (LAMP): A new diagnostic tool lights the world of diagnosis of animal and human pathogens: A review. *Pakistan Journal of Biological Sciences*. 2014;17(2):151-166. doi:10.3923/PJBS.2014.151.166
48. Kubo T, Agoh M, Mai LQ, et al. Development of a reverse transcription-loop-mediated isothermal amplification assay for detection of pandemic (H1N1) 2009 virus as a novel molecular method for diagnosis of pandemic influenza in resource-limited settings. *Journal of Clinical Microbiology*. 2010;48(3):728-735. doi:10.1128/JCM.01481-09/ASSET/E2032253-2056-4D5E-9C5D-60A4953DD84E/ASSETS/GRAPHIC/ZJM9990995710002.JPEG

49. Parida M, Posadas G, Inoue S, Hasebe F, Morita K. Real-Time Reverse Transcription Loop-Mediated Isothermal Amplification for Rapid Detection of West Nile Virus. *Journal of Clinical Microbiology*. 2004;42(1):257-263. doi:10.1128/JCM.42.1.257-263.2004/ASSET/1A5397B0-EC05-4F93-8093-988DB00512FB/ASSETS/GRAPHIC/ZJM0010411750002.JPEG
50. Yuan XY, Wang YL, Meng K, Zhang YX, Xu HY, Ai W. LAMP real-time turbidity detection for fowl adenovirus. *BMC Veterinary Research*. 2019;15(1):1-4. doi:10.1186/S12917-019-2015-5/TABLES/1
51. Augustine R, Hasan A, Das S, et al. Loop-Mediated Isothermal Amplification (LAMP): A Rapid, Sensitive, Specific, and Cost-Effective Point-of-Care Test for Coronaviruses in the Context of COVID-19 Pandemic. *Biology 2020, Vol 9, Page 182*. 2020;9(8):182. doi:10.3390/BIOLOGY9080182
52. Lamb LE, Bartolone SN, Ward E, Chancellor MB. Rapid detection of novel coronavirus/Severe Acute Respiratory Syndrome Coronavirus 2 (SARS-CoV-2) by reverse transcription-loop-mediated isothermal amplification. *PLOS ONE*. 2020;15(6):e0234682. doi:10.1371/JOURNAL.PONE.0234682
53. Oloniniyi OK, Kurosaki Y, Miyamoto H, Takada A, Yasuda J. Rapid detection of all known ebolavirus species by reverse transcription-loop-mediated isothermal amplification (RT-LAMP). *Journal of Virological Methods*. 2017;246:8-14. doi:10.1016/J.JVIROMET.2017.03.011
54. Quoc NB, Phuong NDN, Chau NNB, Linh DTP. Closed tube loop-mediated isothermal amplification assay for rapid detection of hepatitis B virus in human blood. *Heliyon*. 2018;4(3):e00561. doi:10.1016/J.HELIYON.2018.E00561/ATTACHMENT/4F857A1C-852D-494B-A619-7C6BDF289F00/MMC1
55. Kim J, Park BG, Lim DH, et al. Development and evaluation of a multiplex loop-mediated isothermal amplification (LAMP) assay for differentiation of Mycobacterium tuberculosis and non-tuberculosis mycobacterium in clinical samples. *PLOS ONE*. 2021;16(1):e0244753. doi:10.1371/JOURNAL.PONE.0244753
56. Shirato K, Semba S, El-Kafrawy SA, et al. Development of fluorescent reverse transcription loop-mediated isothermal amplification (RT-LAMP) using quenching probes for the detection of the Middle East respiratory syndrome coronavirus. *Journal of Virological Methods*. 2018;258:41-48. doi:10.1016/J.JVIROMET.2018.05.006
57. Foudeh AM, Fatanat Didar T, Veres T, Tabrizian M. Microfluidic designs and techniques using lab-on-a-chip devices for pathogen detection for point-of-care diagnostics. *Lab on a Chip*. 2012;12(18):3249-3266. doi:10.1039/C2LC40630F
58. Monis PT, Giglio S. Nucleic acid amplification-based techniques for pathogen detection and identification. *Infection, Genetics and Evolution*. 2006;6(1):2. doi:10.1016/J.MEEGID.2005.08.004
59. Oliveira BB, Veigas B, Baptista PV. Isothermal Amplification of Nucleic Acids: The Race for the Next “Gold Standard.” *Frontiers in Sensors*. 2021;0:14. doi:10.3389/FSSENS.2021.752600

60. Notomi T, Okayama H, Masubuchi H, et al. Loop-mediated isothermal amplification of DNA. *Nucleic Acids Res.* 2000;28(12):63. doi:10.1093/nar/28.12.e63
61. Shang Y, Sun J, Ye Y, Zhang J, Zhang Y, Sun X. Loop-mediated isothermal amplification-based microfluidic chip for pathogen detection. *Critical Reviews in Food Science and Nutrition.* 2020;60(2):201-224. doi:10.1080/10408398.2018.1518897
62. Azzi L, Maurino V, Baj A, et al. Diagnostic Salivary Tests for SARS-CoV-2. *Journal of Dental Research.* 2021;100(2):115. doi:10.1177/0022034520969670
63. Azzi L, Carcano G, Gianfagna F, et al. Saliva is a reliable tool to detect SARS-CoV-2. *Journal of Infection.* 2020;81(1):e45-e50. doi:10.1016/J.JINF.2020.04.005
64. Liu W, Yue F, Lee LP. Integrated Point-of-Care Molecular Diagnostic Devices for Infectious Diseases. *Accounts of Chemical Research.* 2021;54(22):4107-4119. doi:10.1021/ACS.ACCOUNTS.1C00385/SUPPL\_FILE/AR1C00385\_SI\_001.PDF
65. Paul R, Ostermann E, Wei Q. Advances in point-of-care nucleic acid extraction technologies for rapid diagnosis of human and plant diseases. *Biosensors & Bioelectronics.* 2020;169:112592. doi:10.1016/J.BIOS.2020.112592
66. Ye Q, Lu D, Zhang T, Mao J, Shang S. Recent advances and clinical application in point-of-care testing of SARS-CoV-2. *Journal of Medical Virology.* 2022;94(5):1866-1875. doi:10.1002/JMV.27617
67. Yang M, Ke Y, Wang X, et al. Development and Evaluation of a Rapid and Sensitive EBOV-RPA Test for Rapid Diagnosis of Ebola Virus Disease. *Scientific Reports 2016 6:1.* 2016;6(1):1-7. doi:10.1038/srep26943
68. Priye A, Bird SW, Light YK, Ball CS, Negrete OA, Meagher RJ. A smartphone-based diagnostic platform for rapid detection of Zika, chikungunya, and dengue viruses. *Scientific Reports 2017 7:1.* 2017;7(1):1-11. doi:10.1038/srep44778
69. Packard MM, Wheeler EK, Alocilja EC, Shusteff M. Performance Evaluation of Fast Microfluidic Thermal Lysis of Bacteria for Diagnostic Sample Preparation †. *Diagnostics.* 2013;3(1):105. doi:10.3390/DIAGNOSTICS3010105
70. Cho B, Lee SH, Song J, et al. Nanophotonic Cell Lysis and Polymerase Chain Reaction with Gravity-Driven Cell Enrichment for Rapid Detection of Pathogens. *ACS Nano.* 2019;13(12):13866-13874. doi:10.1021/ACSNANO.9B04685/ASSET/IMAGES/LARGE/NN9B04685\_0004.JPG
71. Yoon J, Yoon YJ, Lee TY, Park MK, Chung J, Shin Y. A disposable lab-on-a-chip platform for highly efficient RNA isolation. *Sensors and Actuators B: Chemical.* 2018;255:1491-1499. doi:10.1016/J.SNB.2017.08.157
72. Ma YD, Chen YS, Lee G bin. An integrated self-driven microfluidic device for rapid detection of the influenza A (H1N1) virus by reverse transcription loop-mediated isothermal amplification. *Sensors and Actuators, B: Chemical.* 2019;296:126647. doi:10.1016/j.snb.2019.126647

73. di Carlo D, Jeong KH, Lee LP. Reagentless mechanical cell lysis by nanoscale barbs in microchannels for sample preparation. *Lab on a Chip*. 2003;3(4):287-291. doi:10.1039/B305162E
74. Yan H, Zhu Y, Zhang Y, et al. Multiplex detection of bacteria on an integrated centrifugal disk using bead-beating lysis and loop-mediated amplification. *Scientific Reports* 2017 7:1. 2017;7(1):1-11. doi:10.1038/s41598-017-01415-x
75. Hügler M, Dame G, Behrmann O, et al. A lab-on-a-chip for preconcentration of bacteria and nucleic acid extraction. *RSC Advances*. 2018;8(36):20124-20130. doi:10.1039/C8RA02177E
76. Walker FM, Hsieh K. Advances in Directly Amplifying Nucleic Acids from Complex Samples. *Biosensors* 2019, Vol 9, Page 117. 2019;9(4):117. doi:10.3390/BIOS9040117
77. Kang JS, Park C, Lee J, Namkung J, Hwang SY, Kim YS. Automated nucleic acids purification from fecal samples on a microfluidic cartridge. *BioChip Journal* 2017 11:1. 2017;11(1):76-84. doi:10.1007/S13206-016-1205-5
78. Branch DW, Vreeland EC, McClain JL, Murton JK, James CD, Achyuthan KE. Rapid Nucleic Acid Extraction and Purification Using a Miniature Ultrasonic Technique. *Micromachines* 2017, Vol 8, Page 228. 2017;8(7):228. doi:10.3390/MI8070228
79. Liu H, Zhao F, Jin CE, et al. Large Instrument- and Detergent-Free Assay for Ultrasensitive Nucleic Acids Isolation via Binary Nanomaterial. *Analytical Chemistry*. 2018;90(8):5108-5115. doi:10.1021/ACS.ANALCHEM.7B05136/SUPPL\_FILE/AC7B05136\_SI\_001.PDF
80. Fu Y, Zhou X, Xing D. Integrated paper-based detection chip with nucleic acid extraction and amplification for automatic and sensitive pathogen detection. *Sensors and Actuators B: Chemical*. 2018;261:288-296. doi:10.1016/J.SNB.2018.01.165
81. Petralia S, Sciuto EL, Conoci S. A novel miniaturized biofilter based on silicon micropillars for nucleic acid extraction. *Analyst*. 2016;142(1):140-146. doi:10.1039/C6AN02049F
82. Almassian DR, Cockrell LM, Nelson WM. Portable nucleic acid thermocyclers. *Chemical Society Reviews*. 2013;42(22):8769-8798. doi:10.1039/C3CS60144G
83. Miralles V, Huerre A, Malloggi F, Jullien MC. A Review of Heating and Temperature Control in Microfluidic Systems: Techniques and Applications. *Diagnostics* 2013, Vol 3, Pages 33-67. 2013;3(1):33-67. doi:10.3390/DIAGNOSTICS3010033
84. Roy E, Stewart G, Mounier M, et al. From cellular lysis to microarray detection, an integrated thermoplastic elastomer (TPE) point of care Lab on a Disc. *Lab on a Chip*. 2014;15(2):406-416. doi:10.1039/C4LC00947A
85. Chen P, Chen C, Su H, et al. Integrated and finger-actuated microfluidic chip for point-of-care testing of multiple pathogens. *Talanta*. 2021;224:121844. doi:10.1016/J.TALANTA.2020.121844

86. Qiu X, Ge S, Gao P, et al. A smartphone-based point-of-care diagnosis of H1N1 with microfluidic convection PCR. *Microsystem Technologies*. 2017;23(7):2951-2956. doi:10.1007/S00542-016-2979-Z/FIGURES/6
87. Deng H, Jayawardena A, Chan J, Tan SM, Alan T, Kwan P. An ultra-portable, self-contained point-of-care nucleic acid amplification test for diagnosis of active COVID-19 infection. *Scientific Reports* 2021 11:1. 2021;11(1):1-12. doi:10.1038/s41598-021-94652-0
88. Park J, Han DH, Park JK. Towards practical sample preparation in point-of-care testing: user-friendly microfluidic devices. *Lab on a Chip*. 2020;20(7):1191-1203. doi:10.1039/D0LC00047G
89. Jagannath A, Cong H, Hassan J, Gonzalez G, Gilchrist MD, Zhang N. Pathogen detection on microfluidic platforms: Recent advances, challenges, and prospects. *Biosensors and Bioelectronics: X*. 2022;10:100134. doi:10.1016/J.BIOSX.2022.100134
90. Laser DJ, Santiago JG. A review of micropumps. *Journal of Micromechanics and Microengineering*. 2004;14(6):R35. doi:10.1088/0960-1317/14/6/R01
91. Wang YN, Fu LM. Micropumps and biomedical applications – A review. *Microelectronic Engineering*. 2018;195:121-138. doi:10.1016/J.MEE.2018.04.008
92. Amirouche F, Zhou Y, Johnson T. Current micropump technologies and their biomedical applications. *Microsystem Technologies*. 2009;15(5):647-666. doi:10.1007/S00542-009-0804-7/FIGURES/26
93. Das PK, Hasan ABMT. Mechanical micropumps and their applications: A review  
ARTICLES YOU MAY BE INTERESTED IN Passive micropumping in microfluidics for point-of-care testing Fabrication of micropump for microfluidics application AIP Conference Mechanical Micropumps And Their Applications: A Review. 2017;1851:20140. doi:10.1063/1.4984739
94. Vashist SK. Point-of-Care Diagnostics: Recent Advances and Trends. *Biosensors* 2017, Vol 7, Page 62. 2017;7(4):62. doi:10.3390/BIOS7040062
95. Niemz A, Ferguson TM, Boyle DS. Point-of-care nucleic acid testing for infectious diseases. *Trends in Biotechnology*. 2011;29(5):240-250. doi:10.1016/J.TIBTECH.2011.01.007
96. Au AK, Lai H, Utela BR, Folch A. Microvalves and Micropumps for BioMEMS. *Micromachines* 2011, Vol 2, Pages 179-220. 2011;2(2):179-220. doi:10.3390/MI2020179
97. Aboubakri A, Ebrahimpour Ahmadi V, Koşar A. Modeling of a Passive-Valve Piezoelectric Micro-Pump: A Parametric Study. *Micromachines* 2020, Vol 11, Page 752. 2020;11(8):752. doi:10.3390/MI11080752
98. Xu L, Wang A, Li X, Oh KW. Passive micropumping in microfluidics for point-of-care testing. *Cite as: Biomicrofluidics*. 2020;14:31503. doi:10.1063/5.0002169

99. Abhari F, Jaafar H, Amziah N, Yunus M. A Comprehensive Study of Micropumps Technologies. *Int J Electrochem Sci*. 2012;7:9765-9780. Accessed May 27, 2022. [www.electrochemsci.org](http://www.electrochemsci.org)
100. Seo JH, Park BH, Oh SJ, et al. Development of a high-throughput centrifugal loop-mediated isothermal amplification microdevice for multiplex foodborne pathogenic bacteria detection. *Sensors and Actuators, B: Chemical*. 2017;246:146-153. doi:10.1016/j.snb.2017.02.051
101. Oh SJ, Park BH, Jung JH, et al. Centrifugal loop-mediated isothermal amplification microdevice for rapid, multiplex and colorimetric foodborne pathogen detection. *Biosensors and Bioelectronics*. 2016;75:293-300. doi:10.1016/J.BIOS.2015.08.052
102. Geissler M, Clime L, Hoa XD, et al. Microfluidic Integration of a Cloth-Based Hybridization Array System (CHAS) for Rapid, Colorimetric Detection of Enterohemorrhagic Escherichia coli (EHEC) Using an Articulated, Centrifugal Platform. *Analytical Chemistry*. 2015;87(20):10565-10572. doi:10.1021/ACS.ANALCHEM.5B03085/ASSET/IMAGES/LARGE/AC-2015-03085U\_0005.JPEG
103. Lee W bin, Fu CY, Chang WH, et al. A microfluidic device for antimicrobial susceptibility testing based on a broth dilution method. *Biosensors and Bioelectronics*. 2017;87:669-678. doi:10.1016/J.BIOS.2016.09.008
104. Sayad A, Ibrahim F, Mukim Uddin S, Cho J, Madou M, Thong KL. A microdevice for rapid, monoplex and colorimetric detection of foodborne pathogens using a centrifugal microfluidic platform. *Biosensors and Bioelectronics*. 2018;100:96-104. doi:10.1016/j.bios.2017.08.060
105. Kim HJ, Kim YJ, Yong DE, et al. Loop-mediated isothermal amplification of vanA gene enables a rapid and naked-eye detection of vancomycin-resistant enterococci infection. *Journal of Microbiological Methods*. 2014;104:61-66. doi:10.1016/j.mimet.2014.05.021
106. Jung JH, Park H, Oh J, Choi G, Seo TS. Integrated centrifugal reverse transcriptase loop-mediated isothermal amplification microdevice for influenza A virus detection. Published online 2014. doi:10.1016/j.bios.2014.12.043
107. Nguyen H van, Nguyen VD, Lee EY, Seo TS. Point-of-care genetic analysis for multiplex pathogenic bacteria on a fully integrated centrifugal microdevice with a large-volume sample. *Biosensors and Bioelectronics*. 2019;136:132-139. doi:10.1016/J.BIOS.2019.04.035
108. Lee W bin, Chien CC, You HL, Kuo FC, Lee MS, Lee G bin. An integrated microfluidic system for antimicrobial susceptibility testing with antibiotic combination. *Lab on a Chip*. 2019;19(16):2699-2708. doi:10.1039/C9LC00585D
109. Clime L, Daoud J, Brassard D, Malic L, Geissler M, Veres T. Active pumping and control of flows in centrifugal microfluidics. *Microfluidics and Nanofluidics*. 2019;23(3):1-22. doi:10.1007/S10404-019-2198-X/FIGURES/12

110. Hassan SU, Tariq A, Noreen Z, et al. Capillary-Driven Flow Microfluidics Combined with Smartphone Detection: An Emerging Tool for Point-of-Care Diagnostics. *Diagnostics* 2020, Vol 10, Page 509. 2020;10(8):509. doi:10.3390/DIAGNOSTICS10080509
111. Arshavsky-Graham S, Segal E. Lab-on-a-Chip Devices for Point-of-Care Medical Diagnostics. Published online 2020:1-19. doi:10.1007/10\_2020\_127
112. Olanrewaju A, Beaugrand M, Yafia M, Juncker D. Capillary microfluidics in microchannels: from microfluidic networks to capillary circuits. *Lab on a Chip*. 2018;18(16):2323-2347. doi:10.1039/C8LC00458G
113. Kaur N, Toley BJ. Paper-based nucleic acid amplification tests for point-of-care diagnostics. *Analyst*. 2018;143(10):2213-2234. doi:10.1039/C7AN01943B
114. Fu Y, Zhou X, Xing D. Lab-on-capillary: a rapid, simple and quantitative genetic analysis platform integrating nucleic acid extraction, amplification and detection. *Lab on a Chip*. 2017;17(24):4334-4341. doi:10.1039/C7LC01107E
115. Magro L, Escadafal C, Garneret P, et al. Paper microfluidics for nucleic acid amplification testing (NAAT) of infectious diseases. *Lab on a Chip*. 2017;17(14):2347-2371. doi:10.1039/C7LC00013H
116. Lafleur LK, Bishop JD, Heiniger EK, et al. A rapid, instrument-free, sample-to-result nucleic acid amplification test. *Lab on a Chip*. 2016;16(19):3777-3787. doi:10.1039/C6LC00677A
117. Nishat S, Jafry AT, Martinez AW, Awan FR. Paper-based microfluidics: Simplified fabrication and assay methods. *Sensors and Actuators B: Chemical*. 2021;336:129681. doi:10.1016/J.SNB.2021.129681
118. Tian T, Bi Y, Xu X, Zhu Z, Yang C. Integrated paper-based microfluidic devices for point-of-care testing. *Analytical Methods*. 2018;10(29):3567-3581. doi:10.1039/C8AY00864G
119. Trieu PT, Lee NY. Paper-Based All-in-One Origami Microdevice for Nucleic Acid Amplification Testing for Rapid Colorimetric Identification of Live Cells for Point-of-Care Testing. *Analytical Chemistry*. 2019;91(17):11013-11022. doi:10.1021/ACS.ANALCHEM.9B01263/ASSET/IMAGES/LARGE/AC-2019-012636\_0010.JPEG
120. Liu D, Wang Y, Li X, et al. Integrated microfluidic devices for in vitro diagnostics at point of care. *Aggregate*. Published online February 16, 2022:e184. doi:10.1002/AGT2.184
121. Xu L, Lee H, Jetta D, Oh KW. Vacuum-driven power-free microfluidics utilizing the gas solubility or permeability of polydimethylsiloxane (PDMS). *Lab on a Chip*. 2015;15(20):3962-3979. doi:10.1039/C5LC00716J
122. Wang A, Koh D, Schneider P, Breloff E, Oh KW. A Compact, Syringe-Assisted, Vacuum-Driven Micropumping Device. *Micromachines* 2019, Vol 10, Page 543. 2019;10(8):543. doi:10.3390/M110080543

123. Ho JY, Cira NJ, Crooks JA, Baeza J, Weibel DB. Rapid Identification of ESKAPE Bacterial Strains Using an Autonomous Microfluidic Device. *PLoS ONE*. 2012;7(7):41245. doi:10.1371/journal.pone.0041245
124. Hosokawa K, Sato K, Ichikawa N, Maeda M. Power-free poly(dimethylsiloxane) microfluidic devices for gold nanoparticle -based DNA analysis. *Lab on a Chip*. 2004;4(3):181-185. doi:10.1039/B403930K
125. Myers FB, Henrikson RH, Bone J, Lee LP. A Handheld Point-of-Care Genomic Diagnostic System. *PLOS ONE*. 2013;8(8):e70266. doi:10.1371/JOURNAL.PONE.0070266
126. Xie C, Chen S, Zhang L, et al. Multiplex detection of blood-borne pathogens on a self-driven microfluidic chip using loop-mediated isothermal amplification. *Analytical and Bioanalytical Chemistry*. 2021;413(11):2923-2931. doi:10.1007/S00216-021-03224-8/FIGURES/5
127. Yeh EC, Fu CC, Hu L, Thakur R, Feng J, Lee LP. Self-powered integrated microfluidic point-of-care low-cost enabling (SIMPLE) chip. *Science Advances*. 2017;3(3). doi:10.1126/SCIADV.1501645/SUPPL\_FILE/1501645\_SM.PDF
128. Li B, Qi J, Fu L, et al. Integrated hand-powered centrifugation and paper-based diagnosis with blood-in/answer-out capabilities. *Biosensors and Bioelectronics*. 2020;165:112282. doi:10.1016/J.BIOS.2020.112282
129. Zhang L, Tian F, Liu C, et al. Hand-powered centrifugal microfluidic platform inspired by the spinning top for sample-to-answer diagnostics of nucleic acids. *Lab on a Chip*. 2018;18(4):610-619. doi:10.1039/C7LC01234A
130. Bhupathi M, Chinna G, Devarapu R. Mobilefuge: A low-cost, portable, open source, 3D-printed centrifuge that can be used for purification of saliva samples for SARS-CoV2 detection. *medRxiv*. Published online January 8, 2021:2021.01.06.21249280. doi:10.1101/2021.01.06.21249280
131. Michael I, Kim D, Gulenko O, et al. A fidget spinner for the point-of-care diagnosis of urinary tract infection. *Nature Biomedical Engineering* 2020 4:6. 2020;4(6):591-600. doi:10.1038/s41551-020-0557-2
132. Jeong SW, Park YM, Jo SH, Lee SJ, Kim YT, Lee KG. Smartphone operable centrifugal system (SOCS) for on-site DNA extraction from foodborne bacterial pathogen. *Biomicrofluidics*. 2019;13(3):34111. doi:10.1063/1.5093752
133. Iwai K, Sochol RD, Lee LP, Lin L. Finger-powered bead-in-droplet microfluidic system for point-of-care diagnostics. *Proceedings of the IEEE International Conference on Micro Electro Mechanical Systems (MEMS)*. Published online 2012:949-952. doi:10.1109/MEMSYS.2012.6170343
134. Pappa AM, Curto VF, Braendlein M, et al. Organic Transistor Arrays Integrated with Finger-Powered Microfluidics for Multianalyte Saliva Testing. *Advanced Healthcare Materials*. 2016;5(17):2295-2302. doi:10.1002/ADHM.201600494

135. Zarei M. Advances in point-of-care technologies for molecular diagnostics. *Biosensors and Bioelectronics*. 2017;98:494-506. doi:10.1016/J.BIOS.2017.07.024
136. Lin TY, Parsenjad S, Tu L, et al. Finger-powered microfluidic electrochemical assay for point-of-care testing. *2017 IEEE 12th International Conference on Nano/Micro Engineered and Molecular Systems, NEMS 2017*. Published online August 25, 2017:313-317. doi:10.1109/NEMS.2017.8017032
137. Lu CH, Shih TS, Shih PC, et al. Finger-powered agglutination lab chip with CMOS image sensing for rapid point-of-care diagnosis applications. *Lab on a Chip*. 2020;20(2):424-433. doi:10.1039/C9LC00961B
138. Li W, Chen T, Chen Z, et al. Squeeze-chip: a finger-controlled microfluidic flow network device and its application to biochemical assays. *Lab on a Chip*. 2012;12(9):1587-1590. doi:10.1039/C2LC40125H
139. Qiu X, Thompson JA, Chen Z, et al. Finger-actuated, self-contained immunoassay cassettes. *Biomedical Microdevices*. 2009;11(6):1175-1186. doi:10.1007/S10544-009-9334-4/FIGURES/11
140. Qi W, Zheng L, Hou Y, et al. A finger-actuated microfluidic biosensor for colorimetric detection of foodborne pathogens. *Food Chemistry*. 2022;381:131801. doi:10.1016/J.FOODCHEM.2021.131801
141. Wang Z, Wang Y, Lin L, et al. A finger-driven disposable micro-platform based on isothermal amplification for the application of multiplexed and point-of-care diagnosis of tuberculosis. *Biosensors and Bioelectronics*. 2022;195:113663. doi:10.1016/J.BIOS.2021.113663
142. Choi Y, Song Y, Kim YT, et al. All-in-one pumpless portable genetic analysis microsystem for rapid naked-eye detection. *Sensors and Actuators B: Chemical*. 2021;344:130307. doi:10.1016/J.SNB.2021.130307
143. Park J, Park JK. Finger-actuated microfluidic device for the blood cross-matching test. *Lab on a Chip*. 2018;18(8):1215-1222. doi:10.1039/C7LC01128H
144. Gong MM, MacDonald BD, Vu Nguyen T, Sinton D. Hand-powered microfluidics: A membrane pump with a patient-to-chip syringe interface. *Biomicrofluidics*. 2012;6(4):044102. doi:10.1063/1.4762851
145. Chan HN, Tan MJA, Wu H. Point-of-care testing: applications of 3D printing. *Lab on a Chip*. 2017;17(16):2713-2739. doi:10.1039/C7LC00397H
146. Au AK, Bhattacharjee N, Horowitz LF, Chang TC, Folch A. 3D-printed microfluidic automation. *Lab on a Chip*. 2015;15(8):1934-1941. doi:10.1039/C5LC00126A
147. Begolo S, Zhukov D v., Selck DA, Li L, Ismagilov RF. The pumping lid: investigating multi-material 3D printing for equipment-free, programmable generation of positive and negative pressures for microfluidic applications. *Lab on a Chip*. 2014;14(24):4616-4628. doi:10.1039/C4LC00910J
148. Chan HN, Shu Y, Xiong B, et al. Simple, Cost-Effective 3D Printed Microfluidic Components for Disposable, Point-of-Care Colorimetric Analysis. *ACS Sensors*.

- 2016;1(3):227-234.  
doi:10.1021/ACSSENSORS.5B00100/SUPPL\_FILE/SE5B00100\_SI\_003.MOV
149. Mak WC, Beni V, Turner APF. Lateral-flow technology: From visual to instrumental. *TrAC Trends in Analytical Chemistry*. 2016;79:297-305.  
doi:10.1016/J.TRAC.2015.10.017
150. Nguyen HQ, Nguyen VD, van Nguyen H, Seo TS. Quantification of colorimetric isothermal amplification on the smartphone and its open-source app for point-of-care pathogen detection. *Scientific Reports*. 2020;10(1):1-10. doi:10.1038/s41598-020-72095-3
151. Zhao F, Liu Z, Gu Y, et al. Detection of *Mycoplasma pneumoniae* by colorimetric loop-mediated isothermal amplification. *Acta Microbiologica et Immunologica Hungarica*. 2013;60(1):1-9. doi:10.1556/AMicr.60.2013.1.1
152. Goto M, Honda E, Ogura A, Nomoto A, Hanaki KI. Colorimetric detection of loop-mediated isothermal amplification reaction by using hydroxy naphthol blue. *Biotechniques*. 2009;46(3):167-172. doi:10.2144/000113072
153. Urusov AE, Zherdev A v., Dzantiev BB. Towards Lateral Flow Quantitative Assays: Detection Approaches. *Biosensors 2019, Vol 9, Page 89*. 2019;9(3):89.  
doi:10.3390/BIOS9030089
154. Lee T, Jang J, Jeong H, Rho J. Plasmonic- and dielectric-based structural coloring: from fundamentals to practical applications. *Nano Convergence 2018 5:1*. 2018;5(1):1-21. doi:10.1186/S40580-017-0133-Y
155. Gramotnev DK, Bozhevolnyi SI. Plasmonics beyond the diffraction limit. *Nature Photonics 2010 4:2*. 2010;4(2):83-91. doi:10.1038/nphoton.2009.282
156. Mudachathi R, Tanaka T. Up Scalable Full Colour Plasmonic Pixels with Controllable Hue, Brightness and Saturation. *Scientific Reports 2017 7:1*. 2017;7(1):1-10.  
doi:10.1038/s41598-017-01266-6
157. Fang B, Yang C, Shen W, Zhang X, Liu X, Zhang Y. Highly efficient omnidirectional structural color tuning method based on dielectric–metal–dielectric structure. *Applied Optics, Vol 56, Issue 4, pp C175-C180*. 2017;56(4):C175-C180.  
doi:10.1364/AO.56.00C175
158. Wang H, Wang X, Yan C, et al. Full Color Generation Using Silver Tandem Nanodisks. *ACS Nano*. 2017;11(5):4419-4427.  
doi:10.1021/ACSNANO.6B08465/ASSET/IMAGES/LARGE/NN-2016-08465B\_0006.JPEG
159. Franklin D, He Z, Ortega PM, et al. Self-assembled plasmonics for angle-independent structural color displays with actively addressed black states. *Proc Natl Acad Sci U S A*. 2020;117(24):13350-13358.  
doi:10.1073/PNAS.2001435117/SUPPL\_FILE/PNAS.2001435117.SM01.AVI

160. Si G, Zhao Y, Leong ESP, Lv J, Liu YJ. Incident-angle dependent color tuning from a single plasmonic chip. *Nanotechnology*. 2014;25(45):455203. doi:10.1088/0957-4484/25/45/455203
161. Xu T, Wu YK, Luo X, Guo LJ. Plasmonic nanoresonators for high-resolution colour filtering and spectral imaging. *Nature Communications* 2010 1:1. 2010;1(1):1-5. doi:10.1038/ncomms1058
162. Nguyen H van, Nguyen VD, Liu F, Seo TS. An Integrated Smartphone-Based Genetic Analyzer for Qualitative and Quantitative Pathogen Detection. *ACS Omega*. 2020;5(35):22208-22214. doi:10.1021/ACSOMEGA.0C02317/ASSET/IMAGES/LARGE/AO0C02317\_0006.JPG EG
163. Nguyen VT, Song S, Park S, Joo C. Recent advances in high-sensitivity detection methods for paper-based lateral-flow assay. *Biosensors and Bioelectronics*. 2020;152:112015. doi:10.1016/J.BIOS.2020.112015
164. Nayak S, Blumenfeld NR, Laksanasopin T, Sia SK. Point-of-Care Diagnostics: Recent Developments in a Connected Age. *Analytical Chemistry*. 2017;89(1):102-123. doi:10.1021/ACS.ANALCHEM.6B04630/ASSET/IMAGES/ACS.ANALCHEM.6B04630.SOCIAL.JPEG\_V03
165. Parker RW, Wilson DJ, Mace CR. Open software platform for automated analysis of paper-based microfluidic devices. *Scientific Reports* 2020 10:1. 2020;10(1):1-10. doi:10.1038/s41598-020-67639-6
166. Abels K, Salvo-Halloran EM, White D, et al. Quantitative Point-of-Care Colorimetric Assay Modeling Using a Handheld Colorimeter. *ACS Omega*. 2021;6. doi:10.1021/ACSOMEGA.1C03460/ASSET/IMAGES/LARGE/AO1C03460\_0005.JPG EG
167. Liu J, Geng Z, Fan Z, Liu J, Chen H. Point-of-care testing based on smartphone: The current state-of-the-art (2017–2018). *Biosensors and Bioelectronics*. 2019;132:17-37. doi:10.1016/J.BIOS.2019.01.068
168. Jung Y, Heo Y, Lee JJ, Deering A, Bae E. Smartphone-based lateral flow imaging system for detection of food-borne bacteria E.coli O157:H7. *Journal of Microbiological Methods*. 2020;168:105800. doi:10.1016/J.MIMET.2019.105800
169. Mudanyali O, Dimitrov S, Sikora U, Padmanabhan S, Navruz I, Ozcan A. Integrated rapid-diagnostic-test reader platform on a cellphone. *Lab on a Chip*. 2012;12(15):2678-2686. doi:10.1039/C2LC40235A/
170. Xiao W, Huang C, Xu F, et al. A simple and compact smartphone-based device for the quantitative readout of colloidal gold lateral flow immunoassay strips. *Sensors and Actuators B: Chemical*. 2018;266:63-70. doi:10.1016/J.SNB.2018.03.110
171. Kaarj K, Akarapipad P, Yoon JY. Simpler, Faster, and Sensitive Zika Virus Assay Using Smartphone Detection of Loop-mediated Isothermal Amplification on Paper Microfluidic Chips. *Scientific Reports*. 2018;8(1):12438. doi:10.1038/s41598-018-30797-9

172. Ganguli A, Mostafa A, Berger J, et al. Rapid isothermal amplification and portable detection system for SARS-CoV-2. *Proc Natl Acad Sci U S A*. 2020;117(37):22727-22735. doi:10.1073/pnas.2014739117
173. Tian F, Liu C, Deng J, et al. A fully automated centrifugal microfluidic system for sample-to-answer viral nucleic acid testing. *Science China Chemistry* 2020 63:10. 2020;63(10):1498-1506. doi:10.1007/S11426-020-9800-6
174. Wang S, Liu N, Zheng L, Cai G, Lin J. A lab-on-chip device for the sample-in-result-out detection of viable: Salmonella using loop-mediated isothermal amplification and real-time turbidity monitoring. *Lab on a Chip*. 2020;20(13):2296-2305. doi:10.1039/d0lc00290a
175. Liu D, Zhu Y, Li N, Lu Y, Cheng J, Xu Y. A portable microfluidic analyzer for integrated bacterial detection using visible loop-mediated amplification. *Sensors and Actuators, B: Chemical*. 2020;310:127834. doi:10.1016/j.snb.2020.127834
176. Trinh KTL, Trinh TND, Lee NY. Fully integrated and slidable paper-embedded plastic microdevice for point-of-care testing of multiple foodborne pathogens. *Biosensors and Bioelectronics*. 2019;135:120-128. doi:10.1016/j.bios.2019.04.011
177. Seo JH, Park BH, Oh SJ, et al. Development of a high-throughput centrifugal loop-mediated isothermal amplification microdevice for multiplex foodborne pathogenic bacteria detection. *Sensors and Actuators, B: Chemical*. 2017;246:146-153. doi:10.1016/j.snb.2017.02.051
178. Smith S, Korvink JG, Mager D, Land K. The potential of paper-based diagnostics to meet the ASSURED criteria. *RSC Advances*. 2018;8(59):34012-34034. doi:10.1039/C8RA06132G
179. Marcel S, Christian AL, Richard N, et al. COVID-19 epidemic in Switzerland: on the importance of testing, contact tracing and isolation. *Swiss Medical Weekly* 2020 :11. 2020;150(11). doi:10.4414/SMW.2020.20225
180. Rodríguez-Lázaro D, Cook N, Hernández M. Real-Time PCR in Food Science: PCR Diagnostics. *Current Issues in Molecular Biology* 2013, Vol 15, Pages 39-44. 2013;15(2):39-44. doi:10.21775/CIMB.015.039
181. Verma J, Saxena S, Babu SG. ELISA-Based Identification and Detection of Microbes. Published online 2013:169-186. doi:10.1007/978-3-642-34410-7\_13
182. Waheed S, Cabot JM, Macdonald NP, et al. 3D printed microfluidic devices: enablers and barriers. *Lab on a Chip*. 2016;16(11):1993-2013. doi:10.1039/C6LC00284F
183. Kadimisetty K, Song J, Doto AM, et al. Fully 3D printed integrated reactor array for point-of-care molecular diagnostics. *Biosensors and Bioelectronics*. 2018;109:156-163. doi:10.1016/J.BIOS.2018.03.009